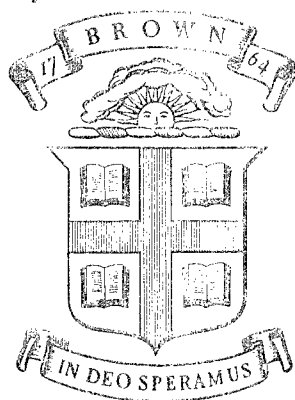


Bu :  
DA-358/8



Division  
of  
APPLIED MATHEMATICS

Best Available Copy

BROWN UNIVERSITY

RECEIVED  
R. M. B.  
LIBRARY OF THE  
BROWN UNIVERSITY  
PROVIDENCE, R.I.  
SEP 19 1964

This document has been approved for public release, and its distribution is unlimited.  
It is to be controlled and not to be con- sidered as an official document of the Department of Defense, and its use is to be limited to the purposes for which it was prepared.

Providence  
Rhode Island

Bu :  
DA-358/8

DEPARTMENT OF THE ARMY  
U. S. ARMY RESEARCH OFFICE -- DURHAM

DA-31-124-ARO(D)-358

540 + 2  
1. Information (Mechanics)

Technical Report No. 8

An Experimental Investigation of the  
Dynamic Tangent Moduli of Polyethylene  
by

James P. Walsh

DA-358/8


AD 680 202

20060110133

DA-358/8

TECHNICAL LIBRARY  
BLDG 313  
ABERDEEN PROVING GROUND MD.  
STEAP-TL

August 1968



## Abstract of An Experimental Investigation of the Dynamic Tangent Moduli of Polyethylene

The research presented in this thesis is on the study of the behavior of the dynamic tangent moduli of polyethylene under large quasi-static deformations. This involved both the determination of the complex shear modulus  $G^*$  and the complex Youngs modulus  $E^*$  as a function of longitudinal and torsional strains.

Tubular specimens were subjected to longitudinal strains of up to 150% or torsional strains of up to 30% by applying constant loads and allowing the sample to creep. At various levels of these static strains, as the sample is undergoing creep, small oscillatory strains are superimposed on the specimen through a coil and magnet system. These small dynamic strains may be imposed in either a lateral, longitudinal, or torsional mode depending on the moduli being investigated. From the decay curve of the vibrations or the resonant frequency and half-breadth of the frequency-amplitude curve, the value of the relevant storage and loss moduli are obtained.

Upon removal of the static load, the specimen will start to recover and the moduli can be determined during the recovery cycle. In addition, the variation of the different moduli under stress relaxation were also obtained for both fixed torsional and longitudinal strains.

Both the shear modulus  $G^*$  and Youngs modulus  $E^*$  were obtained in this manner, the Youngs modulus being determined from either longitudinal or lateral vibrations of the specimen, and the shear modulus by torsional vibrations.

## I. Introduction

The research work presented herein is an effort to increase our understanding of the behavior of a class of materials referred to as high polymers. Specifically, this research is concerned with the behavior of a low density polyethylene with a specific gravity of 0.92.

High polymers are materials which differ greatly in their mechanical behavior from crystalline solids as a result of their being composed of long chain molecules. The bonds within these molecules are usually single pairs of covalent electrons and such molecules possess strong intramolecular forces. The forces between neighboring molecules are usually much weaker, depending to a great extent on the size and shape of the polymer chain. Due to these weak intermolecular forces, these chains may act rather independently of one another and are randomly oriented and may be in a highly coiled form.

Many high polymers, however, are partly crystalline, and in such polymers there are regions of different degrees of order, from the completely amorphous to the ordered crystalline. In the crystalline region, the crystallization has resulted in a tying together of random chain ends and an increase in order, and in these regions the forces between neighboring molecules are higher. The low

density polyethylene that has been used in this investigation is partly crystalline, of the order of 40 to 50%, and hence consists of regions of different degrees of order. In such a partly crystalline polymer a valid molecular interpretation of the observed macroscopic behavior under applied forces is made even more difficult. This is especially true since the growth and decay of crystalline regions must be considered, since under the action of forces which tend to orient the molecular chains, such changes are apt to take place.

However, in such polymers some of the observed macroscopic behavior can be explained on a molecular basis. These materials often show both retarded elastic behavior and viscous flow. For small deformations the "instantaneous" elastic behavior can be explained as due to the small changes in valence angles and valence distances, while the retarded elasticity is due to the coiling and uncoiling of the molecular chains. Such behavior is time-dependent but recoverable. Viscous flow is also time-dependent but such deformations are not recoverable and this is due to the slippage of the molecular chains past one another.

There has been a vast amount of research carried out on the study of high polymers in order to determine their viscoelastic behavior. The primary purpose of these investigations has been to predict the stresses or deformations resulting from prescribed displacements or forces applied to the material and to gain some knowledge of the relations between the observed mechanical behavior and the molecular arrangement in order better to understand the mechanical behavior resulting from different molecular mechanisms. Hitherto more success has been achieved in the first aim than in the

latter, and this is especially true for crystalline polymers.

Under applied forces, the response of polyethylene as expected for a viscoelastic material is both time and temperature dependent. The usual viscoelastic phenomena of creep, stress relaxation, delayed recovery, permanent deformation and viscous flow are all observable, their relative importance depending on the temperature and the experimental time scale.

This time and temperature dependence has led quite naturally to the use of a large number of experimental techniques, since to predict the general behavior of a viscoelastic material its response over a wide time and temperature range must be known. For instance, the applied forces might be impact forces whose time of application is in the microsecond range whereas the study of creep may encompass many years.

The most common experimental methods are stress relaxation, creep, and dynamic loading. In stress relaxation an initial strain is imparted to the material, and the stress relaxation function  $\psi(t)$  is measured. In creep, a constant stress is suddenly applied and the observation of the resulting deformation enables one to find the creep function  $\phi(t)$ . There are experimental difficulties involved in both of these procedures and usually the first readings cannot be taken until about 0.1 seconds after loading because of inertia effects in the apparatus. Dynamic experimental techniques include wave propagation and vibrational methods. In wave propagation methods the velocity and attenuation of the wave are measured and these can then be related to the viscoelastic constants. Vibrational methods can be classified as forced oscillation, resonance, and free vibrations.

In these vibrational methods, a time dependent sinusoidal deformation is applied and for small deformations where linear viscoelasticity applies the resulting stress response will also be sinusoidal though not in phase with the strain. Thus if

$$\epsilon(t) = \epsilon_0 \cos(pt)$$

then

$$\sigma(t) = \sigma_0 \cos(pt - \delta)$$

or in complex notation

$$\epsilon(t) = \epsilon_0 e^{ipt}$$

then

$$\sigma(t) = \sigma_0 e^{i(pt + \delta)} = E^* \epsilon(t)$$

where we have the following relations

$$E^* = E_1 + iE_2, \quad E_1 = \frac{\sigma_0}{\epsilon_0} \cos \delta, \quad E_2 = \frac{\sigma_0}{\epsilon_0} \sin \delta, \quad \text{and} \quad \tan \delta = \frac{E_2}{E_1}$$

In a similar manner if the stress is given as

$$\sigma(t) = \sigma_0 e^{ipt}$$

then for a linear viscoelastic material

$$\epsilon(t) = \epsilon_0 e^{i(pt - \delta)} = J^* \sigma(t)$$

where

$$J^* = J_1 - iJ_2 = \frac{1}{E^*}$$

The relevant modulus used will depend on the method of applying the imposed forces, and in this report it will be either Young's modulus  $E^*$  or the shear modulus  $G^*$ . In this notation  $E_1$  is usually referred to as the storage modulus and gives the stress which is in phase with the applied strain, whereas  $E_2$  is referred to as the loss modulus and it gives the stress which is  $90^\circ$  out of phase with the strain. That is  $E_1$  gives the elastic response of the material and  $E_2$  gives the viscous response which is a measure of the internal loss.

In forced oscillation techniques the sample is deformed mechanically, the values of  $\sigma_0$ ,  $\epsilon_0$ , and the phase angle  $\delta$  between stress and strain have to be measured. From these observed quantities the complex modulus can be determined by employing the relationships previously discussed. This method is used at frequencies where the inertia of the specimen and apparatus can be neglected, i.e., for frequencies which are very low compared to the resonant frequency.

At higher frequencies which approach the natural frequency of the specimen and its apparatus, the inertia forces cannot be neglected and either free vibration or resonance methods are used. In the experimental investigations discussed in this report both of these methods were used. Neither the stress amplitude  $\sigma_0$ , strain amplitude  $\epsilon_0$ , or phase angle  $\delta$  between stress and strain are measured directly. In the resonance method a variable frequency oscillator with a constant amplitude is needed to drive the specimen and the resulting pickup is observed on an oscilloscope. By observing the frequency-amplitude curve, the frequency at which the amplitude is a maximum is found, this being the resonant frequency, and from this value  $E_1$  can be calculated. In addition, the frequencies on either side of the resonant frequency at which the amplitude is half of the resonant amplitude are found. From the ratio of the resonant frequency to the difference of the half amplitude frequencies, a value of the relevant loss modulus can be obtained. There are some experimental difficulties involved in this method, due to the electro-mechanical coupling. This can be accounted for by running a series of tests at different field currents and extrapolating the results to a zero field current. Another difficulty is



the fact that the response of the material is being determined over the frequency range encompassing the half-amplitude frequencies rather than at one frequency. That is,  $E_1$  is determined at the resonant frequency but  $E_2$  is not. However, for most polymers the change in  $E_2$  over such a small frequency range is negligible, especially if  $E_2 \ll E_1$ .

In the method of free vibrations, the specimen and its associated mass is set into free vibration and the decay of the vibrations is recorded. The frequency of the vibrations is used to determine the storage modulus and the decay of the vibrations gives a value of the loss modulus. One difficulty presented by this method is that the damped vibrations contain not one, but a whole spectrum of frequencies. However, it can be shown that for small damping where  $\tan \delta \ll 1$ , it can be treated as a vibration at the natural frequency. In the case of polyethylene,  $\tan \delta$  is comparatively small and both of the above methods give reasonably good results.

In both the resonance method and free vibrations neither  $E_1$  nor  $E_2$  is measured directly, but both are related to the quantities measured through the stress-strain relations of the material. The geometry and mass of the specimen and the attached vibrating system must also be considered. In the dynamic tests that have been run, the specimen itself is tubular shaped and a center mass  $M$  is attached to it. Depending on the way in which the vibrations are applied, either the shear modulus  $G^*$  or Youngs modulus  $E^*$  can be determined.

Figures 1 and 2 show the polyethylene specimen and the center mass  $M$ , together with the driving and pickup coils which

were used in this investigation. The details of the experimental techniques will be discussed later but a brief introduction is needed here. By using an oscillator, a sinusoidal current whose frequency can be varied is applied to the driving coils and the specimen is set into vibration. By using the pickup coils, the frequency amplitude curve or the decay curve of the vibrations can be observed on an oscilloscope.

By applying small torsional strains to the sample the relevant modulus will be the shear modulus  $G^* = G_1 + i G_2$ ,  $G_1$  being a measure of the elastic response,  $G_2$  being a measure of the viscous losses and  $\tan \delta = G_2/G_1$  then being an indication of the relative importance of the viscous losses or internal friction.

For the determination of the shear modulus  $G^*$ , the experimental system will consist of the tubular shaped polyethylene specimen which is clamped at both ends to prevent rotational movement, and with a mass  $M$  mounted at the midlength of the sample.

$I$  - mass moment of inertia of the center mass  $M$  with respect to the axis of rotation.

$I_x$  - mass moment of inertia of the polyethylene specimen with respect to the longitudinal axis.

$I_p$  - area moment of inertia of the polyethylene specimen with respect to its longitudinal axis.

$l$  - overall free length of the polyethylene specimen between the clamped ends.

The equation of motion for the specimen itself will be

$$I_x \frac{\partial^2 \theta}{\partial t^2} = \frac{\partial T}{\partial x}$$

where  $T$  is the torque, and from strength of materials, for the

elastic case

$$T = GI_p \frac{\partial \theta}{\partial x}$$

which then gives

$$I_x \frac{\partial^2 \theta}{\partial t^2} = GI_p \frac{\partial^2 \theta}{\partial x^2}$$

or for a tubular specimen

$$\frac{\partial^2 \theta}{\partial t^2} = \frac{G}{\rho} \frac{\partial^2 \theta}{\partial x^2} \quad (1)$$

where  $\rho$  is the density of the material. This can be generalized to the viscoelastic case by assuming a proper stress-strain law.

If

$$\tau = G\gamma + G'\dot{\gamma}$$

then by replacing  $G$  by  $G + G' \frac{\partial}{\partial t}$  in equation (1), we have

$$\frac{\partial^2 \theta}{\partial t^2} = \frac{G}{\rho} \frac{\partial^2 \theta}{\partial x^2} + \frac{G'}{\rho} \frac{\partial^3 \theta}{\partial t \partial x^2} \quad (2)$$

Try a solution by using separation of variables

$$\theta(x,t) = g(x)f(t)$$

and after substituting in equation (2), the following relation is obtained

$$\frac{g''(x)}{g(x)} = \frac{\rho f''(t)}{Gf(t) + G'f'(t)} = -k^2$$

where  $k$  is a constant and this gives us two equations, a space equation in  $x$  and a time equation

$$g''(x) + k^2 g(x) = 0 \quad (3a)$$

$$f''(t) + af'(t) + bf(t) = 0 \quad (3b)$$

where

$$a = \frac{G'k^2}{\rho}, \quad b = \frac{Gk^2}{\rho}$$

The solution of the space equation is the same as that of the elastic case

$$g(x) = A \cos kx + B \sin kx$$

and  $k$  is found from the boundary conditions.

For the case of free vibrations, assume  $f(t)$  has a solution of the following form

$$f(t) = \text{Re}^{-t(\gamma - ip)}$$

By substituting this into equation (3b) we have

$$\gamma^2 - p^2 - 2\gamma pi - \gamma a + pai + b = 0$$

By equating the real and imaginary parts to zero, the following two relations are obtained.

$$\gamma = \frac{a}{2}$$

$$p^2 = b - \frac{a^2}{4}$$

which then gives us  $\gamma$  and  $p$ , where  $\gamma$  is related to the decay of the vibrations and  $p$  is the angular frequency.

By taking the derivative of  $f(t)$  with respect to  $t$  and setting it equal to zero, we have the time period for successive maxima or minima and this is found to be

$$\Delta T = -\frac{2\pi}{p}$$

The amplitude is reduced by  $e^{-\gamma t}$  in time  $t$  and hence in one  $\frac{2\pi\gamma}{p}$  period of the oscillations it will be reduced by the factor  $e^{\frac{2\pi\gamma}{p}}$

By defining  $\Delta'$  to be the natural logarithm of the ratio of successive maxima or minima, we have

$$\Delta' = \ln \frac{\theta_n}{\theta_{n+1}} = \frac{2\pi\gamma}{p}$$

The value of  $k$  must be determined from the boundary conditions which are as follows, at the clamped end  $x = 0$ , there is no rotation

$$\theta(0, t) = 0, \quad \text{for all } t$$

and at the midlength of the specimen,  $x = \frac{\ell}{2}$ , the torque is due to the mass moment of inertia of the center mass  $M$ , giving the relation

$$I_p \left( G + G' \frac{\partial}{\partial t} \right) \frac{\partial \theta}{\partial x} \bigg|_{x=\frac{\ell}{2}} = -\frac{I}{2} \frac{\partial^2 \theta}{\partial t^2} \bigg|_{x=\frac{\ell}{2}}$$

and these result in the following frequency equation

$$Z \tan Z = \frac{I_x}{I}$$

where  $Z = \frac{k\ell}{2}$  and when the ratio of the mass moment of inertia of the specimen to that of the center mass is known  $k$  can then be found. In order to agree with the notation used for the complex moduli, i.e.,  $G^* = G_1 + iG_2$ , let  $G = G_1$  and  $G' = \frac{G_2}{p}$ .

The following relations have been obtained previously

$$p^2 = b - a^2/4 \quad (4a)$$

$$\gamma = a/2 \quad (4b)$$

$$\Delta' = \frac{2\pi\gamma}{p} \quad (4c)$$

$$\text{where } a = \frac{G_2 k^2}{\rho p}, \quad b = \frac{G_1 k^2}{\rho}$$

By substitution these can be written as

$$G_1 = \frac{\pi^2 p^2 \ell I_x}{Z^2 I_p} \left( 1 + \frac{\Delta'^2}{4\pi^2} \right)$$

$$\tan \delta = \frac{G_2}{G_1} = \frac{\Delta'/\pi}{(1 + \Delta'^2/4\pi^2)}$$

or for small damping

$$G_1 = \frac{\pi^2 p^2 l I_x}{Z^2 I_p} \quad (5)$$

$$\tan \delta = \frac{G_2}{G_1} = \frac{\Delta'}{\pi} \quad (6)$$

Now in this solution, it was assumed that the time function was of the form  $f(t) = \text{Re}^{-t(\gamma - ip)}$  where there is only one frequency component  $p$ . In reality there would be a whole spectrum of frequencies  $p$  but as mentioned earlier, for small values of  $\Delta'$  the assumption of a single frequency will not result in serious errors.

For the case of resonance, assume that the applied torque at the center mass  $M$  is of the form

$$T = T_0 e^{i\omega t}$$

and that  $f(t)$  has a solution of the following form

$$f(t) = T_0 f(\omega) e^{i(\omega t - \alpha)}$$

substitute this into

$$f''(t) + af'(t) + bf(t) = T_0 e^{i\omega t}$$

By equating the real and imaginary parts, we find

$$\tan \alpha = \frac{a\omega}{b - \omega^2}$$

and

$$f(\omega) = \frac{1}{\sqrt{(b - \omega^2)^2 + a^2 \omega^2}}$$

The value of  $\omega$  at resonance will be that value of  $\omega$  for which  $f(\omega)$  is a maximum and this can be found by taking the derivative of  $[(b - \omega^2)^2 + a^2 \omega^2]$  with respect to  $\omega$  and setting it equal to zero.

This then gives us for the value of the resonant frequency  $\omega_r$ ,

$$\omega_r^2 = b - \frac{a^2}{2} \quad (7)$$

and

$$\text{maximum } f(\omega) = \frac{1}{ap}$$

In order to find the values of  $\omega$  for which the amplitude is half the resonant amplitude, set

$$f(\omega) = \frac{1}{2ap}$$

hence

$$\sqrt{(b-\omega^2)^2 + a^2\omega^2} = 2ap$$

which gives us a quadratic equation in  $\omega^2$

$$(\omega^2)^2 + (a^2 - 2b)\omega^2 + b^2 - 4a^2p^2 = 0$$

The two roots, which will be denoted by  $\omega_1^2$  and  $\omega_2^2$  are

$$\omega_1^2, \omega_2^2 = (b - \frac{a^2}{2}) \pm \sqrt{3} ap$$

and

$$\omega_1^2 - \omega_2^2 = 2\sqrt{3} ap \quad (8)$$

Now the half-breadth of the resonance peak is defined as

$$\frac{\Delta\omega}{\omega_r} = \frac{\omega_1 - \omega_2}{\omega_r}$$

and for the case of small damping, this can be written as

$$\frac{\Delta\omega}{\omega_r} \approx \frac{\omega_1 - \omega_2}{p} \approx \frac{\omega_1^2 - \omega_2^2}{2p^2}$$

and from equations (4) and (8) we have

$$\frac{\Delta\omega}{\omega_r} = \sqrt{3} \frac{\Delta'}{\pi} = \sqrt{3} \tan \delta$$

In addition, for small damping, by using equations (4), equation (7) can be written as

$$G_1 = \frac{\pi^2 \omega_r^2 \ell I_x}{Z^2 I_p}$$

where  $Z$  is determined from the frequency equation

$$Z \tan Z = \frac{I_x}{I}$$

By applying small longitudinal vibrations to the specimen, the relevant modulus will be Young's modulus  $E^* = E_1 + iE_2$ , where  $E_1$  is a measure of the elastic response and  $E_2$  is a measure of the viscous losses. The governing equation for longitudinal vibrations will be of the same form as for torsional vibrations, i.e.,

$$\frac{\partial^2 u}{\partial t^2} = \frac{E}{\rho} \frac{\partial^2 u}{\partial x^2} + \frac{E'}{\rho} \frac{\partial^3 u}{\partial t \partial x^2}$$

and the solution for either resonance or free vibration will also be of a similar form. For free vibration with small damping we have

$$\tan \delta = \frac{E_2}{E_1} = \frac{\Delta'}{\pi}$$

$$E_1 = \frac{\pi^2 p^2 \ell m}{Z^2 A}$$

where  $m$  is the mass of the specimen, and  $A$  is the cross-sectional area. The value of  $Z$  is found from the following frequency equation

$$Z \tan Z = \frac{m}{M}$$



For resonance we have the following,

$$\tan \delta = \frac{E_2}{E_1} = \frac{1}{\sqrt{3}} \frac{\Delta \omega}{\omega_r}$$

and

$$E_1 = \frac{\pi^2 \omega_r^2 \ell m}{Z^2 A}$$

In order to determine the complex Young's modulus from flexural vibrations, the experimental setup can be classified as a fixed-fixed beam with an attached mass  $M$  at the middle of the specimen. Assuming a stress-strain law of the form  $\sigma = E\epsilon + E'\dot{\epsilon}$  the equation of motion for the lateral vibration of a beam is

$$EI_z \frac{\partial^4 y}{\partial x^4} + E'I_z \frac{\partial^5 y}{\partial t \partial x^4} + \frac{m}{\ell} \frac{\partial^2 y}{\partial t^2} = 0$$

where  $I_z$  is the area moment of inertia of the cross section. By assuming a solution by separation of variables of the form

$$y(x,t) = g(x)f(t)$$

the following relation is obtained

$$\frac{g''''(x)}{g(x)} = \frac{-mf''(t)}{EI_z \ell f(t) + E'I_z \ell f'(t)} = k^4$$

which gives us two equations, a space equation in  $x$  and a time equation

$$g''''(x) - k^4 g(x) = 0$$

$$f''(t) + af(t) + bf'(t) = 0$$

where

$$a = \frac{E'I_z \ell k^4}{m} \quad b = \frac{EI_z \ell k^4}{m}$$

The solution for the space equation will be the same as for the elastic case

$$g(x) = A(\cos kx + \cosh kx) + B(\cos kx - \cosh kx) \\ + C(\sin kx + \sinh kx) + D(\sin kx - \sinh kx)$$

where  $k$  is determined from the boundary conditions.

For free vibrations, assume a solution of the following form

$$f(t) = \text{Re}^{-t(\gamma - ip)}$$

which is the same as that used in the previous cases, and in a similar manner leads to

$$E_1 = \frac{m p^2}{I_z k^4} \left(1 + \frac{\Delta'^2}{4\pi^2}\right) \\ \tan \delta = \frac{E_2}{E_1} = \frac{\frac{\Delta'}{\pi}}{1 + \frac{\Delta'^2}{4\pi^2}}$$

The boundary conditions are as follows, at  $x = 0$ , both  $y$  and  $\frac{\partial y}{\partial x}$  are zero, which gives us  $A = C$  and hence

$$g(x) = B(\cos kx - \cosh kx) + D(\sin kx - \sinh kx)$$

At  $x = \frac{l}{2}$ , the slope  $\frac{\partial y}{\partial x} = 0$  which gives

$$\frac{B}{D} = \frac{\cos \frac{kl}{2} - \cosh \frac{kl}{2}}{\sin \frac{kl}{2} + \sinh \frac{kl}{2}}$$

the second condition at  $x = \frac{l}{2}$  is that the shearing force results from the inertia of the center mass  $M$ ,

$$EI_z \frac{\partial^3 y}{\partial x^3} + E'I_z \frac{\partial^4 y}{\partial t \partial x^3} = M \frac{\partial^2 y}{\partial t^2}$$

This gives another relation for  $\frac{B}{D}$ . By equating the two equations

the following frequency equation is determined

$$\frac{\sin Z \cosh Z + \cos Z \sinh Z}{1 - \cos Z \cosh Z} = \frac{M_z}{m}$$

where

$$Z = k \frac{\ell}{2}$$

By substituting for  $k$ , and assuming small damping, the following relations are obtained

$$E_1 = \frac{\pi^2 m p^2 \ell^3}{4 Z^4 I_z} \quad (9a)$$

$$\tan \delta = \frac{E_2}{E_1} = \frac{\Delta'}{\pi} \quad (9b)$$

where, as before, it is assumed that due to the damping being small the use of only one frequency component instead of a spectrum of such frequencies will not be greatly in error. For resonance, the derivation is similar to the previous cases and with the assumption of small damping leads to

$$E_1 = \frac{\pi^2 m \omega_r^2 \ell^3}{4 Z^4 I_z} \quad (10)$$

$$\tan \delta = \frac{E_2}{E_1} = \frac{1}{\sqrt{3}} \frac{\Delta \omega}{\omega_r}$$

However, in obtaining the relation between the complex Young's modulus  $E^*$  and the observed quantities, any longitudinal tension present in the beam must be taken into consideration. For the elastic beam with axial tension  $T$  the equation of motion is

$$EI_z \frac{\partial^4 y}{\partial x^4} - T \frac{\partial^2 y}{\partial x^2} = -m \frac{\partial^2 y}{\partial t^2}$$

and by substituting a solution of the form

$$y(x,t) = g(x)f(t)$$

the following two relations are obtained

$$f''(t) + pf(t) = 0$$

$$EI_z g''''(x) - Tg''(x) = p^2 \frac{m}{\ell} g(x) \quad (11)$$

The solution for  $g(x)$  is

$$g(x) = A \cosh 2\gamma x + B \sinh 2\gamma x + C \sin 2\delta x + D \cos 2\delta x$$

where

$$\begin{aligned} 4\gamma^2 &= \alpha^2 + \sqrt{\alpha^4 + \beta^4} \\ 4\delta^2 &= \alpha^2 - \sqrt{\alpha^4 + \beta^4} \\ \alpha^2 &= \frac{T}{2EI_z} \quad \beta^4 = \frac{mp^2}{EI_z \ell} \end{aligned}$$

The only end conditions which will give us an analytic solution is a simply supported beam. For a fixed-fixed beam an approximate solution can be obtained if we assume that the tension is the more important restoring force, i.e., assuming  $T \gg 4\pi^2 EI_z$  but this is not true for our case even if we had these end conditions. For the end conditions which we have, the resulting frequency equation is much more complicated and it is doubtful whether any approximation could be made.

However, if we multiply both sides of equation (11) by  $g(x)$  and integrate twice by parts between  $x = 0$  and  $x = \frac{\ell}{2}$  we have

$$p^2 = \frac{\frac{EI_z \ell}{m} \int_0^{\frac{\ell}{2}} g''(x)^2 dx + \frac{T\ell}{m} \int_0^{\frac{\ell}{2}} g'(x)^2 dx}{\int_0^{\frac{\ell}{2}} g(x)^2 dx + \frac{\ell M}{m} g(\frac{\ell}{2})} \quad (12)$$

where the boundary conditions discussed previously have been used.

Rayleighs principle states that if we put in an assumed value for  $g(x)$  the resulting frequency will be too high. Let us put into equation (12) the solution of the beam equation when there is no tension present and denote the frequency obtained by  $p_1^2$  and this is found to be

$$p_1^2 = \frac{4EI_z Z^4}{\pi^2 m l^3} + 0.102 \frac{T Z^2}{\pi^2 m l}$$

If only flexural rigidity were present we would have

$$p_s^2 = \frac{4EI_z Z^4}{\pi^2 m l^3}$$

and if we considered a string of mass  $m$  with a concentrated mass  $M$  at the midlength, the relation would be

$$p_t^2 = \frac{Q^2 T}{\pi^2 m l}$$

where  $Q$  is found from the frequency equation

$$Q \tan Q = \frac{m}{M}$$

Let  $g(x)$  be the correct solution for equation (12). If we put this solution into the energy relation for the beam without an axial load and denote the frequency obtained by  $\bar{p}_s^2$ , by Rayleighs principle we have

$$p_s^2 \leq \bar{p}_s^2$$

and if we put  $g(x)$  into the energy equation for the vibrating string and denote this frequency by  $\bar{p}_t^2$  we again have

$$p_t^2 \leq \bar{p}_t^2$$

Now equation (12) can be written as

$$p^2 = \frac{\frac{EI_z \ell}{m} \int_0^{\frac{\ell}{2}} g''(x)^2 dx}{\int_0^{\frac{\ell}{2}} g(x)^2 dx + \frac{\ell M}{m} g(\frac{\ell}{2})} + \frac{\frac{T \ell}{m} \int_0^{\frac{\ell}{2}} g'(x)^2 dx}{\int_0^{\frac{\ell}{2}} g(x)^2 dx + \frac{\ell M}{m} g(\frac{\ell}{2})} = \bar{p}_s^2 + \bar{p}_t^2$$

Hence we have

$$p_s^2 + p_t^2 \leq p^2 \leq p_1^2$$

or

$$\frac{4EI_z Z^4}{\pi^2 m \ell^3} + \frac{Q^2 T}{\pi^2 m \ell} \leq p^2 \leq \frac{4EI_z Z^4}{\pi^2 m \ell^3} + 0.102 \frac{T Z^2}{\pi^2 m \ell} \quad (13)$$

and this together with experimental observations of the change in frequency due to applying a tension load will enable us to make reasonable corrections on the observed values of  $E^*$  obtained from flexural vibration in the presence of a tension load.

## II. Experimental Equipment

In this section the equipment used in the experimental investigation will be described.

### (A) The material and its preparation.

The polyethylene that was used in this investigation was obtained from the Monsanto Chemical Company, which kindly supplied us with 30 feet of the material. It was a tubular shaped, low density polyethylene with a specific gravity of 0.92. The nominal O.D. was 1/2 inch and the nominal I.D. was 3/8 inch. All of the polyethylene that was used in this test program came from the same mix in order to avoid as much as possible any variation in the material properties from one test specimen to another, due to the manufacturing process.

In order to remove any residual strains and leave the sample in a stress free state, the specimen had to be annealed. Since the polyethylene was supplied in a coiled form it was found that an annealing temperature of 100° Centigrade was necessary. The individual specimens which were approximately  $9\frac{1}{4}$  inches in length were thus put in an oven at 100° Centigrade for 24 hours and were then found to be quite straight.

The trueness of a specimen was determined by measuring the inside and outside diameters at a number of points along its length. The variation in the inside diameter was found to be within two thousandths, e.g., from 0.374 to 0.376 inches for a typical specimen. The variation in the outside diameter was found to be much greater, some specimens showing a variation of over ten thousandths. However, in all the specimens actually used in the test program, the variation of the outside diameter was kept to within two

thousandths, e.g., for a typical specimen from 0.494 to 0.496 inches. Since the material supplied to us was a commercial product for general customer use this variation was unavoidable and no attempt at remolding was made.

(B) Description of the testing machine.

In order to carry out the series of tests that was contemplated it was decided to design and construct a test machine on which the tubular specimen together with its center mass could be mounted and the desired loading program carried out without removing the specimen or the center mass. That is, a machine where the specimen could be mounted, together with the center mass M, and a combination of creep in torsion or tension, followed by either stress relaxation or recovery.

The machine so constructed is shown in Figure 1 and an explanation of the various parts follows. The ends of the specimen are mounted as shown at A and B with U shaped clamps. The position of A is fixed with respect to its vertical position while the other end of the specimen at B is attached to the movable testing head. The movable testing head can move in the vertical direction along the guide rods shown. Through a pulley and cable system loads can be transmitted to the movable testing head, via the brake rod C, in order to run a creep test in tension. At any stage of the creep test the strain can be kept constant by applying the brake, shown at D, and the decay of stress with time can then be measured with the load cell shown at E. Alternatively, as a certain strain in creep is reached the tension load can be removed and the specimen allowed to recover under zero load, since the



weight of the testing head and load cell has been counterbalanced. The initial length of the specimen is about  $9\frac{1}{4}$  inches, with  $1\frac{1}{2}$  inches being clamped at both ends. This leaves the initial free length to be about  $6\frac{1}{4}$  inches and a maximum longitudinal strain of 150% can be achieved with this arrangement.

While the lower end of the sample which is clamped at A is prevented from moving in a vertical direction, it can rotate about its center on a shaft which is connected to the lower pulley marked F. Torsional creep tests can then be run by applying loads to this pulley and with a brake arrangement similar to the one previously described the torsional strain can be kept constant for relaxation tests, or the load can be removed and torsional recovery allowed. This allows unlimited torsional strain, i.e., up to the point at which the specimen buckles.

At G is shown the movable magnet holder which can move along the guide rods as the specimen is stretched in tension and thus keep the magnets in alignment with the coils of the center mass. This part actually consists of two rings, the outer one which can move along the guide rods as just explained and the inner ring which can rotate and keep the magnets and coils aligned during torsional creep.

In order to reduce frictional forces to as small a value as possible, high quality bearings were used where needed such as on the movable head B, on the torsional pulley F, as well as on the other pulleys through which the loads were applied. The frictional forces were thus kept to less than 1% of the loads actually used in the experiment.

Except for the guide rods and bearings the machine was made

from a high grade of structural aluminium. This was done mainly in order to keep spurious magnetic effects at a minimum.

The machine was constructed in such a manner as to be used in either a vertical or horizontal position, but for the tests discussed in this report, it was used only in the vertical position. Due to the added weight of the center mass which was much greater than that of the sample, the specimen would bend during the recovery tests if the horizontal position was used, and for this reason it was used only in the vertical position.

(C) Added center mass M.

As discussed earlier, the small oscillatory strains from which the relevant dynamic data is gathered are applied to the sample through the center mass M with the four coils as shown in Figure 2. In order to avoid any difficulties due to slippage between the center mass M and the polyethylene specimen the bond between the two would have to be reasonably constant and this proved to be a problem due to the large changes in the geometry of the sample during the loading program. During the longitudinal creep test, the outside diameter would change from about 0.500 inch to 0.320 inch at 145% strain. However, by inserting an aluminum core at the midlength of the specimen, the overall change in the outside diameter at this point could be kept to about 40 thousandths and this variation could more easily be dealt with.

For this reason, the circular center mass M which was made from aluminum was bored out to a diameter of 0.475 inches and then cut in two lengthwise. Two coiled extension springs of  $\frac{1}{8}$  inch O.D., length of  $1\frac{7}{8}$  inches, and wire diameter of 0.016 inches were

then used to keep the mass M fixed to the sample and it is believed that this worked very well as there was no indication of any slippage between the specimen and center mass. The outside diameter of the aluminum mass was 1 inch and its length was 1 inch.

The four coils are positioned on the center mass at ninety degree intervals. Two of the coils are the driving coils, which were made by winding seven layers of #28 gage wire on an aluminum core,  $\frac{1}{4}$  inch in diameter and 1 inch in length. The other two coils are the pickup coils which were also made on an aluminum core by winding on nine layers of #38 gage wire. Both driving coils were collinear as well as both pickup coils. The lead wires from all four coils to the power and recording equipment were made of #38 gage wire. In order to apply longitudinal vibrations to the specimen, iron cores were substituted for the aluminum ones. This created some problems due to the four coils being so close together and attempts to shield the coils were not very successful.

(D) Recording the changing geometry of the specimen.

The relevant geometrical data that had to be recorded for the determination of the dynamic moduli included the strain, overall length of the sample, and the diameter. These had to be determined at each strain level with a high degree of accuracy. At first, the direct reading of these measurements with a Garret microscope and micrometer was tried. This, however, necessitated stopping the test for a matter of minutes, while the data was being taken. For this reason, it was decided to try to take a photograph of the sample, and then take the measurements off the photograph after the test had been run. For this purpose, an Exacter

camera was tried. After experimenting with the camera, it was found that the most reliable measurements could be obtained by using a telephoto lens and taking measurements off the negative.

In Figure 3a is shown a picture of the specimen at zero strain and in Figure 3b the same specimen after it had been strained to 143.5% in the longitudinal direction. The marker shown in the photograph was used as a reference length. In order to measure the longitudinal strain, two ink dots were applied to the specimen between the center mass M and the clamped end. These dots were initially about 1 inch apart. The strain was then determined from the change in distance between these dots. The distance between the dots and the outside diameter of the specimen were then measured from the negative by the use of the Garret microscope and micrometer. Though these measurements were not quite as accurate as the direct measurements, the saving in time more than offset this. The degree of accuracy was found by taking direct measurements of a sample with the microscope, and comparing these to values taken off of a negative of the same sample. It was found, that the strain and the outside diameter were within 1%, using the direct readings as the true readings.

Before the specimen was mounted, the diameter and distance between the dots were measured. After the specimen was mounted, the initial negative that was taken should give us the same readings unless the specimen was deformed while mounting the specimen on the test machine. It was found that very little distortion occurred except very near to the clamp. In addition, the overall length of the specimen was recorded when needed from a rule which is shown at H in Figure 1. These readings were taken to within

$\frac{1}{64}$  of an inch. During torsional creep, the angle through which one end of the test specimen was rotated was found by reading the vernier dial shown at I in Figure 1. This could be read to a tenth of a degree which was more than accurate enough for our purposes.

(E) Constant temperature chamber.

As is well known, the dynamic moduli of polymers are temperature dependent and during each test the temperature would have to be kept reasonably constant. For this reason, the tests were carried out with the testing machine in a constant temperature chamber. This consisted of a small storage room in a corner of the laboratory which was then thermally insulated. It was found that the temperature in the room could be kept to within  $1/2^{\circ}$  Centigrade in the range from 24 to 74 degrees. For most of the tests reported on in this report, the test temperature was  $25^{\circ}$  Centigrade. The temperature was brought up to this level by using a rheostat connected to light bulbs placed in the room. For higher temperatures, heating coils were used and connected to a 220 volt Variac and with this arrangement a maximum temperature of  $74^{\circ}$  Centigrade could be achieved. The temperature was checked by having a number of thermocouples placed in different positions around the chamber and reading them on a potentiometer. A small window was made in one wall through which pictures of the sample could be taken as the camera was outside. However, the light source for the camera was in the chamber and since this was triggered each time a picture was taken, led to an increase of temperature. This was, however, kept to a minimum and for the duration of a test a temperature increase

of no more than one half of a degree Centigrade usually occurred.

(F) Electrical circuit and equipment.

A schematic diagram of the electrical circuit is shown in Figure 4. The function generator puts out a sinusoidal wave, the frequency of which can be varied. This was sent on to a 30 watt amplifier and then on to the two driving coils which are connected to the center mass. Depending upon the type and position of the magnets, the sample will then be forced into either lateral, longitudinal or torsional oscillations. The other two magnets and coils constitute the pickup network which feeds the signal to the oscilloscope where the decay curve of the vibrations or the resonant frequency and half-breadth of the frequency-amplitude curve can be observed. The triggering circuit shown is to trigger the oscilloscope in order to pick up the decay curve with a polaroid camera. Also shown is the decade counter which was used to determine the frequency of the oscillatory strain.

### III. Discussion of the Experimental Results and Conclusions.

In this section, the experimental results on the behavior of the dynamic tangent moduli in shear  $G^*$  and  $E^*$  in both flexure and extension will be discussed. The values of the moduli are obtained as a function of large quasi-static strains in either the longitudinal or torsional direction.

All of these tests have been carried out at a standard temperature of  $25^{\circ}$  Centigrade. However, the temperature dependence of both the shear modulus  $G^*$  and Youngs modulus  $E^*$  have been investigated for specimens under conditions of zero strain. In addition, the effect of the amplitude of the imposed sinusoidal oscillations on the moduli has been determined. These effects will be discussed in more detail in subsequent sections.

#### (A) Determination of the dynamic shear modulus $G^*$ .

In this series of tests the observed behavior of both the storage and loss moduli in shear are obtained by superimposing small torsional oscillations on the specimen. The shear modulus  $G^*$  is determined in this way under longitudinal creep followed by recovery or relaxation, and in addition under torsional creep followed by recovery or relaxation. The effect of a static torsional strain upon the behavior of  $G^*$  in longitudinal creep, and the effect of a static longitudinal strain on  $G^*$  in torsional creep are also determined.

The effect on the shear modulus of the amplitude of the sinusoidal oscillations was determined by observing the variation in the natural frequency or resonant frequency with change in amplitude. It was found that the frequency showed a slight de-

crease with increasing amplitude and since  $G_1$  is proportional to the square of the frequency, this led to a decrease in  $G_1$  with increasing amplitude. By observing the decay curve of the vibrations or the half-breadth of the frequency-amplitude curve it was found that  $\tan \delta$  showed a small increase with increasing amplitude. These effects were very small and since the amplitude of the sinusoidal vibrations was kept constant during the tests, these effects did not have to be considered.

The temperature dependence of the shear modulus was also determined, and as expected the temperature effects were much more significant. The dependence of the shear modulus on temperature is shown in Figure 5 for a specimen in the unstrained state. The value of  $\tan \delta$  as may be seen from Figure 5 shows a gradual increase in magnitude over the temperature range used. The observed points were determined from the decay curve of the vibrations by the relation

$$\tan \delta = \frac{\Delta'}{\pi}$$

and the value of  $\tan \delta$  was found to increase from 0.1020 at  $24^\circ$  to 0.1630 at  $74^\circ$  Centigrade. The values of the natural frequency  $p$  were also obtained from the decay curve of the vibrations. The equation for the determination of  $G_1$  is

$$G_1 = \frac{\pi^2 p^2 l I_x}{Z^2 I_p}$$

where in these tests  $p$  is the only variable, and the values of  $G_1$  determined by this relation are also shown in Figure 5. The value of  $G_1$  shows a continuous decrease from  $2.69 \times 10^9$  to  $0.45 \times 10^9$  dynes/cm<sup>2</sup> over the range of  $24^\circ$  to  $74^\circ$  Centigrade.



### Longitudinal creep and recovery.

The first series of tests that will be discussed is the behavior of the dynamic shear modulus  $G^*$  of the polyethylene specimen as it undergoes creep in the longitudinal direction under the influence of an applied tension load, followed by recovery upon removal of the load.

When a load is applied to the specimen via the pulley arrangement, which was discussed previously, the specimen is strained in the longitudinal direction, the strain increasing with time. At various intervals of creep, small torsional oscillations are superimposed on the specimen and either the natural frequency  $p$  or the resonant frequency  $\omega_r$  together with the loss modulus are obtained. In addition, at each of these intervals the overall length of the specimen is recorded and a photograph of the sample is taken.

After a certain strain is reached, the creep test is terminated and the tension load on the specimen is removed. This allows the specimen to recover in the longitudinal direction. At various intervals of the recovery strain, the torsional oscillations are again superimposed on the sample, the value of the overall length is recorded and a photograph taken and this gives us similar information to that obtained during the creep phase of the test.

The maximum strain that is reached during creep depends upon the tension load that is applied. For the specimens discussed in this section, the tension load varied from  $2.7 \times 10^7$  to  $4.6 \times 10^7$  dynes, giving an initial engineering stress of  $5.2 \times 10^7$  to  $8.8 \times 10^7$

dynes/cm<sup>2</sup>. In Figure 6, are shown the variations of the creep strain  $\epsilon_x$  in the longitudinal direction versus the time of creep for three specimens. The creep test is terminated when the change of strain with time becomes small as there is no appreciable viscous flow at this stage. After removal of the tension load, due to the large strains which had been achieved, the specimens did not show complete recovery. The amount of permanent strain remaining in the specimen was dependent upon the maximum creep that the specimen was subjected to. In Figure 7, are shown the recovery curves for the three specimens that were tested. When the rate of recovery became very small, the temperature in the test chamber was increased and this resulted in significant additional recovery for some specimens. The temperature was increased from the test temperature of 25° to a maximum of 74° Centigrade. No data were taken at the higher temperatures but as additional recovery occurred the temperature was reduced back down to the test temperature and the data were then taken. One additional remark about these creep and recovery curves is needed at this time. At the various intervals of strain at which the data were recorded, the creep or recovery was stopped for the period of time needed to collect this data. This time interval was usually of the order of one minute.

The equation for the determination of  $G_1$  is given by

$$G_1 = \frac{\pi^2 p^2 \ell I_x}{Z^2 I_p}$$

where

$$Z \tan Z = \frac{I_x}{I}$$

and the value of  $Z$  will change with longitudinal strain. For values of  $I_x \ll I$ , the frequency equation can be written as

$$Z \tan Z \approx Z^2 \approx \frac{I_x}{I}$$

and by substituting this into the equation for  $G_1$  we have

$$G_1 = \frac{\pi^2 p^2 \ell I}{I_p}$$

For the specimens and center mass that are used in this experimental investigation,  $\frac{I_x}{I}$  is about 0.007. From the negatives of the photographs taken at the various strain intervals, the outside diameter and strain of the specimen are determined, as explained in the previous section. In order to determine  $G_1$ , the storage component of the complex shear modulus  $G^*$ , the following variables must be known as a function of the longitudinal strain, the value of  $\ell$  which is the overall length of the specimen, the value of  $I_p$  which is the area moment of inertia of the specimen, and the value of either the natural frequency  $p$  or the resonant frequency  $\omega_r$ . The value of  $I_p$  for a tubular specimen is given as

$$I_p = \frac{\pi}{32} (d_o^4 - d_i^4)$$

$d_o$  being the outside diameter and  $d_i$  being the inside diameter.

By expressing the inside diameter as  $d_i = \frac{\bar{d}_i}{\bar{d}_o} d_o$ , where the bar means the values at zero strain,  $I_p$  can then be expressed in terms of the outside diameter.

For the discrete strain intervals at which the data were recorded, the values of  $\ell$ ,  $d_o$ , and either  $p$  or  $\omega_r$  are then known. These values can then be plotted versus the strain and continuous

curves which best fit these observed quantities are then drawn on the graphs.

The values of the natural frequency  $p$  raised to the second power for specimen No. 3 are shown in Figure 8 for both creep and recovery together with a best fit curve, this curve being determined visually. The dashed portion of the recovery curve is for the values of  $p$  which were determined after the temperature had been increased to facilitate recovery and the values seem to be questionable. In Figure 8 are also shown the values of the natural frequency  $p$  that were calculated by assuming the storage modulus  $G_1$  remained constant with respect to strain, and this will be discussed later. The curves of the natural frequency  $p$  for the other specimens are similar. In order to determine the variation of the storage component of the shear modulus  $G^*$ , values for  $\ell$ ,  $I_p$ , and  $p$  are determined from the best fit curves on the appropriate graphs. These values are taken at certain intervals of strain, i.e., every 10% and are then used in the relation

$$G_1 = \frac{\pi^2 p^2 \ell I}{I_p}$$

and the values of  $G_1$  obtained in this manner are shown in Figures 9, 10, and 11 for specimens No. 1, 2, and 3.

The reason for using the "smoothed values" of  $\ell$ ,  $I_p$ , and  $p$  in the equation for  $G_1$  instead of the observed values, was to reduce the amount of scatter that would have occurred in plotting the value of  $G_1$ . The overall change in the value of  $G_1$  is very small compared to the overall changes in  $\ell$ ,  $I_p$ , and  $p$ . Since  $G_1$  is proportional to the product of  $\frac{\ell}{I_p}$  and  $p^2$ , let us take a look at how they change with longitudinal strain. For specimen No. 3

which had a maximum creep strain of 143.5%, the ratio of  $\frac{\ell}{I_p}$  increased by a factor of about 14 while at the same time the value of  $p^2$  was decreasing by almost the same amount. Since the two quantities,  $\frac{\ell}{I_p}$  and  $p^2$ , are experimentally measured, the error in the product of the two will be much greater than their separate errors, especially since the values of the two factors are changing in opposite directions, i.e., one increasing, and one decreasing with strain.

In Figure 12 are shown the values of  $p^2$  during the creep phase of the tests for specimens No. 1, 2, and 3, and in Figure 13 are the smoothed values of  $\frac{\ell}{I_p}$  for the same specimens. Though the difference among the values of  $p^2$  or  $\frac{\ell}{I_p}$  between the different specimens are small compared to the overall changes in  $p^2$  or  $\frac{\ell}{I_p}$ , the values of  $G_1$  for the three specimens show significant differences, these differences being as large as the overall changes in  $G_1$  for any one specimen during creep.

At this time all that can be said about the variation of  $G_1$  with respect to longitudinal strain is that for all three specimens the value of  $G_1$  shows an initial decrease with increasing strain up to a value of 20 to 30%, and then tends to level off before starting to increase slowly in value with larger strains. For specimen No. 3, the value of  $G_1$  seems to remain constant for about an interval of 80% strain before starting to increase while the other two specimens seem to show an increase starting much sooner.

That there is definitely a decrease in the value of  $G_1$  as the specimens are strained in the longitudinal direction can be seen from Figure 8. In addition to the experimentally observed values of the natural frequency  $p$  for specimen No. 3, are the

values of the frequency calculated by assuming that  $G_1$  remains constant. The value of  $G_1$  at zero strain is  $2.68 \times 10^9$  dynes/cm<sup>2</sup> and if we write

$$p^2 = \frac{2.68 \times 10^9 I}{\pi^2 \ell I} p$$

the variation in the value of  $p$  can then be found. From Figure 8 it can be seen that there is an initial decrease in  $G_1$  and that at larger longitudinal strains  $G_1$  starts to increase, approaching its value at zero strain.

The behavior of  $G_1$  during recovery for all three specimens show similar behavior. Upon removal of the tension load the value of  $G_1$  tends to decrease at first, this decrease being larger for the specimens which had been strained more, and then upon greater recovery it starts to increase. This led to a larger value of  $G_1$  compared to the corresponding creep value when recovery was completed at the test temperature. As mentioned earlier, the temperature was then raised in order to achieve more recovery, and though these values are questionable it appears that  $G_1$  is approaching its initial stress free value. At the maximum recovery that was achieved for the three specimens, the final value of  $G_1$  for both specimen No. 2 and 3 was higher while that of specimen No. 1 was lower than the corresponding creep value.

For the three specimens used in this phase of the test program, there does not appear to be any correlation between the values of  $G_1$  and the tension load used, nor to the rate of straining. The values of  $G_1$ , depend only upon the value of the strain in the specimen, though this dependence is different for creep then

for recovery. The difference between the value of  $G_1$  during recovery compared to its value in creep seems to be dependent upon the maximum strain achieved. The initial decrease in  $G_1$  on recovery being greater for specimen No. 3 than for the other two specimens.

The values of  $\tan \delta$  were obtained from the decay curve of the vibrations by the following relation

$$\tan \delta = \frac{\Delta'}{\pi}$$

and for all three specimens showed similar behavior. The values of  $\tan \delta$  for specimen No. 3 are shown in Figure 14 for both creep and recovery. The value of  $\tan \delta$  showed an initial increase with longitudinal strain though the rate of increase becomes smaller with increasing strain and then appears to be approaching a constant value. During the recovery, the value of  $\tan \delta$  shows an initial increase but then tends to decrease and at the end of recovery the value is lower than the corresponding creep value. The values of  $\tan \delta$  obtained after the test temperature was increased in order to induce greater recovery also fall below the corresponding creep values of  $\tan \delta$ . The initial increase in  $\tan \delta$  at the start of recovery appears to be greater for the specimens which had been strained more during creep.

By using the resonance method, comparable values of  $\tan \delta$  and  $G_1$  were also obtained, the value of  $G_1$  being slightly higher. However, in plotting  $\omega_r^2$  versus  $\epsilon_x$  there was more scatter about the best fit curve and for this reason the moduli discussed herein were found by using the free vibration data.

For specimens No. 4 and 5, quasi-static torsional strains of 8 and 14% respectively were applied to the specimens and a suitable time was allowed to elapse before longitudinal creep tests were started. These tests were run in order to determine if a static torsional strain had any effect on the behavior of  $G^*$  during longitudinal creep. Both of these specimens showed similar behavior and it was found that the torsional prestrain had very little effect on  $G^*$ . As in the previous tests, the values of  $\tan \delta$  showed an initial increase and then appeared to approach a constant value. This increase in  $\tan \delta$  was smaller than that experienced by the specimens which had not been prestrained in the torsional direction, though the difference was not large. The values of  $G_1$  decreased at first with longitudinal strain but then started to increase again with increasing strain. Both of these specimens showed a greater increase in  $G_1$  than the specimens which had not been prestrained but again this difference was small.

#### Relaxation at fixed longitudinal strains.

In addition to the longitudinal creep and recovery tests, a number of specimens were allowed to undergo longitudinal deformation up to a certain strain, and at this point the strain was kept constant and the behavior of the dynamic shear modulus  $G^*$  during stress relaxation was observed.

The specimens were strained in the longitudinal direction by applying constant loads as explained in the previous section, and as a certain strain was reached, the brake shown at D in Figure 1 was applied and this ensured that the specimen was held at a fixed deformation. By applying small torsional oscillations,



the decay curve of the vibrations was observed and the value of the natural frequency  $p$  and logarithmic decrement  $\Delta'$  were thus obtained. The decay curve of the vibrations was obtained at various intervals of time,  $t = 0$  being the time at which the brake was applied. The moduli, are given by the following relations

$$\tan \delta = \frac{\Delta'}{\pi}$$

$$G_1 = \left( \frac{\pi^2 I l}{I_p} \right) p^2$$

where the quantity in brackets for  $G_1$  is a constant during the relaxation tests, and this value was determined from a photograph of the specimen. Thus by multiplying the square of the observed natural frequency  $p$  by the appropriate constant the values of  $G_1$  were then known with respect to time. The values of  $G_1$  and  $\tan \delta$  for three specimens No. 6, 7, and 8 were obtained during stress relaxation at the fixed longitudinal strains of 8, 22, and 115% respectively. The behavior of  $G_1$  and  $\tan \delta$  during stress relaxation at strains of 8 and 22% were similar and in Figure 15 the results for specimen No. 7 with  $\epsilon_x = 22\%$  are shown. In Figure 16, are shown the behavior of  $G_1$  and  $\tan \delta$  for specimen No. 8 during stress relaxation at a longitudinal strain of 115%.

The behavior of  $\tan \delta$  and  $G_1$  for specimens No. 6 and 7 are quite similar, the behavior of specimen No. 8 showing slightly larger changes with respect to time. For specimens No. 6 and 7 the values of  $G_1$  remain fairly constant up until a value of  $t = 10$  minutes, there is then a gradual increase up until  $t = 400$  minutes, and for longer times the value of  $G_1$  seems to be approaching a constant value. For specimens No. 6 and 7, the values of  $G_1$  increased

from 2.48 to 2.78 and from  $2.46$  to  $2.75 \times 10^9$  dynes/cm<sup>2</sup> respectively. For specimen No. 8 with a longitudinal strain of 115%, the change in  $G_1$  was from 2.56 to  $2.94 \times 10^9$  dynes/cm<sup>2</sup> and this increase occurred in the interval  $t = 5$  to  $t = 40$  minutes.

These results appear to indicate that the relaxation behavior of the storage modulus  $G_1$  at fixed longitudinal strains is dependent on the value of the strain, though this dependence appears to be slight. In addition, the time interval over which  $G_1$  shows its greatest change appears to be shifted to shorter times for larger strains.

The values of  $\tan \delta$  for all three specimens showed similar behavior although the change in  $\tan \delta$  for specimen No. 8 was slightly larger. For all three specimens, the values of  $\tan \delta$  appear to remain reasonably constant for about 10 minutes, after which there is a decrease in their value. After a time of about 100 minutes, the values of  $\tan \delta$  appear to be approaching constant values. Unlike the behavior of  $G_1$ , this change appears to occur in the same time interval for all three specimens. For specimens No. 6 and 7 the decrease in  $\tan \delta$  is 0.0090 while the change of  $\tan \delta$  for specimen No. 8 is 0.0120. This would seem to indicate a larger overall change in  $\tan \delta$  during stress relaxation with increasing fixed longitudinal strain.

#### Torsional creep and recovery.

In this series of tests, the behavior of the dynamic shear modulus  $G^*$  of the polyethylene specimen as it undergoes creep in the torsional direction is discussed. For some of the specimens the torsional creep is allowed to continue until buckling of the

tubular specimen occurs, while for other specimens, the creep test is terminated and upon removal of the load the sample is allowed to recover in the torsional direction. In addition, some of the specimens were prestrained in the longitudinal direction, to determine what effect a static torsional strain would have on the dynamic shear modulus  $G^*$  during torsional creep.

By applying a load to the pulley system shown at F in Figure 1, the specimen will be strained in the torsional direction since the end of the specimen at B is clamped against rotation while the other end shown at A will rotate as the pulley turns. At certain intervals of the torsional creep strain, the small torsional oscillations are applied to the specimen, and by observing the decay curve of the vibrations both the natural frequency  $p$  and the logarithmic decrement  $\Delta'$  can be found. As in the longitudinal creep tests, the torsional creep test is stopped for the interval of time needed to obtain the decay curve of the vibrations. At each of the intervals at which the decay curve is obtained, the torsional strain is recorded by reading the rotating dial disc and the vernier scale shown at I in Figure 1. For those specimens which were not allowed to buckle, at a certain torsional strain the load is removed and this will then allow the specimen to recover in the torsional direction. During the recovery cycle, the recovery creep is stopped at various intervals of strain, the decay curve of the vibrations is obtained and the vernier dial is read.

The maximum strain that is attained during torsional creep will depend upon the stress that has been applied, and this varied from  $3.5 \times 10^7$  to  $5.9 \times 10^7$  dynes/cm<sup>2</sup>. For those tests in which the creep test was terminated and either recovery or relaxation al-

lowed, the torsional creep was stopped when the change of strain became small. However, for the larger stresses used, the specimen was found to buckle before the creep rate had appreciably slowed down. For those specimens which were allowed to recover in the torsional direction, the amount of recovery was dependent upon the creep strain that had been reached. For these tests, additional recovery was attained by raising the temperature in the test chamber from 25° to 74° Centigrade. In Figure 17 are shown some initial creep curves under different stresses, and in Figure 18 are the recovery curves for the same specimens.

In order to obtain the storage and loss moduli of  $G^*$  we have as before the following relations

$$\tan \delta = \frac{\Delta'}{\pi}$$

$$G_1 = \frac{\pi^2 p^2 l I}{I_p}$$

where both the logarithmic decrement  $\Delta'$  and the natural frequency  $p$  are determined from the decay curve of the torsional vibrations. For this series of tests, the only variable in the determination of  $G_1$  is the natural frequency  $p$  since geometry changes are negligible until the specimen starts to buckle. Hence, for each interval of creep or recovery, the only data that must be recorded are the decay curve of the vibrations and the reading of the vernier dial. The vernier dial is graduated in degrees and the torsional strain is then given by

$$\epsilon_\theta = \frac{d_o \theta}{l} \frac{\pi}{360}$$

where  $d_o$  is the outside diameter of the specimen.

Three specimens, No. 9, 10, and 11 were tested in creep and recovery with stresses of 3.5, 4.7, and  $5.9 \times 10^7$  dynes/cm<sup>2</sup> and these specimens were allowed to undergo torsional creep up to 12.1, 13.7 and 16.9% strain respectively, before the torsional loads were removed and the specimens allowed to recover. Since the only variable in the equation for  $G_1$  is the natural frequency  $p$  raised to the second power we can write

$$G_1 = \left( \frac{\pi^2 l I}{I_p} \right) p^2$$

where the quantity in brackets is a constant for each specimen throughout the test. In order to plot the value of  $G_1$  as a function of the torsional strain during both creep and recovery, the experimentally observed values of the natural frequency  $p$  raised to the second power are multiplied by the appropriate constants and in Figures 19, 20, and 21 are shown the values of  $G_1$  for the three specimens. The values of  $G_1$  for all three specimens show a continuous decrease with increasing torsional strain, though at a decreasing rate. The curves of  $G_1$  for all three specimens are quite similar as opposed to the curves of  $G_1$  for different specimens obtained during longitudinal creep. The closer agreement between the curves of  $G_1$  versus torsional strains is due to the fact that no geometry changes and their attendant errors had to be considered. It is seen that there is no effect due to the different stresses used nor to the rate of straining, and hence  $G_1$  during torsional creep is a function only of the static strain.

All three specimens also showed similar behavior during recovery, the value of  $G_1$  at first decreasing and then starting to increase. It seems that the greater the initial creep strain, the

greater is the difference in  $G_1$  between creep and recovery. For all three specimens, the value of  $G_1$  started to increase with further recovery and the dashed lines on the graphs are for those portions of recovery which were achieved by increasing the temperature. However, in none of the specimens did  $G_1$  on recovery become greater than its corresponding creep value as occurred in the longitudinal recovery tests. In addition, it can be seen that the values of  $G_1$  are approaching their initial stress free values.

In Figure 22 is shown the creep and recovery curves of  $\tan \delta$  for specimen No. 11, the values of  $\tan \delta$  being determined from the decay curve of the vibrations. The behavior of  $\tan \delta$  for all three specimens was similar, showing a very small increase in the value of  $\tan \delta$  with increasing creep, and upon recovery showing another increase and then decreasing below the corresponding creep values. Though the recovery curves of  $G_1$  did not cross the initial creep curves, the curves of  $\tan \delta$  do, all three specimens showing a smaller value of  $\tan \delta$  at maximum recovery as compared to its corresponding creep value. As in the case for  $G_1$  the values of  $\tan \delta$  appear to be a function of the strain alone.

In addition, the values of  $\tan \delta$  and  $G_1$  were obtained for specimen No. 12 which was allowed to creep until buckling occurred. The curves were similar to those of the previous specimens until a strain of 19% was reached, where  $G_1$  then started to decrease and the value of  $\tan \delta$  started to increase, thus indicating the start of buckling. By observing photographs of the specimen under torsional creep, it was found that changes in the outside diameter started to occur at about 18% strain.

The effect of a longitudinal prestrain on the behavior of

$G^*$  in torsional creep was also investigated. A number of specimens were strained in the longitudinal direction and a suitable time was allowed for relaxation effects to cease before torsional creep tests were started. Three specimens with longitudinal pre-strain of  $\epsilon_x = 3, 22, \text{ and } 112\%$  were tested in this manner. The only apparent effect on the behavior of  $G_1$  in torsional creep was an overall smaller change in  $G_1$  with increasing longitudinal pre-strain, though this difference was slight. The values of  $\tan \delta$  showed a greater increase as compared to the specimens which had not been prestrained, but again this difference was small.

#### Relaxation at fixed torsional strains.

In addition to the torsional creep and recovery tests, two specimens were subjected to torsional creep and at the torsional quasi-static strains of 8 and 16% respectively, the strains were kept constant and the behavior of the dynamic moduli in shear were observed during stress relaxation.

The specimens were subjected to the torsional creep as explained previously and when the desired strain was reached, a brake was applied to the pulley shown at F in Figure 1, thus keeping the strain constant. Since the value of  $G_1$  is given by the relation

$$G_1 = \left( \frac{\pi^2 l I}{I_p} \right) p^2$$

and the quantity in brackets is a constant, the only relevant data that needs to be recorded for the relaxation tests were the natural frequency  $p$  and the value of the logarithmic decrement  $\Delta'$ . These give us the values of  $\tan \delta$  and  $G_1$ , and these can both be obtained

from the decay curve of the torsional vibrations. The decay curve was obtained at various intervals of time,  $t = 0$  corresponding to the time that the brake was applied.

The values of  $\tan \delta$  and  $G_1$  are shown in Figure 23 for specimen No. 14 with a torsional static strain of 16%. There did not appear to be any difference in the relaxation behavior of the two specimens. The values of  $G_1$  for specimen No. 14 shows a gradual increase in value from 2.41 to  $2.74 \times 10^9$  dynes/cm<sup>2</sup> and then appears to remain constant with increasing time. The value of  $\tan \delta$  over the same period shows a gradual decrease in value from 0.1125 to 0.1070 and then appears to be approaching a constant value. The values of  $G_1$  and  $\tan \delta$  for specimen No. 13 show similar changes. Since there are no apparent differences in the relaxation behavior of the two specimens, this would seem to indicate that the relaxation behavior of  $G^*$ , is independent of the static torsional strain at least in the region of large strains to which the two specimens were subjected. Both the variation in  $G_1$  and  $\tan \delta$  observed from these tests are similar to the behavior observed in relaxation at fixed longitudinal strains, and this would seem to indicate that the same molecular mechanisms are involved in both cases.

(B) Determination of the dynamic Youngs modulus  $E^*$  from longitudinal vibrations.

In this section of the report, the observed behavior of the dynamic Youngs modulus, obtained by imposing longitudinal vibrations on the specimen was observed. This behavior was observed under longitudinal creep and recovery, and in addition the behavior in relaxation at various longitudinal strains was obtained.



The data gathered in this phase of the investigation was not as complete as that obtained by using flexural vibrations and which will be discussed in a later section. This was due to two reasons, the first being the experimental difficulties involved in obtaining the decay curve or the resonant frequency and half-breadth, and secondly this data was desired mainly in order to check on the results obtained from flexural vibrations where the effect of the tension load on the values of  $E^*$  were corrected by approximate methods. The experimental difficulties were due to the fact that the amplitude of vibrations in the longitudinal direction were very small even though coils with iron cores were used and, the decay curve of the vibrations was then badly distorted because of the available equipment. The values of the natural frequency  $p$  and logarithmic decrement that were obtained were rather inaccurate and the resonance method was used for this phase of the experimental program. The resonant frequencies were more reliable and these were the values used in determining the value of  $E_1$  versus longitudinal strain in creep and recovery, as well as the time variation during relaxation behavior. The values of  $\tan \delta$  could not be obtained from the resonance method due to the interaction of the four iron cores and attempts at shielding them proved to be unsuccessful.

However, in order to serve as a check on the results obtained from the flexural vibrations, the values of  $E_1$  under longitudinal creep and recovery, and under relaxation will be sufficient and these results are presented in this section.

In addition, the behavior of  $E_1$  with respect to temperature was determined for an undeformed specimen, and this could also be

compared to the value of  $E_1$  obtained from flexural vibrations over the same temperature range. The temperature range that was used was from 24 to 74° Centigrade and these results will be discussed later. No attempt was made to determine the amplitude effects on  $E_1$ , but the amplitude of the oscillations at resonance were kept constant throughout the tests.

#### Longitudinal creep and recovery.

The specimens were subjected to longitudinal creep by applying constant loads, these being applied in the manner described in a previous section. At various intervals of strain, the creep test was stopped for a period of time sufficient to enable the resonance frequency to be obtained, and to record the relevant geometric data. As in the previous tests, this consisted of obtaining the overall length of the specimen from reading a rule and taking a photograph of the specimen from which the strain and diameter could be obtained. When the creep test was terminated the specimen was allowed to recover and the same information was recorded during the recovery phase. The creep and recovery curves with respect to time are similar to those shown in Figures 6 and 7 for comparable loads. The specimens in this section had applied tension loads of from  $2.7 \times 10^7$  to  $4.6 \times 10^7$  dynes, giving an initial stress of  $5.2 \times 10^7$  to  $8.8 \times 10^7$  dynes/cm<sup>2</sup>. In addition, as in previous tests the temperature in the test chamber was increased in order to obtain additional recovery for one specimen.

For longitudinal vibrations the equation for  $E_1$  is given as

$$E_1 = \frac{\pi^2 \omega_r^2 l m}{Z^2 A}$$

where  $Z$  is determined from the frequency equation

$$Z \tan Z = \frac{m}{M}$$

$m$  being the mass of the polyethylene specimen,  $M$  the center mass,  $A$  the cross sectional area of the polyethylene specimen,  $\ell$  the overall length, and  $\omega_r$  the resonant frequency. The value of  $Z$  obtained from the frequency equation is a constant throughout the test. The area  $A$  is determined from the photographs and the overall length  $\ell$  of the specimen is obtained by reading the rule. The relation for  $E_1$  can be written as

$$E_1 = \left( \frac{\pi^2 m}{Z^2} \right) \frac{\ell}{A} \omega_r^2$$

the quantity in brackets being a constant for each specimen. Hence to determine  $E_1$ , the values of  $\omega_r^2$  and  $\frac{\ell}{A}$  must be known. The values of  $\omega_r^2$  that are obtained at discrete strain levels are plotted against the longitudinal strain  $\epsilon_x$  and a smooth continuous curve which best fits the data was drawn through the points. The values of  $A$  and  $\ell$  were also plotted in the same manner and a continuous curve drawn through the points. Then at various intervals of both the creep and recovery strain, say at 10% intervals, values of  $\ell$ ,  $A$ , and  $\omega_r^2$  are obtained from the best fit curve and these are then used in the relation for  $E_1$ .

The values of  $E_1$  so determined are shown in Figure 24 for specimen No. 15 in both creep and recovery. The value of  $E_1$  for this specimen showed a slight decrease in value with the onset of creep, but then started to increase again at about 10% strain. The overall change in  $E_1$  was from an initial value of  $4.92 \times 10^9$  to

$11.51 \times 10^9$  dynes/cm<sup>2</sup> at a strain of  $\epsilon_x = 140\%$ . The recovery curve showed an initial decrease when recovery started and then started to level off, remaining below the creep curve of  $E_1$  until  $\epsilon_x = 30\%$  where it crosses and then gives a higher value of  $E_1$  for recovery as compared to the corresponding creep value. The maximum amount of recovery at the test temperature was at  $\epsilon_x = 38\%$  and at this point the temperature was increased to  $74^\circ$  Centigrade in order to achieve additional recovery. These values of  $E_1$  are shown by the dashed lines and it appears that  $E_1$  is approaching its initial stress free value. The creep and recovery curves for the other specimens that were tested showed similar behavior, the only difference being that the specimens which had been strained more in creep showed a greater decrease in  $E_1$  at the start of recovery. For the different specimens used, the curves of  $E_1$  versus longitudinal creep were in better agreement than those of  $G_1$  and this was probably due to the fact that the two factors in  $E_1$ ,  $\omega_r^2$  and  $\frac{l}{A}$  were not changing as rapidly as were the corresponding factors of  $p^2$  and  $\frac{l}{I_p}$  in  $G_1$ .

There was no indication that the value of  $E_1$  was dependent on the tension load used nor to the rate of straining and hence the value of  $E_1$  during longitudinal creep and recovery is then a function of the strains alone.

#### Relaxation at fixed longitudinal strains.

During the relaxation tests at fixed longitudinal strains, there are no geometry changes and the equation for determining  $E_1$  from longitudinal vibrations can be written as

$$E_1 = \left( \frac{\pi^2 m l}{Z^2 A} \right) \omega_r^2$$

where at fixed longitudinal strains the quantity in brackets is a constant and  $E_1$  is proportional to the square of the resonant frequency. By observing the resonant frequency with respect to time,  $t = 0$  starting at the time the deformation is held constant, the values of  $E_1$  can be plotted by multiplying the square of the observed frequencies by the appropriate constant and these values are shown in Figure 25 for various values of static longitudinal strain. It appears that there is little if any change in the value of  $E_1$  during relaxation.

The results obtained in this phase of the testing program will be discussed in more detail in the following section, where a comparison between this data and the values of  $E_1$  obtained by flexural vibrations is made.

(C) Determination of the dynamic Youngs modulus  $E^*$  from lateral vibrations.

In this section of the report, the observed behavior of both the dynamic storage and loss moduli of  $E^*$  are obtained by superimposing small oscillatory strains on the specimen in the lateral direction. The dynamic Youngs modulus  $E^*$  is determined in this way under longitudinal creep followed by recovery or relaxation, and in addition under torsional creep followed by recovery or relaxation. The effect of a static torsional strain upon the behavior of  $E^*$  in longitudinal creep and the effect of a static longitudinal strain on  $E^*$  in torsional creep are also determined.

The effect on Youngs modulus  $E^*$  of the amplitude of the sinusoidal oscillations was determined by observing the variation of the natural frequency  $p$  and the logarithmic decrement

$\Delta'$  with change in amplitude. It was found that  $E_1$  slowly decreases in an apparently linear manner with increasing amplitude while  $\tan \delta$  increases, though not linearly. As in the previous tests, the amplitude was kept constant during each test and these small effects were ignored.

The temperature dependence of Young's modulus  $E^*$  for an undeformed specimen is shown in Figure 26 for the temperature range of 24 to 74° Centigrade. These results were obtained from the decay curve of the lateral vibrations and the values of  $p$  and  $\Delta'$  were then used in equations 9. The value of  $E_1$  shows a continuous decrease from  $5.2 \times 10^9$  to  $0.9 \times 10^9$  dynes/cm<sup>2</sup> over this temperature range. The value of  $\tan \delta$  showed an increase from 0.1280 to 0.1910 over the same temperature range. The value of  $E_1$  obtained from longitudinal vibrations is also shown on the graph and both curves of  $E_1$  are similar.

#### Longitudinal creep and recovery.

In this series of tests, the behavior of  $E^*$  of the polyethylene specimen as it undergoes creep in the longitudinal direction under an applied tension load followed by recovery upon removal of the load will be discussed.

The specimen is subjected to longitudinal strains by applying loads as described previously, and allowing the specimen to creep. At various intervals of strain the creep test is stopped long enough to obtain the relevant data which includes a photograph of the specimen, the decay curve of the vibrations, rule reading, and in addition readings taken from the load cell. After a certain strain is reached the creep test is terminated and the specimen is

allowed to recover. At various intervals of the recovery strain the relevant data is again recorded.

The maximum strain reached during the recovery tests was different for the specimens used and depended on the tension load that was applied. The strain versus time curves for the three specimens tested are similar to those shown in Figures 6 and 7. The amount of recovery was dependent upon the maximum strain and as in the previous tests, additional recovery was achieved by increasing the temperature in the test chamber.

In the introduction the following relation (equation 13) was derived,

$$\frac{4EI_z Z^4}{\pi^2 m l^3} + \frac{Q^2 T}{\pi^2 m l} \leq p^2 \leq \frac{4EI_z Z^4}{\pi^2 m l^3} + 0.102 \frac{Z^2 T}{\pi^2 m l}$$

It was hoped that this would enable us to make corrections for the effect of the tension load on the values of  $E_1$  obtained by superimposing flexural vibrations on the specimen. In this phase of the testing program, three specimens were tested under tension loads of 2.7, 3.6, and  $4.6 \times 10^7$  dynes and the initial stresses were 5.2, 7.0, and  $8.8 \times 10^7$  dynes/cm<sup>2</sup>. The specimens with increasing load were subjected to a larger longitudinal strain. However, before these tests were run, an estimation of the effect of tension on each of the specimens was made. This was done in the following manner, the decay curve of the vibrations was obtained for the undeformed specimen and then a tension load of  $0.4 \times 10^7$  dynes, giving an initial stress of  $0.76 \times 10^7$  dynes/cm<sup>2</sup> was applied and the decay curve of the vibrations was again obtained. The change in the geometry of the specimens due to this tension load was small and

was not considered. By finding the increase in the frequency after the load was applied we were able to obtain an approximation of the effect on the frequency due to the load. For each separate specimen at zero strain equation 13 can be written as

$$C_1 E_1 + C_2 T \leq p^2 \leq C_1 E_1 + C_3 T$$

where the values of  $C$  will then be known constants, though different for each specimen. The value of the two frequencies found for each specimen before and after a small load was applied are given by

$$p_1^2 = \frac{4E_1 I_z Z^4}{\pi^2 m l^3} = C_1 E_1$$

$$p_2^2 = \frac{4E_1 I_z Z^4}{\pi^2 m l^3} + \frac{C_4 T Z^2}{\pi^2 m l} = C_1 E_1 + C_4 T$$

and  $C_4$  can then be found, i.e.,

$$C_4 = \frac{p_2^2 - p_1^2}{T}$$

and this value of  $C_4$  will tend to be on the low side since the frequency will decrease with strain, no matter how small the strain is. Hence we would expect  $C_4$  to be less than  $C_3$  though not necessarily greater than  $C_2$ . The values of  $C_2$ ,  $C_3$ , and  $C_4$  are as follows for the three specimens.

	<u><math>C_2</math></u>	<u><math>C_3</math></u>	<u><math>C_4</math></u>
specimen No. 16	0.094	0.107	0.088
specimen No. 17	0.094	0.108	0.090
specimen No. 18	0.095	0.109	0.090

and we see that the values of  $C_4$  are less than the corresponding



values of  $C_3$  which they should be. Now from our derivation of equation (13) we know the true value  $C$ , should be between  $C_2$  and  $C_3$  and from the experiments we know that  $C$  is greater than  $C_4$  but this did not give us a lower bound. If we used the value of  $C_3$  this would make the correction too large and this could even give us a negative value of  $E_1$ . For this reason it was decided to use the values of  $C_2$  for the corrections, hence we have from equation (13)

$$p_1^2 = \frac{4E_1 I_z Z^4}{\pi^2 m \ell^3} + \frac{Q^2 T}{\pi^2 m \ell}$$

or

$$E_1 = \frac{\pi^2 m \ell^3 p_1^2}{4 I_z Z^4} - \frac{Q^2 T \ell^2}{4 I_z Z^4}$$

which can be written

$$E_1 = \left( \frac{\pi^2 m}{4 Z^4} \right) \frac{\ell^3}{I_z} p_1^2 - \left( \frac{Q^2}{4 Z^4} \right) \frac{\ell^2}{I_z} T \quad (14)$$

the quantities in brackets being constants, though different for each specimen.

At certain intervals of strain during either creep or recovery the test was stopped long enough to obtain the decay curve of the vibrations and the needed geometric data. This was then plotted on a graph versus the longitudinal strain  $\epsilon_x$  and a curve which best fitted the data was then drawn. Then at certain strain intervals, say every 10%, the values of  $\ell$  and  $I_z$  were taken from the best fit curves and together with the value of the frequency obtained from the decay curve, the value of  $E_1$  was calculated from equation 14. The values of  $E_1$  are shown in Figures 27, 28, and 29 for the three specimens. Since a constant load was used the

value of  $T$  in equation 14 was considered a constant during the creep phase after a strain of about 5% was reached. This was due to the fact that the brake was not completely released until this strain was reached. At each interval of strain at which the test was stopped, the tension load would start to relax but since the decay curve of the vibrations was obtained quickly the change in  $T$  was not significant. The recording of the tension load  $T$  during recovery was more difficult. During the first one or two readings made after the sample started to recover, the tension on the specimen would increase quite rapidly and for this reason the decay curve was not obtained until about 1 minute had passed, at which time the tension was not changing as fast and the load cell could then be read. For subsequent recovery stops the decay curve was obtained as soon as the brake was applied and the load cell could then be read without much difficulty. The dashed lines on the graphs are for those values of  $E_1$  which were obtained after the temperature was increased in order to achieve greater recovery.

From the graphs of  $E_1$  versus longitudinal strain for the three different specimens, it can be seen that the values of  $E_1$  are quite similar. The value of  $E_1$  showing a slight decrease at first and then starting to increase with increasing longitudinal strain. For specimen No. 18 which was strained to  $\epsilon_x = 140\%$ , the value of  $E_1$  increased from  $4.98 \times 10^9$  to  $12.61 \times 10^9$  dynes/cm<sup>2</sup>. These values of  $E_1$  can be compared to the values of  $E_1$  obtained by applying longitudinal oscillations. While the values do not agree exactly they are in reasonably good agreement, the values of  $E_1$  from flexural vibrations being slightly higher during creep than those obtained from longitudinal vibrations.

The values of  $\tan \delta$  which were obtained from the decay curve of the vibrations by the relation

$$\tan \delta = \frac{\Delta'}{\pi}$$

are shown in Figure 30 for specimen No. 18 during both creep and recovery. The values of  $\tan \delta$  for the other specimens show similar behavior. As can be seen from the graph, there is a large decrease in  $\tan \delta$  with increasing longitudinal strain. For specimen No. 18 the value of  $\tan \delta$  at zero strain was 0.1350 and it then decreased to 0.03 at  $\epsilon_x = 140\%$  strain. The value of  $\tan \delta$  upon recovery is higher than its corresponding creep value, but the values obtained at later stages of recovery seem to indicate that  $\tan \delta$  is starting to approach its initial stress free value.

In addition to these specimens, one other specimen with a torsional prestrain of  $\epsilon_\theta = 12\%$  was also tested in longitudinal creep and there were no apparent differences in the values of  $E_1$  or  $\tan \delta$ , and hence the effect of a torsional prestrain on  $E^*$  during longitudinal creep would appear to be negligible.

#### Relaxation at fixed longitudinal strains.

A number of specimens were allowed to creep in a longitudinal direction and at a certain strain the deformation was held constant and the relaxation behavior of the specimens was observed. Since there were no geometry changes during relaxation, equation 14 can be written as

$$E_1 = \left( \frac{\pi^2 m \ell^3}{4Z^4 I_z} \right) p_1^2 - \left( \frac{Q^2 \ell^2}{4Z^4 I_z} \right) T$$

where the quantities in brackets are constants. By obtaining the

values of the natural frequency from the decay curve of the vibrations and recording the tension  $T$  from the load cell at various intervals of time the value of  $E_1$  can then be calculated. These values of  $E_1$  can then be compared to those obtained from longitudinal vibrations which showed a constant value of  $E_1$  with respect to time. This will give us another indication of the correctness of our approximation on the effects due to the tension.

In Figure 31 are shown the values of  $E_1$  and  $\tan \delta$  obtained in this manner for a specimen in relaxation at a longitudinal strain of  $\epsilon_x = 142\%$ . The value of  $E_1$  showed an initial decrease in value during the first few minutes of relaxation, but at longer times seemed to remain constant. There was no apparent variation in  $\tan \delta$  over the time range observed. A number of specimens were tested in relaxation at other values of fixed longitudinal strain and the above behavior was observed in all cases. These values of  $E_1$  can be compared to the values of  $E_1$  obtained from longitudinal vibrations and it seems that the behavior of  $E_1$  in both cases is similar. The only difference is that the values of  $E_1$  from lateral vibrations show a slight decrease in value during the first few minutes and this difference could be due to errors involved in reading the load cell.

#### Torsional creep and recovery.

In this series of tests the behavior of the complex Young's modulus  $E^*$  of the polyethylene specimen as it undergoes creep and recovery in the torsional direction is discussed. For some of the specimens the torsional creep is allowed to continue until buckling occurs while for other specimens the creep test is terminated and

upon removal of the load, the specimen is allowed to recover in the torsional direction. In addition some of the specimens were prestrained in the longitudinal direction to see what effect this would have on the moduli.

The specimen is strained in the torsional direction by applying a constant load to the specimen via the pulley shown at F in Figure 1. The angle through which one end of the specimen is twisted is determined by reading the vernier dial shown at I in Figure 1, and the torsional strain  $\epsilon_\theta$  is then determined. Since the geometry changes are negligible until buckling starts to occur, the data that must be recorded are the strain and the decay curve of the flexural vibrations. At each interval of strain for which the data is recorded, the creep test is stopped long enough to read the dial and obtain the decay curve of the vibrations. This time was usually about one minute. For those tests in which the specimen was allowed to recover, the load was removed from the specimen and at various intervals of the recovery strain the needed data was again recorded. As in the previous tests the amount of recovery was dependent upon the maximum creep strain that had been reached. In order to achieve greater recovery the test temperature was increased from 25 to 74° Centigrade. The creep and recovery curves are similar to those shown in Figure 17 and 18.

In order to obtain the storage and loss moduli of  $E^*$  we have the following relations

$$\tan \delta = \frac{\Delta'}{\pi}$$

$$E_1 = \left( \frac{\pi^2 m \ell^3}{4Z^4 I_z} \right) p^2 - \left( \frac{Q^2}{4Z^4 I_z} \right) T$$

where the quantities in brackets are constants for each specimen throughout the test. For those specimens which had not been prestrained in the longitudinal direction, no correction for  $E_1$  was needed and the second term is zero. For those specimens which had been prestrained in the longitudinal direction, the tension present must be corrected for, and this is taken care of in the second term.

For those specimens which were prestrained in the longitudinal direction, a suitable time was allowed to elapse in order for the tensile stress to approach a constant value, before a torsional creep test was started and the tension  $T$  could then be taken as a constant. By taking readings of the load cell during torsional creep and recovery, the change in  $T$  was in fact very small and the above assumption is then certainly reasonable. Since we are concerned here with the behavior of  $E_1$  with respect to the torsional strain  $\epsilon_\theta$ , the correction term for  $E_1$  will in effect only move the  $E_1$  versus  $\epsilon_\theta$  curve along the  $E_1$  axis and the overall change in  $E_1$  will not be effected.

Three different specimens with stresses of 3.5, 4.7, and  $5.9 \times 10^7$  dynes/cm<sup>2</sup> were tested in torsional creep and then allowed to recover. These specimens had not been prestrained in the longitudinal direction. In Figure 32 is shown the variation of  $E_1$  with torsional strain  $\epsilon_\theta$  for specimen No. 19 during both creep and recovery. For the other specimens tested the behavior of  $E_1$  was similar. The value of  $E_1$  shows a continuous decrease from  $4.94 \times 10^9$  to  $4.7 \times 10^9$  dynes/cm<sup>2</sup> at a strain of  $\epsilon_\theta = 18\%$ . During recovery the value of  $E_1$  decreases at first then starts to increase, and it ap-

pears that the value of  $E_1$  is approaching its stress free value. The dashed portion of the recovery curve is for the values of  $E_1$  obtained after the temperature was increased in order to achieve further recovery. In Figure 33 the value of  $\tan \delta$  for this specimen is shown during creep and recovery. The values of  $\tan \delta$  for the other specimens also show similar behavior. The value of  $\tan \delta$  during creep appears to be constant or decreasing at a very small rate with increasing torsional strain. Upon recovery the value of  $\tan \delta$  at first increases and then starts to decrease with further recovery. The dashed portions of the recovery curve are for those values of  $\tan \delta$  obtained after the temperature had been increased. For all three specimens, the final value of  $\tan \delta$  when recovery was completed was lower than the corresponding creep value. The values of  $E_1$  and  $\tan \delta$  do not appear to depend on the stress nor the rate of straining, and are dependent upon the static strain alone.

In addition, a number of specimens were tested in torsional creep after they had been prestrained in the longitudinal direction. The value of  $\tan \delta$  for all of these specimens showed a constant value during torsional creep. However, the longitudinal prestrain did effect the values of  $E_1$ . It was found that with increasing longitudinal prestrain, the decrease in  $E_1$  with torsional creep became smaller, and with a prestrain of  $\epsilon_x = 140\%$ ,  $E_1$  remained constant during torsional creep. This behavior is probably due to the long chain molecules becoming more oriented with longitudinal prestrain and hence less opportunity for any additional movement of these chains during torsional creep.

Relaxation at fixed torsional strains.

In this series of tests, the specimens were subjected to torsional creep and at a certain strain the deformation was kept constant and the behavior of  $E^*$  observed during stress relaxation. In Figure 34 are shown the values of  $E_1$  and  $\tan \delta$  during stress relaxation at a torsional strain of 14%. The value of  $\tan \delta$  remains constant but the value of  $E_1$  shows an increase. It appears that  $E_1$  is constant at first, and then gradually increases in the interval  $t = 10$  to 200 minutes, and then approaches a constant value for longer times. The increase in  $E_1$  was from  $4.69 \times 10^9$  to  $4.90 \times 10^9$  dynes/cm<sup>2</sup>. Two other specimens which were strained to 6 and 10% respectively showed similar behavior although the increase in  $E_1$  was not as large.



#### IV. Conclusions.

From the wealth of experimental data that has been obtained during this investigation, some conclusions on the behavior of one high polymer, specifically a low density polyethylene, will be presented.

As described in the introduction, the mechanical behavior of high polymers are highly dependent on temperature and time effects. For the tests which were carried out in this investigation, temperature effects were generally avoided by using a constant temperature chamber and keeping the specimen at one temperature throughout the test. In those tests where the temperature was increased to facilitate additional recovery, the temperature was lowered back down to the test temperature before additional readings were taken. What effect this temperature cycle had on subsequent recovery behavior is, however, not known for sure. Since the high polymer we are using is partly crystalline, with a melting temperature of around  $112^{\circ}$  Centigrade and the temperature was raised to as high a value as  $74^{\circ}$  Centigrade, certain molecular changes with respect to the amount of crystallization undoubtedly occurred at the higher temperature, thus contributing to additional recovery. Thus by lowering the temperature back to the test temperature and stating that the observed behavior is the true recovery behavior, could easily be debated. The results obtained after the temperature increase, are shown by dashed lines on the appropriate graphs for the above reasons. However, we did obtain some data on the variation of  $E^*$  and  $G^*$  with temperature from  $24^{\circ}$  to  $74^{\circ}$  Centigrade for undeformed specimens. This in general showed the values

of the storage moduli, both  $G_1$  and  $E_1$  decreasing with increasing temperature as expected. The values of  $\tan \delta$  both showed an increase in value with increasing temperature but no peaks were observed in the temperature range that was used.

Of the two experimental techniques that were used in this investigation, resonance and free vibrations, there are certain disadvantages in using either. In determining the values of  $G^*$  in torsional oscillations and  $E^*$  in flexural oscillations, the data obtained from free vibrations was used. It was found that the values of the frequency and logarithmic decrement were more reliable and the amount of scatter with respect to the best fit curves was less than if the resonance method was used. The free vibration method also had the advantage that the decay curve of the vibrations could be obtained more quickly than the corresponding data for resonance. For those tests in which the value of  $E^*$  was determined by longitudinal vibrations, the free vibration method was not used. This was due to not being able to get sufficient amplitude of vibration, and at these low amplitudes the decay curve was visibly distorted due to the equipment available. The use of iron cores did not overcome this problem. Hence, for these tests, the resonance frequency was used to obtain value of  $E_1$ . Due to the inability to shield the coils and lead wires, a value of  $\tan \delta$  from the resonance method was also found to be unreliable.

The experimental determination of the dynamic Young's modulus was obtained by using lateral vibrations and making a correction for the tension present in the specimen. Though this correction was an approximation, the corrected values of  $E_1$  were found to

be in good agreement with the limited results obtained by using longitudinal vibrations. Values of  $E_1$  from both methods were obtained as a function of the static longitudinal strain  $\epsilon_x$ , and in addition as a function of time during relaxation at fixed longitudinal strains. These results usually showed a difference of less than 8% in value. It would thus seem to indicate that the correction that was made was a reasonable one. The difference in the value of  $E_1$  obtained by the two methods may be due in part to the way in which the specimen is strained. During flexural vibrations the molecular chains near the surface of the specimen will undergo a greater strain than those chains closer to the center. In longitudinal vibrations, each chain will be subjected to the same strain. What we are observing from longitudinal vibrations is an average  $E_1$  over the whole cross section, but in flexural vibrations it is a weighted average.

The values of  $E_1$  during longitudinal creep showed an initial decrease in value between a strain of 0 to 10% but then started to increase with increasing strain. The initial decrease in the value of  $E_1$  during the beginning of creep could possibly be attributed to changes in the crystalline region. The increase in the value of  $E_1$  was due mainly to the orientation of the long chain molecules in the longitudinal direction.

The value of  $\tan \delta$  showed a rapid decrease in value from 0.1350 at  $\epsilon_x = 0$  to a value of 0.03 at  $\epsilon_x = 140\%$ . This is undoubtedly due to the orientation of the polymer chains, which results in greater forces of attraction between the polymer molecules and reduces the chances of any additional movement of the molecules.

During recovery the values of  $E_1$  were generally lower and the values of  $\tan \delta$  higher and this was probably due to the movement of some of the polymer chains back to a more coiled configuration. However, when additional recovery was achieved by raising the temperature the values of  $E_1$  were then higher than the corresponding creep values and this would seem to indicate that some orientation effects due to stretching remained.

The values of  $E_1$  and  $\tan \delta$  during torsional creep showed only small changes,  $E_1$  decreasing with strain while  $\tan \delta$  increased. From the recovery data it appears that both  $E_1$  and  $\tan \delta$  are approaching their initial stress free values.

There were no apparent changes in the values of either  $E_1$  or  $\tan \delta$  during relaxation at fixed longitudinal strains but during relaxation at fixed torsional strains there was an increase in  $E_1$ , though  $\tan \delta$  remained constant. This increase in  $E_1$  was about equal to the decrease of  $E_1$  during the torsional creep.

The values of  $G_1$  that were obtained during longitudinal creep and recovery for different specimens did appear to show some differences, but as was mentioned before this was probably due mainly to the way the two factors  $\frac{l}{I_p}$  and  $p^2$  were changing. A slight error in either factor would produce a much greater error in  $G_1$ . However, there is definitely an initial decrease in the value of  $G_1$  and with increasing strain it tends to increase again. The value of  $\tan \delta$  showed an initial increase and then appeared to approach a constant value. During recovery  $G_1$  was initially lower while  $\tan \delta$  was higher as compared to their creep values, but on further recovery they both crossed their respective creep curves. Again this may be due to molecular changes brought about by an increase

in temperature.

The value of  $G_1$  during torsional creep also showed an initial decrease in value but then remained constant up until buckling occurred. The values of  $\tan \delta$  showed a small increase and then approached a constant value. Both  $G_1$  and  $\tan \delta$  showed relaxation effects at fixed longitudinal and torsional strains, these time effects being similar. The values of  $G_1$  and  $\tan \delta$  were constant for the first few minutes of relaxation and then  $G_1$  showed a gradual increase while  $\tan \delta$  showed a decrease in value. At longer times both  $G_1$  and  $\tan \delta$  appeared to become constant again.

In this investigation, there did not appear to be any effects due to the rate of straining, nor did it appear that the value of the stresses used during creep had any effect on the different moduli.

### References

1. Alfrey, T., Mechanical Behavior of High Polymers, Interscience, New York, 1948.
2. Ferry, J. D., Viscoelastic Properties of Polymers, Wiley, New York, 1961.
3. Kolsky, H., Stress Waves in Solids, Dover, New York, 1963.
4. Kolsky, H., and Hillier, K. W., "An Investigation of the Dynamic Elastic Properties of Some High Polymers," Proceedings of the Physical Society, 62, p. 111, 1949.
5. Kolsky, H., "The Mechanical Testing of High Polymers," Progress in Non-Destructive Testing, 2, Heywood, London, 1959.
6. Lurie, H., "Lateral Vibrations as Related to Structural Stability," Journal of Applied Mechanics, 19, p. 195, 1952.
7. Morse, P. M., Vibration and Sound, McGraw-Hill, New York, 1948.
8. Stephans, B. C., "Natural Vibration Frequencies of Structural Members," Journal of the Aeronautical Society, 4, p. 54, 1936.
9. Stuart, H. A., Die Physik Der Hochpolymeren, 4, Springer-Verlog, Berlin, 1956.

### Acknowledgement

The author wishes to express his appreciation to Professor H. Kolsky for suggesting the investigation discussed herein, and for his guidance and encouragement during the work. Thanks are also due to Mr. R. Stanton for his assistance in the performance of the experiments and the construction of the test equipment.

TECHNICAL LIBRARY  
BLDG 313  
ABERDEEN PROVING GROUND MD.  
STRAP-TL

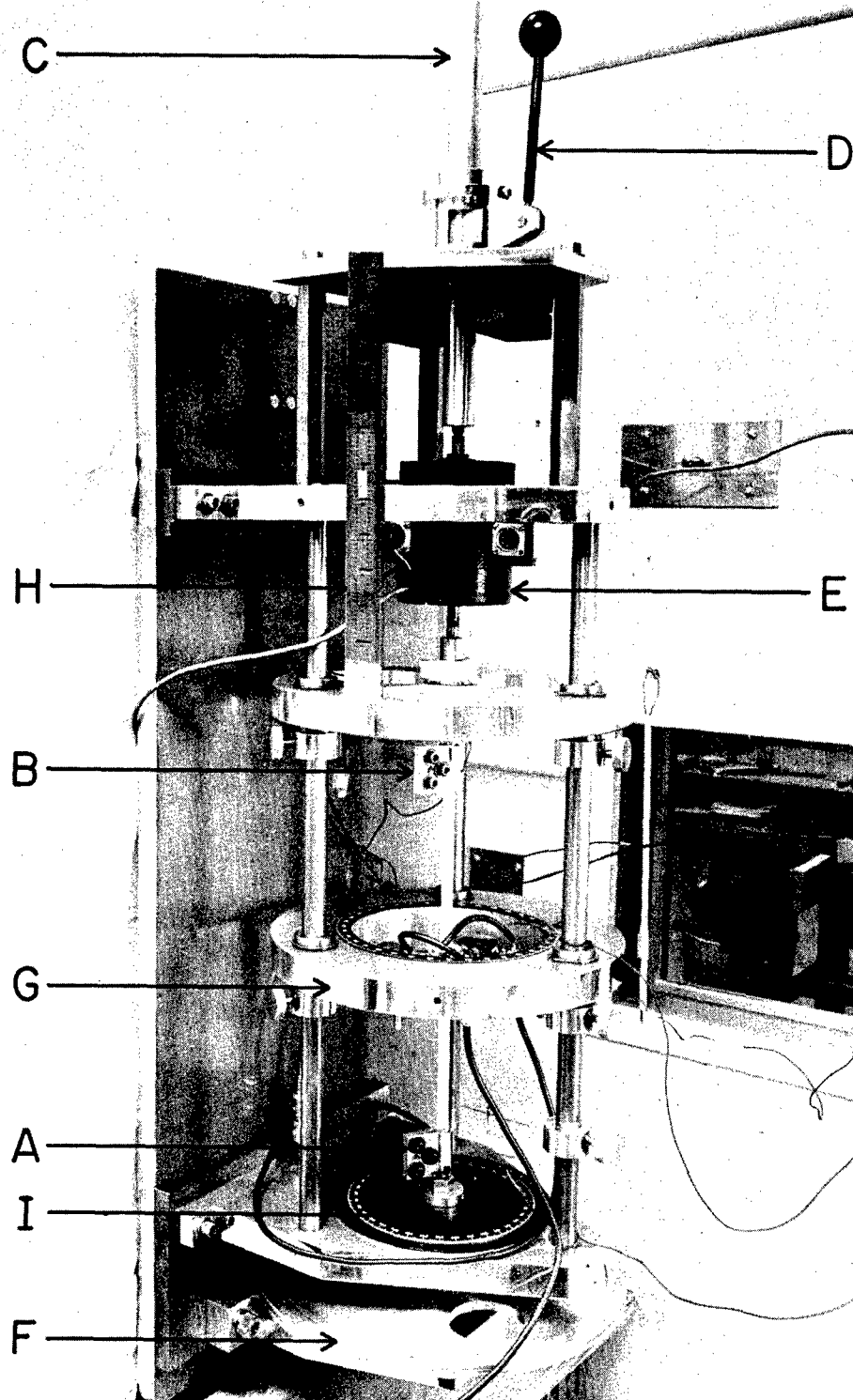


FIG. 1 TESTING MACHINE



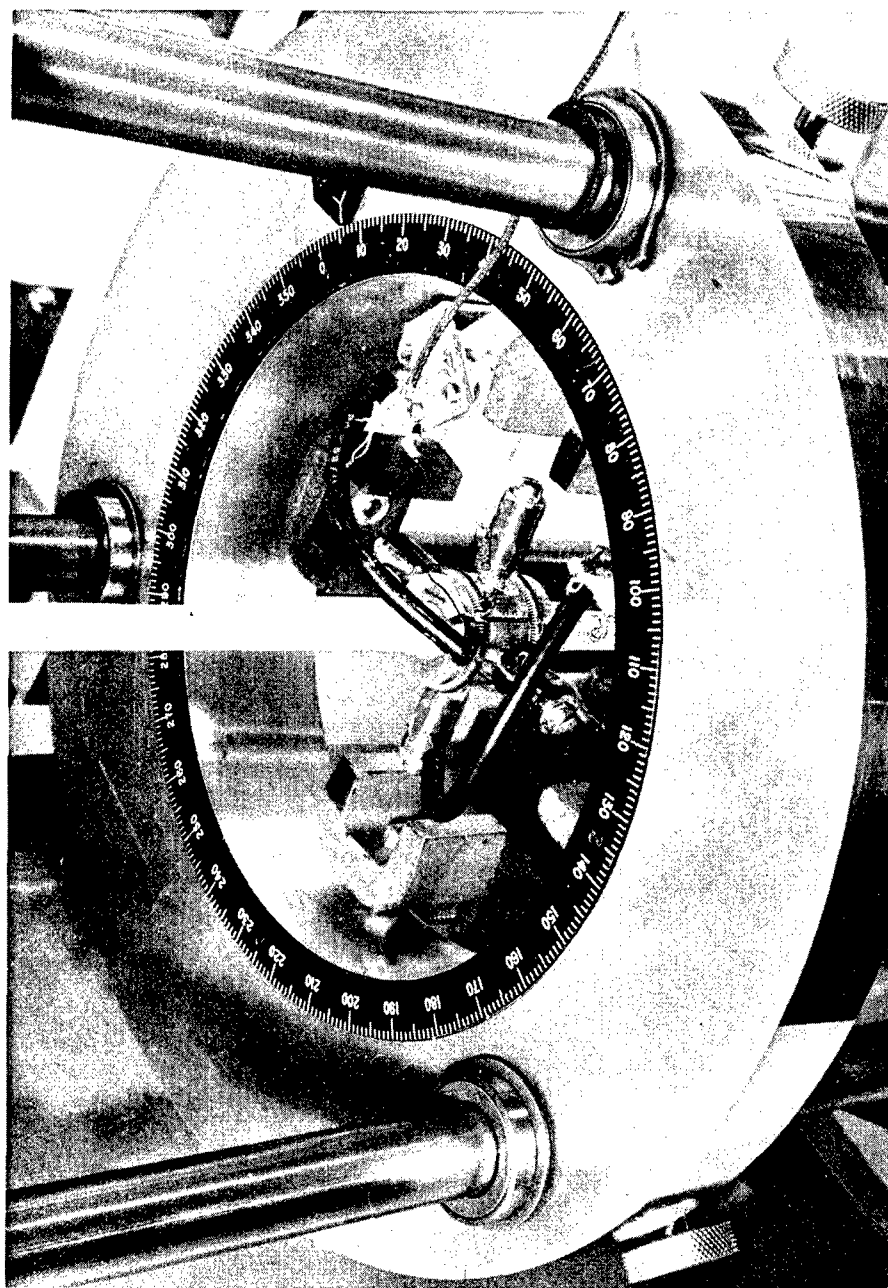
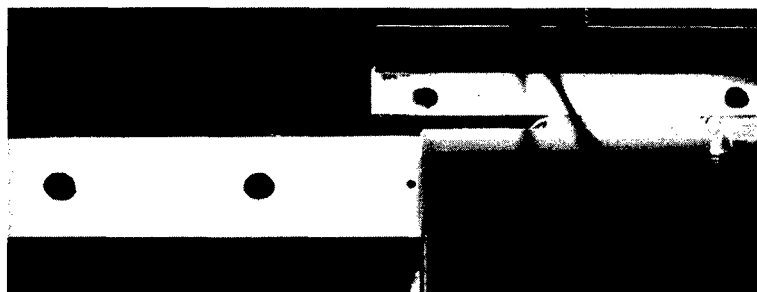
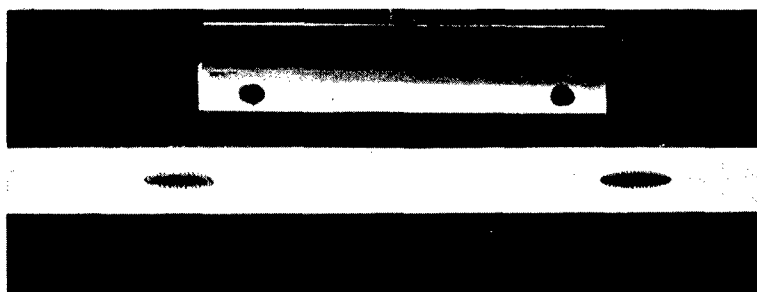


FIG. 2 POLYETHYLENE SPECIMEN WITH THE COIL AND MAGNET SYSTEM



(a)  $\epsilon_x = 0$



(b)  $\epsilon_x = 143.5\%$

FIG. 3 PHOTOGRAPHS OF A SPECIMEN

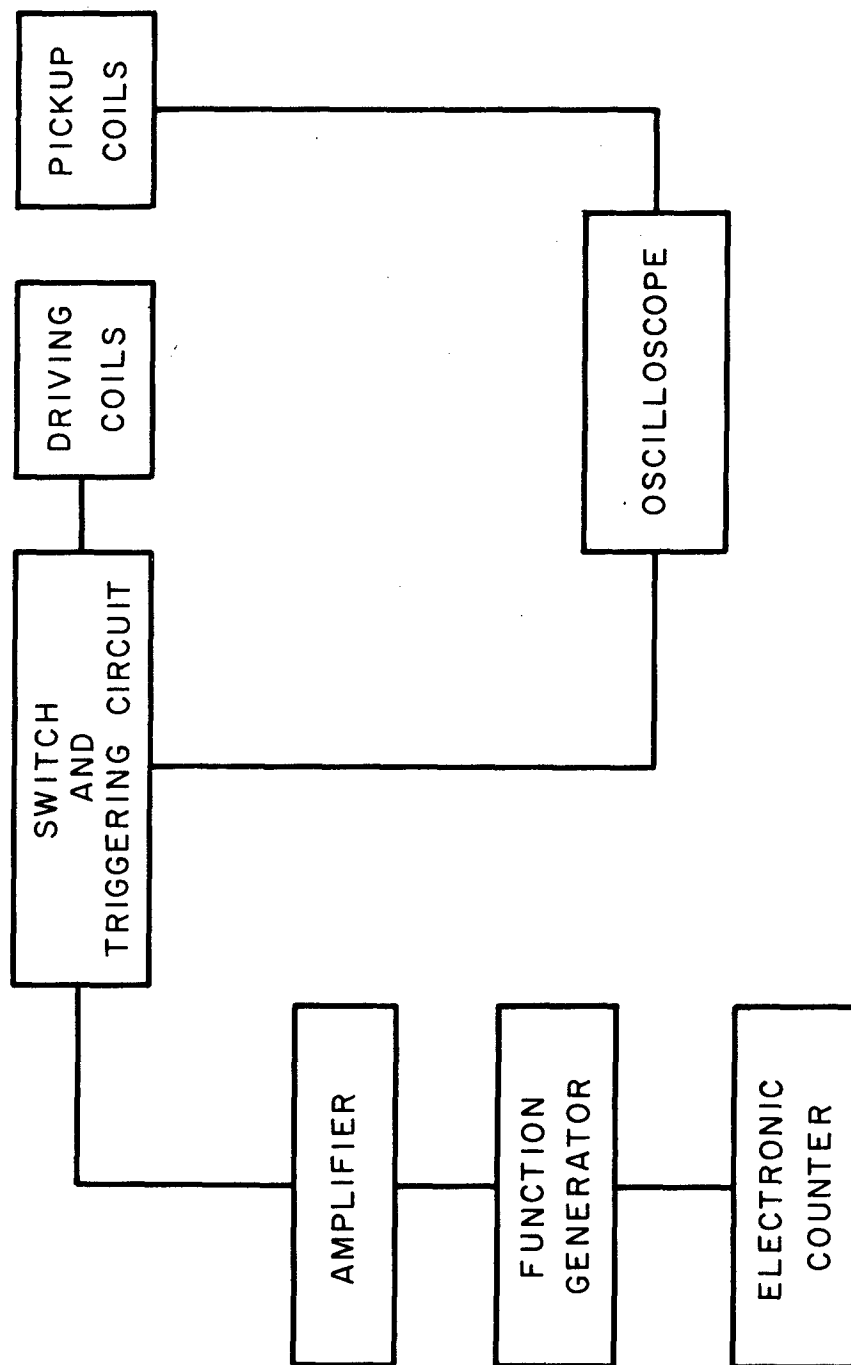


FIG. 4 EXPERIMENTAL ARRANGEMENT OF THE ELECTRICAL SYSTEM.

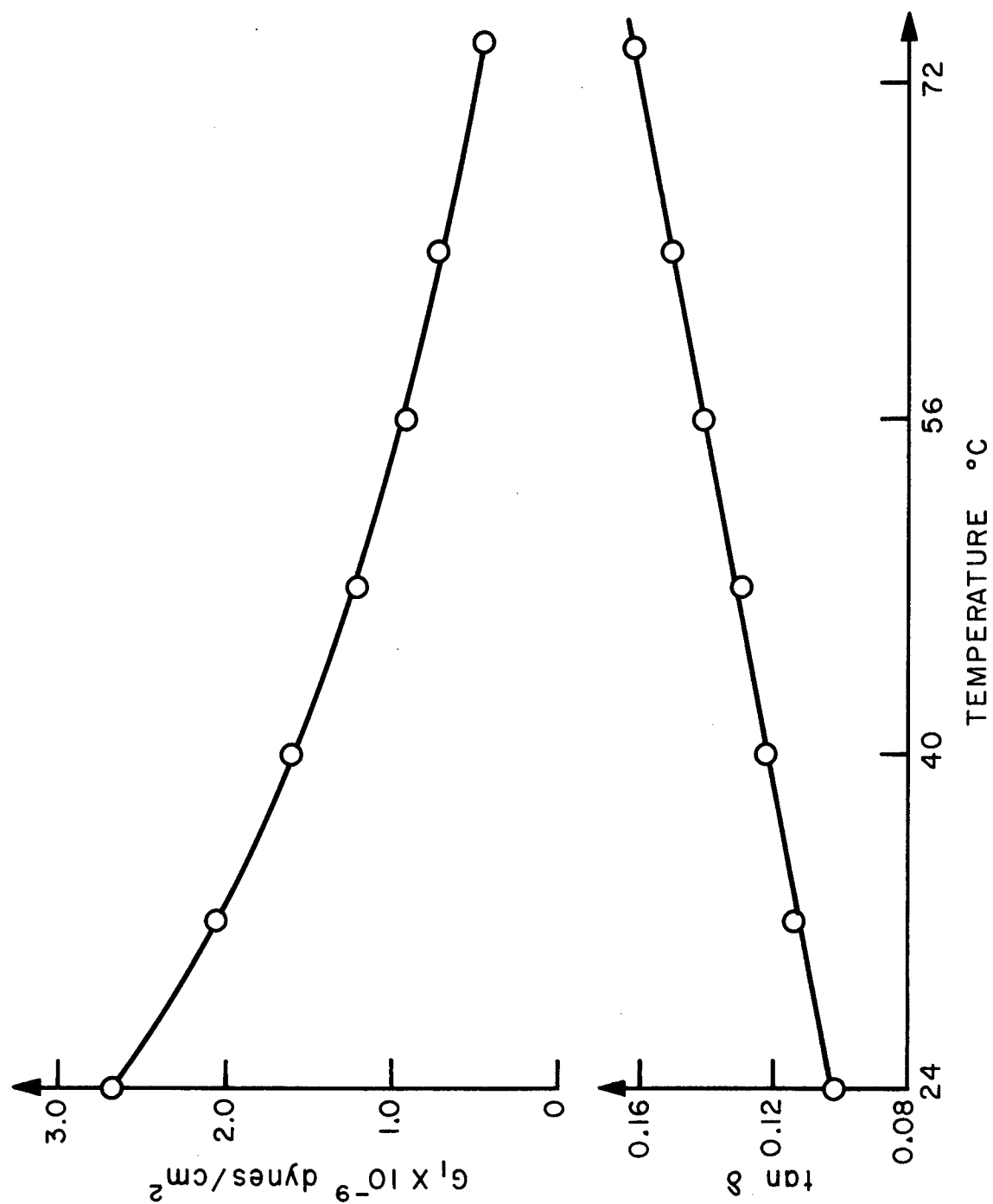


FIG. 5 TEMPERATURE VARIATION OF  $G'$  AND  $\tan \delta$

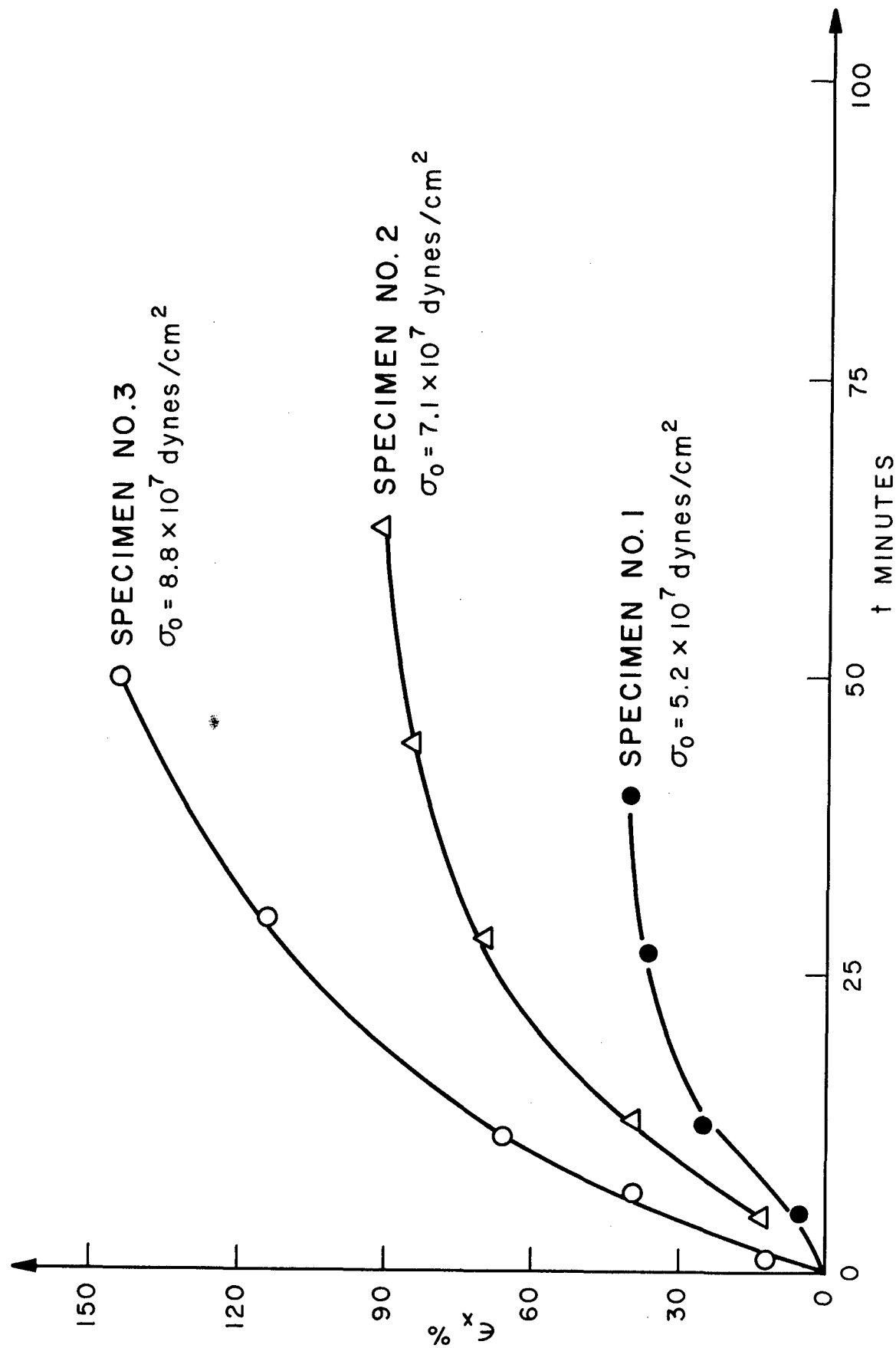


FIG. 6 STRAIN VERSUS TIME DURING LONGITUDINAL CREEP.

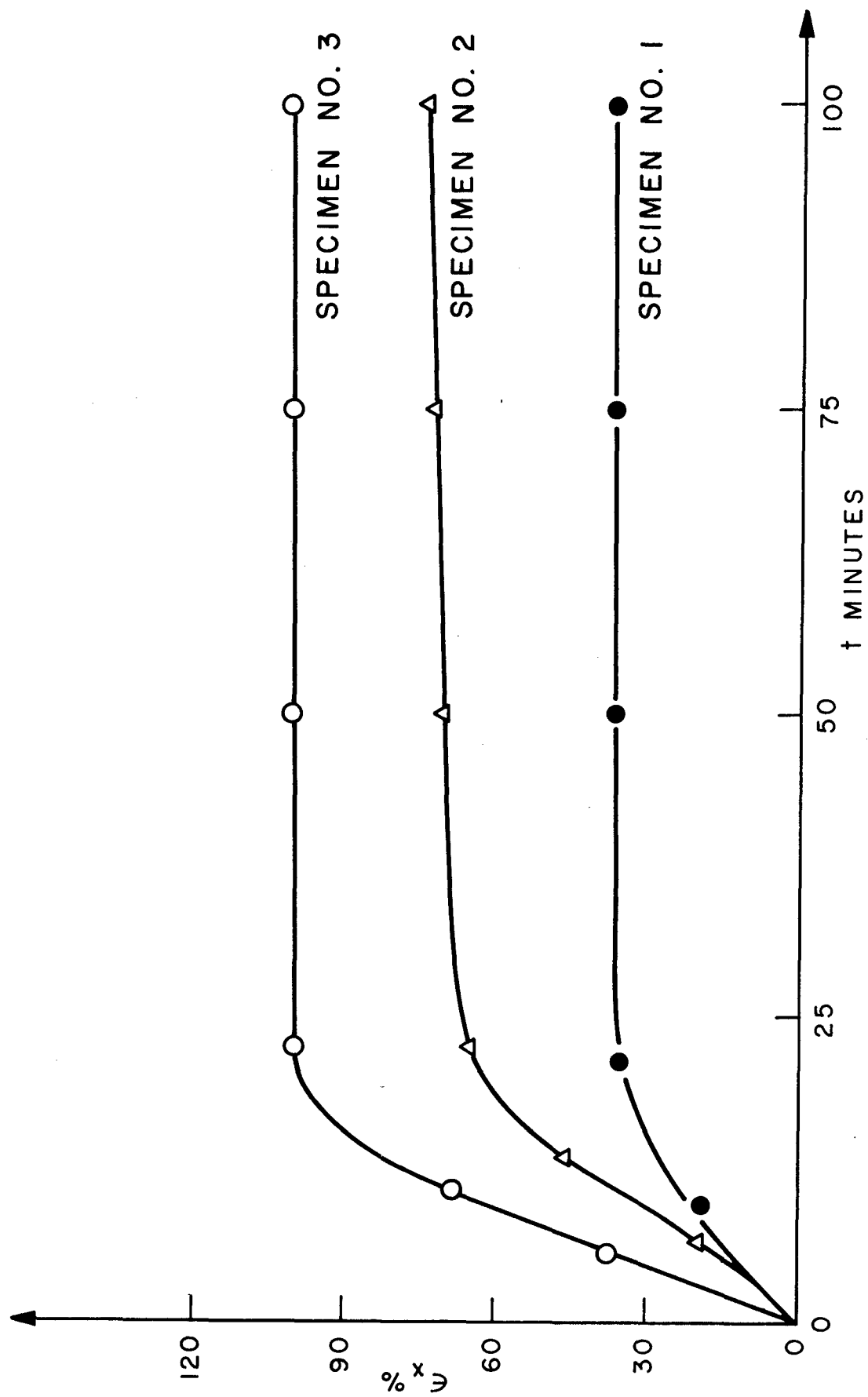


FIG. 7 STRAIN VERSUS TIME CURVES DURING LONGITUDINAL RECOVERY.

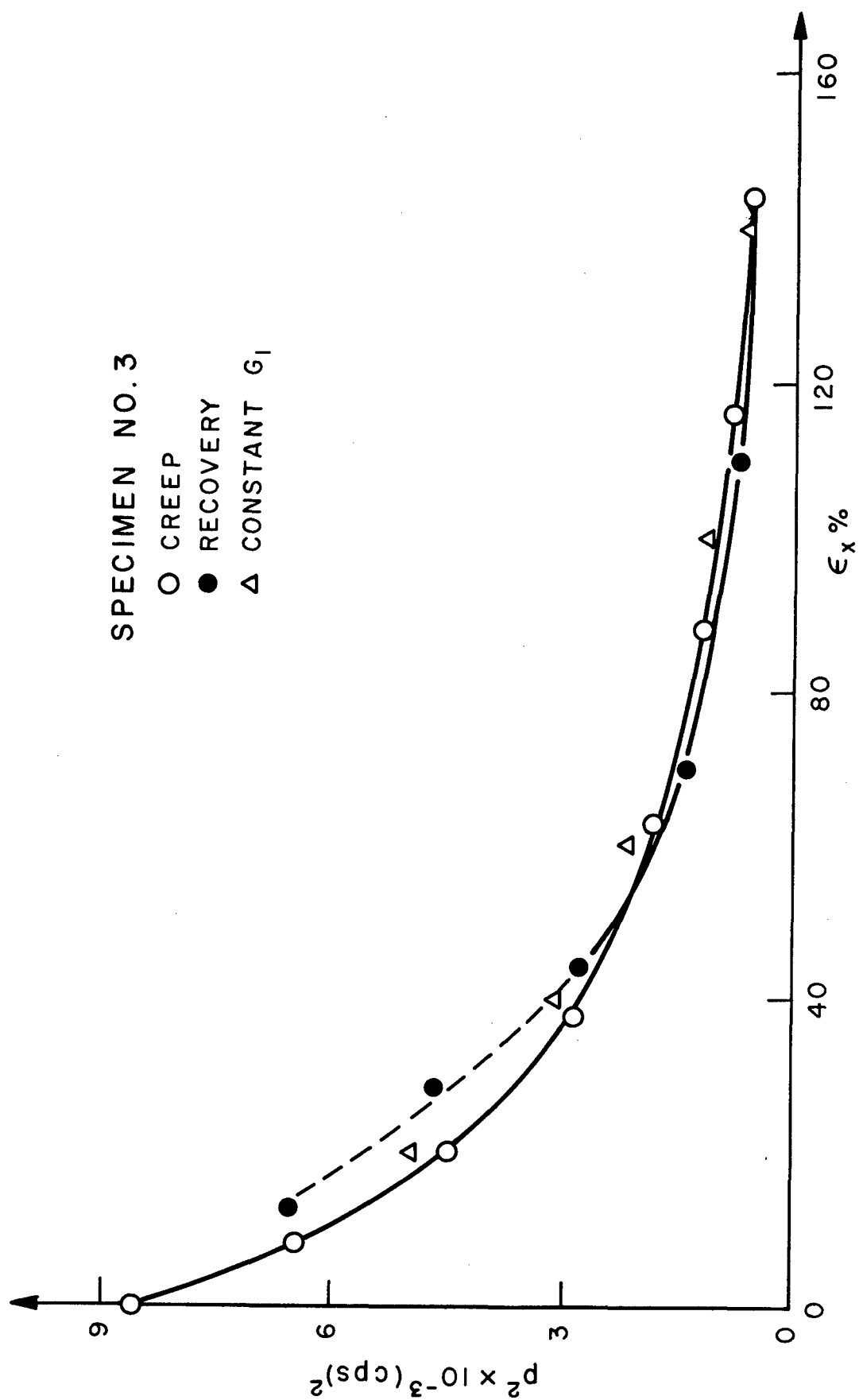


FIG. 8 VARIATION OF THE SQUARE OF THE NATURAL FREQUENCY  $p$  DURING LONGITUDINAL CREEP AND RECOVERY.

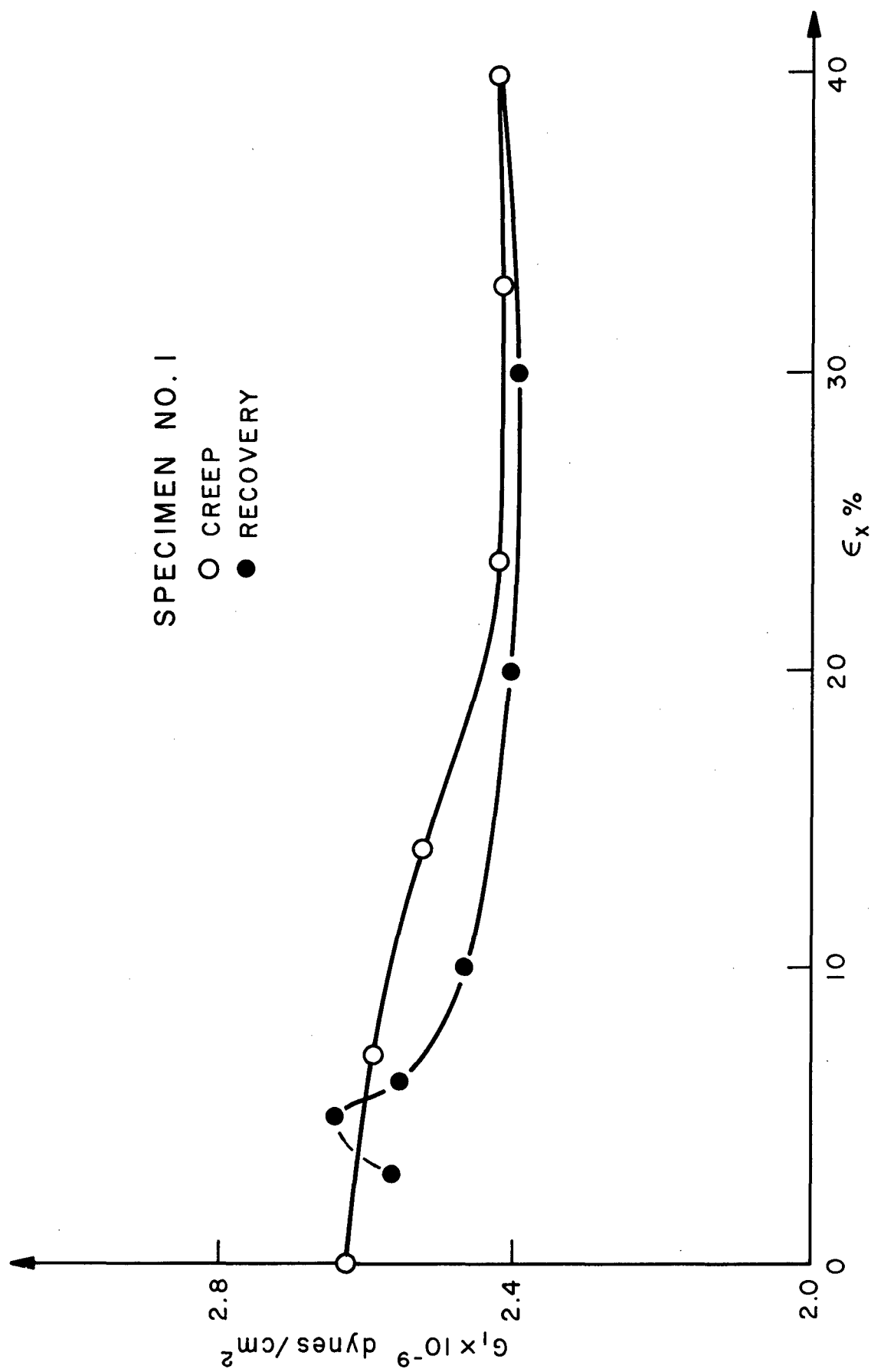


FIG. 9  $G_1$  DURING LONGITUDINAL CREEP AND RECOVERY.



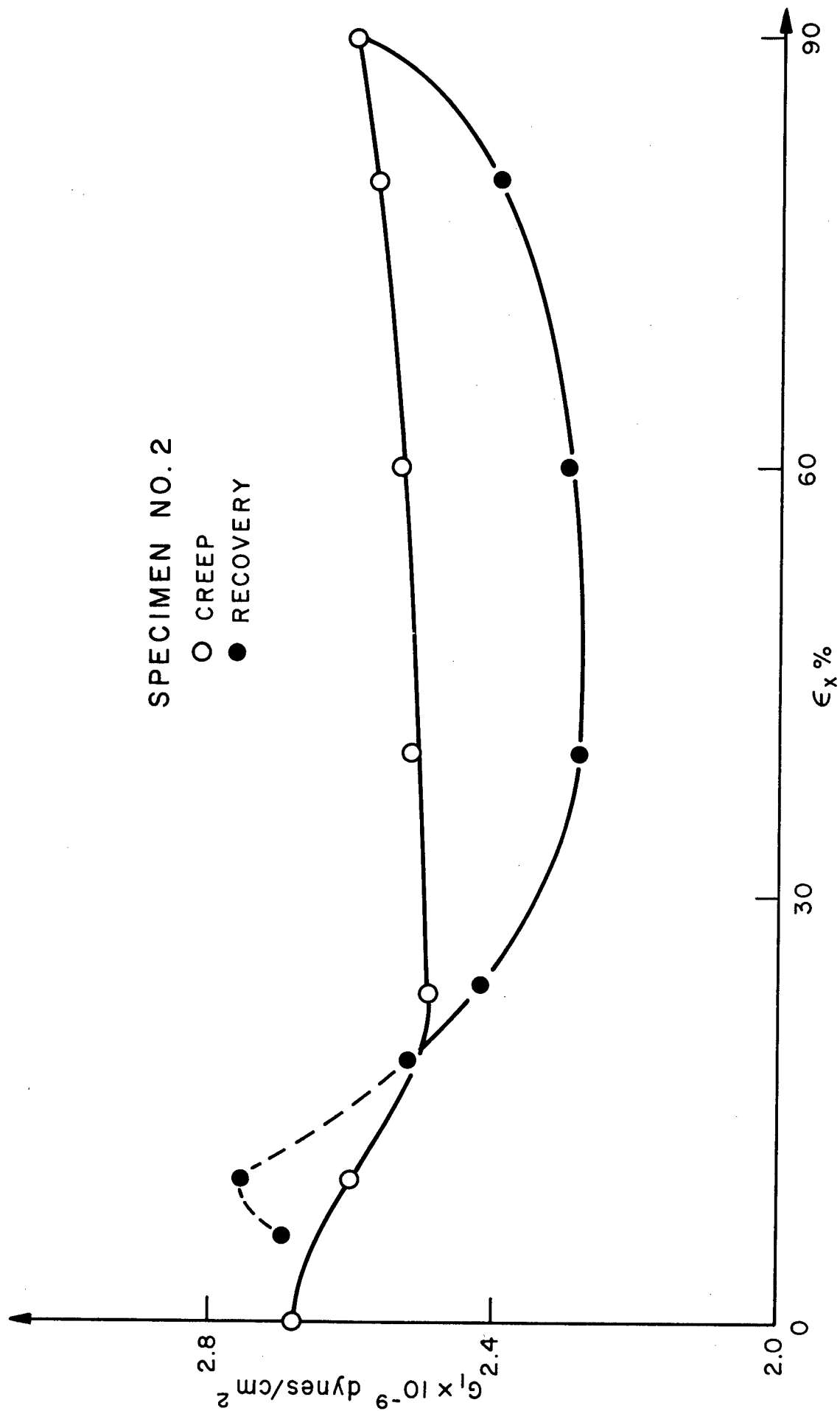


FIG. 10  $G_1$  DURING LONGITUDINAL CREEP AND RECOVERY.

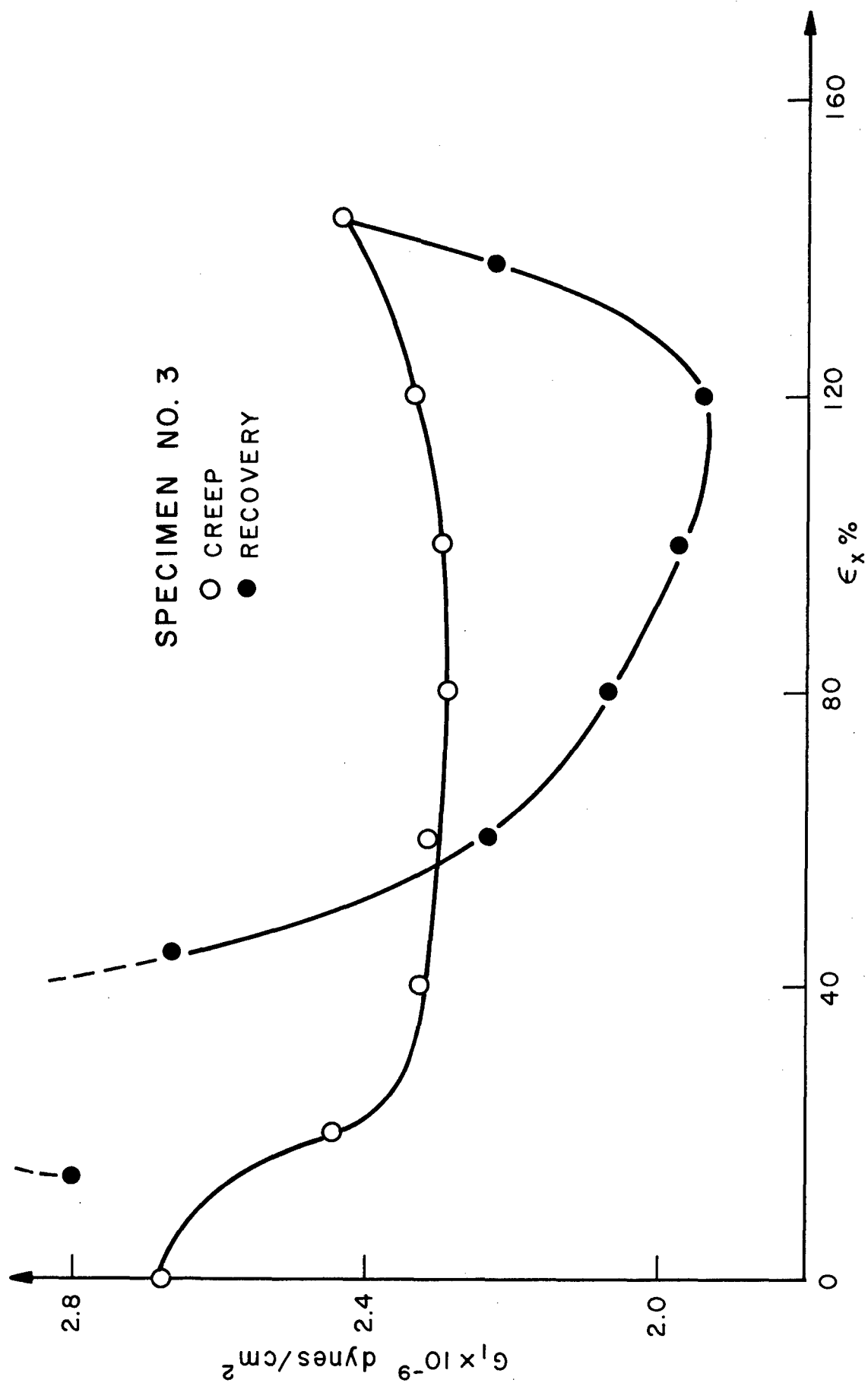


FIG. II  $G_1$  DURING LONGITUDINAL CREEP AND RECOVERY.

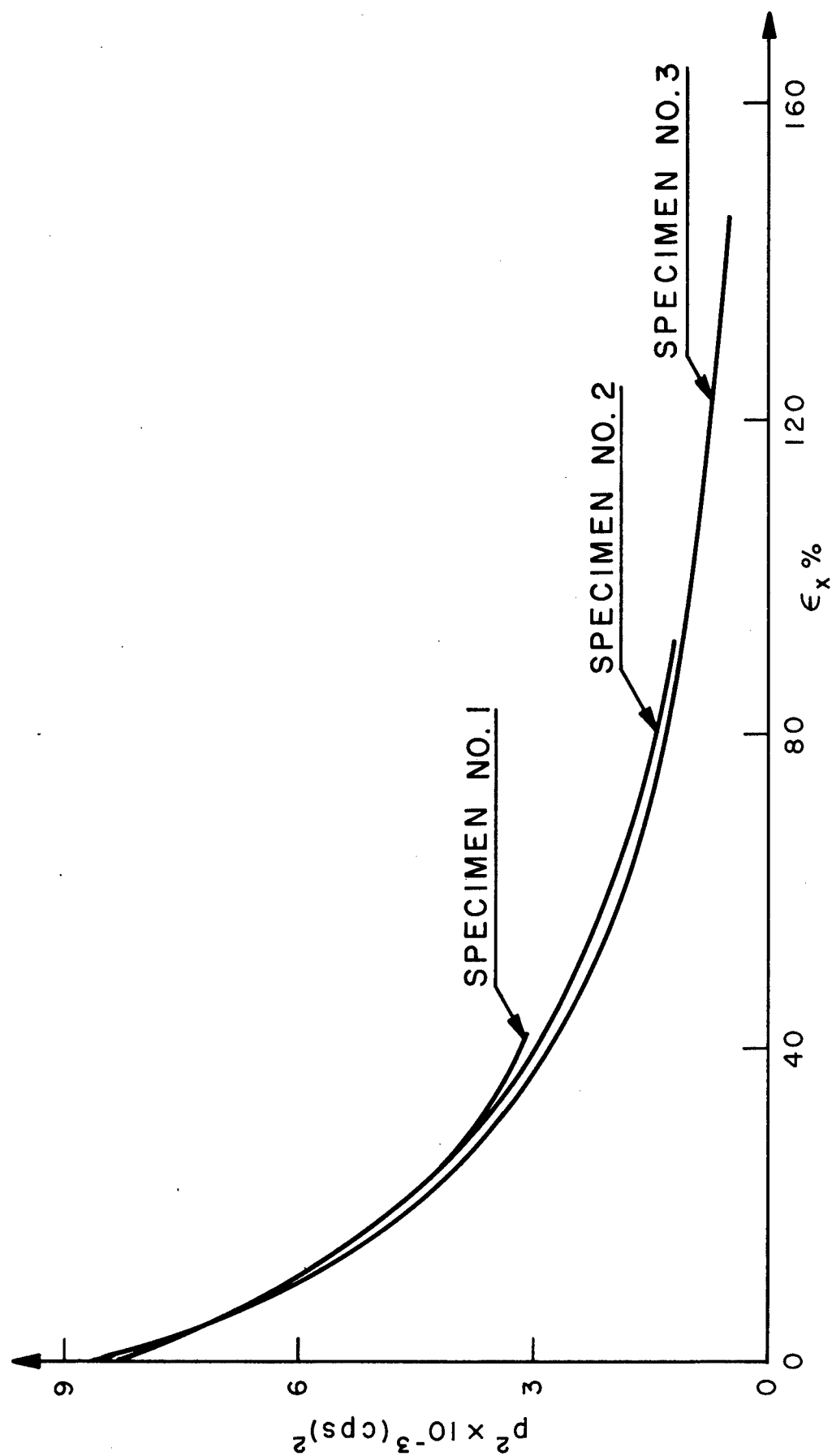


FIG. 12 COMPARISON OF THE SQUARE OF THE NATURAL FREQUENCY  $p$  FOR THREE SPECIMENS.

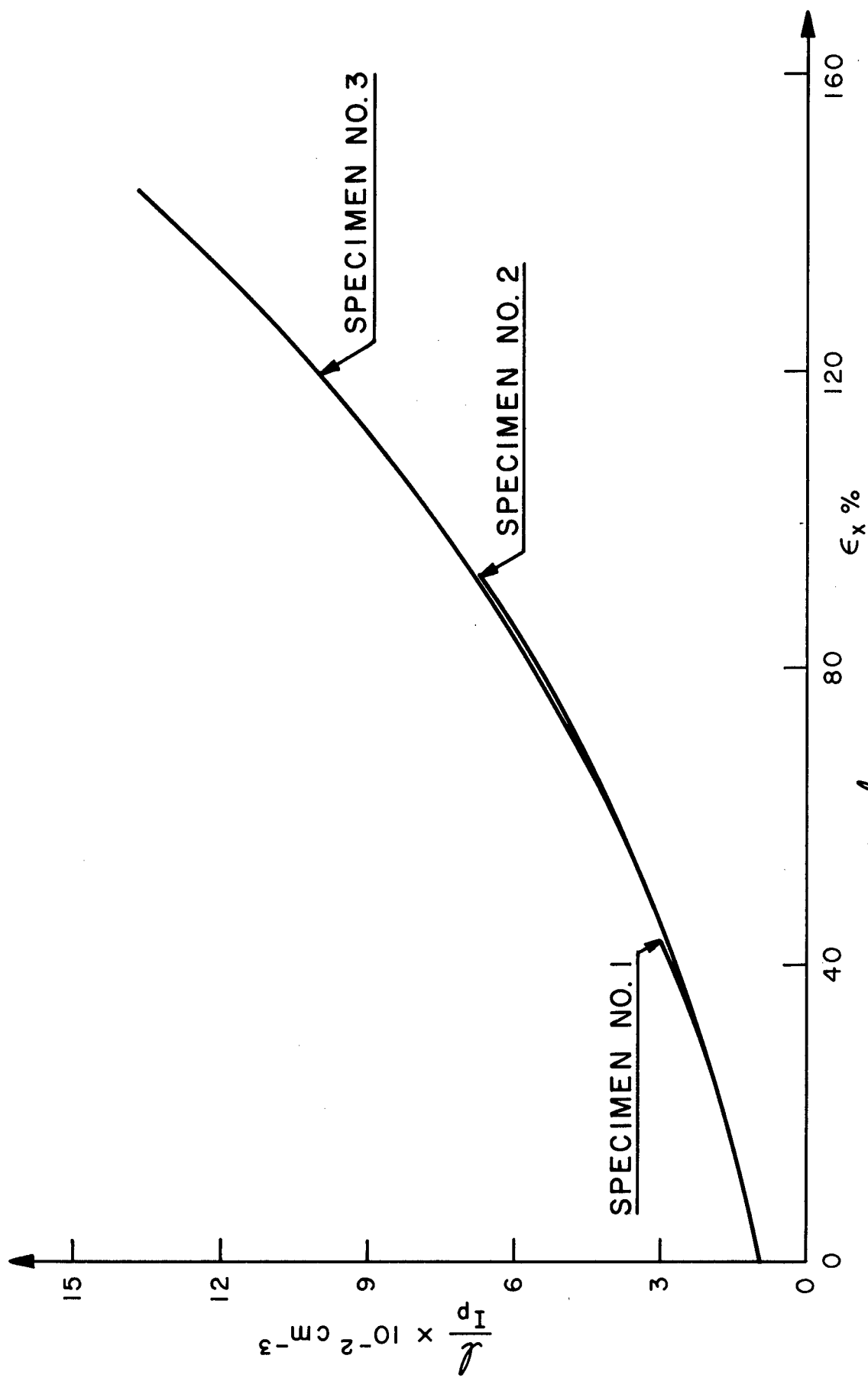


FIG. 13 COMPARISON OF  $\frac{l}{I_p}$  FOR THREE SPECIMENS.

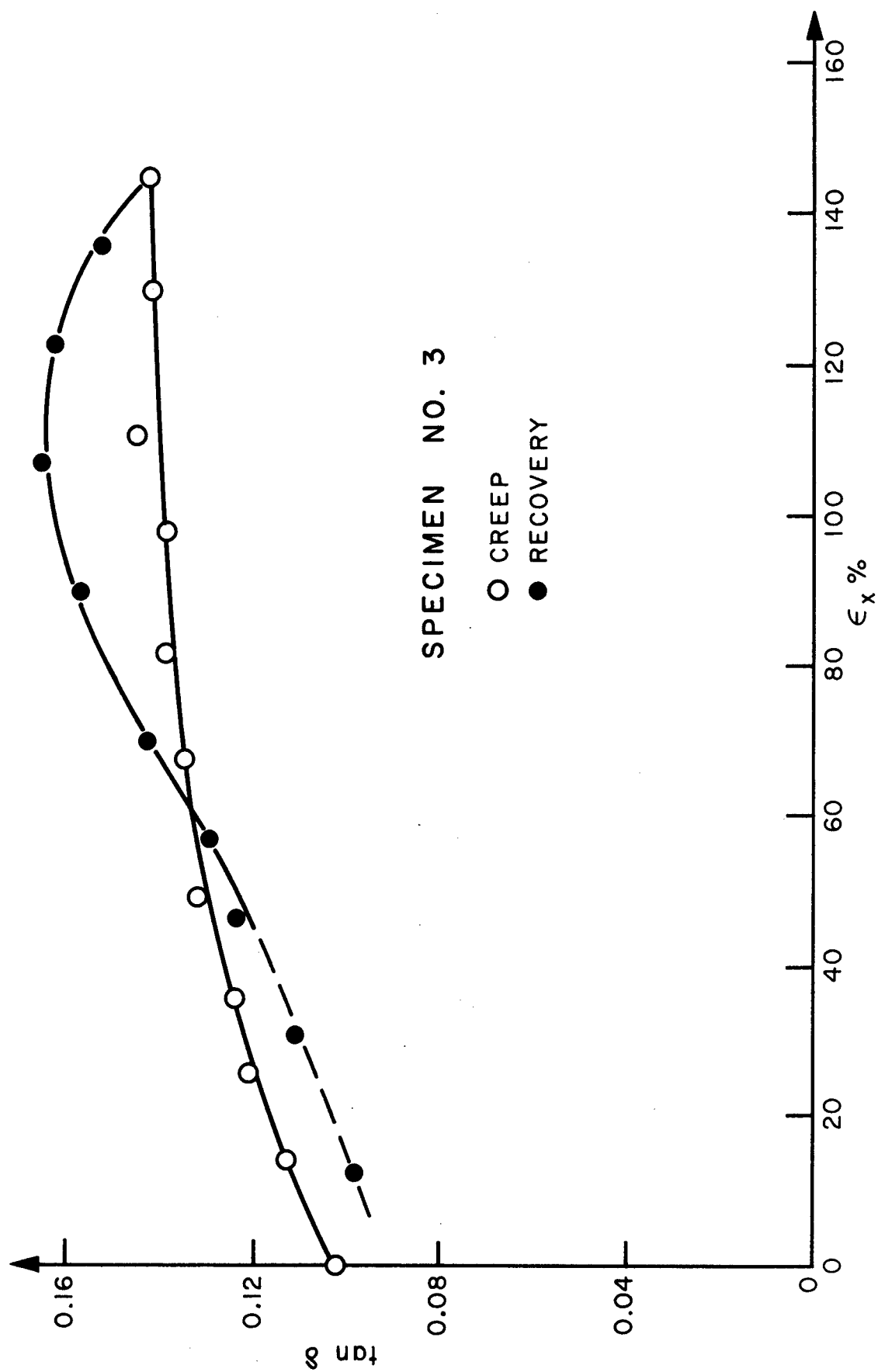


FIG. 14  $\tan \delta = \frac{G_2}{G_1}$  DURING LONGITUDINAL CREEP AND RECOVERY

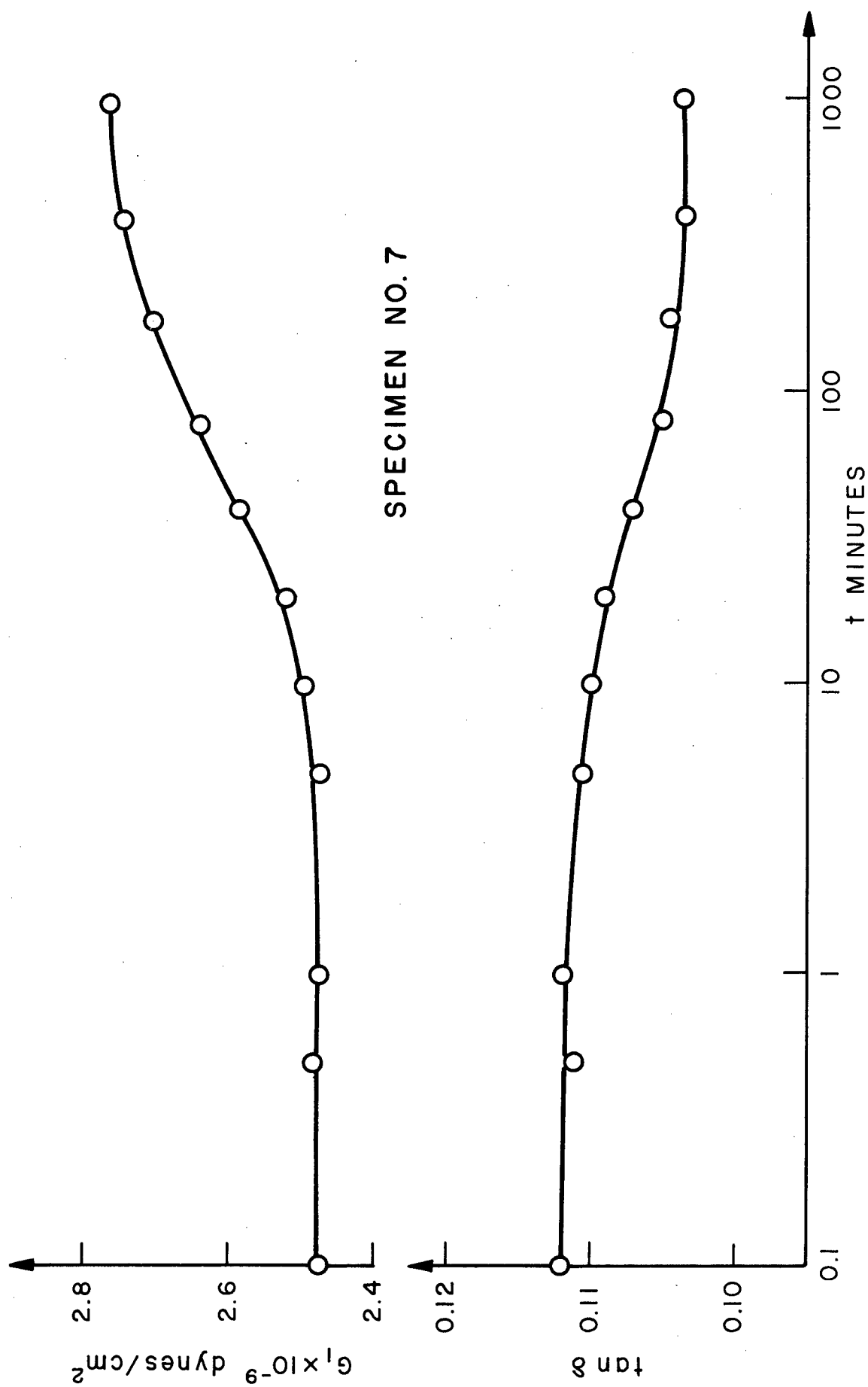


FIG. 15  $G'$  AND  $\tan \delta$  DURING STRESS RELAXATION AT  $\epsilon_x = 22\%$

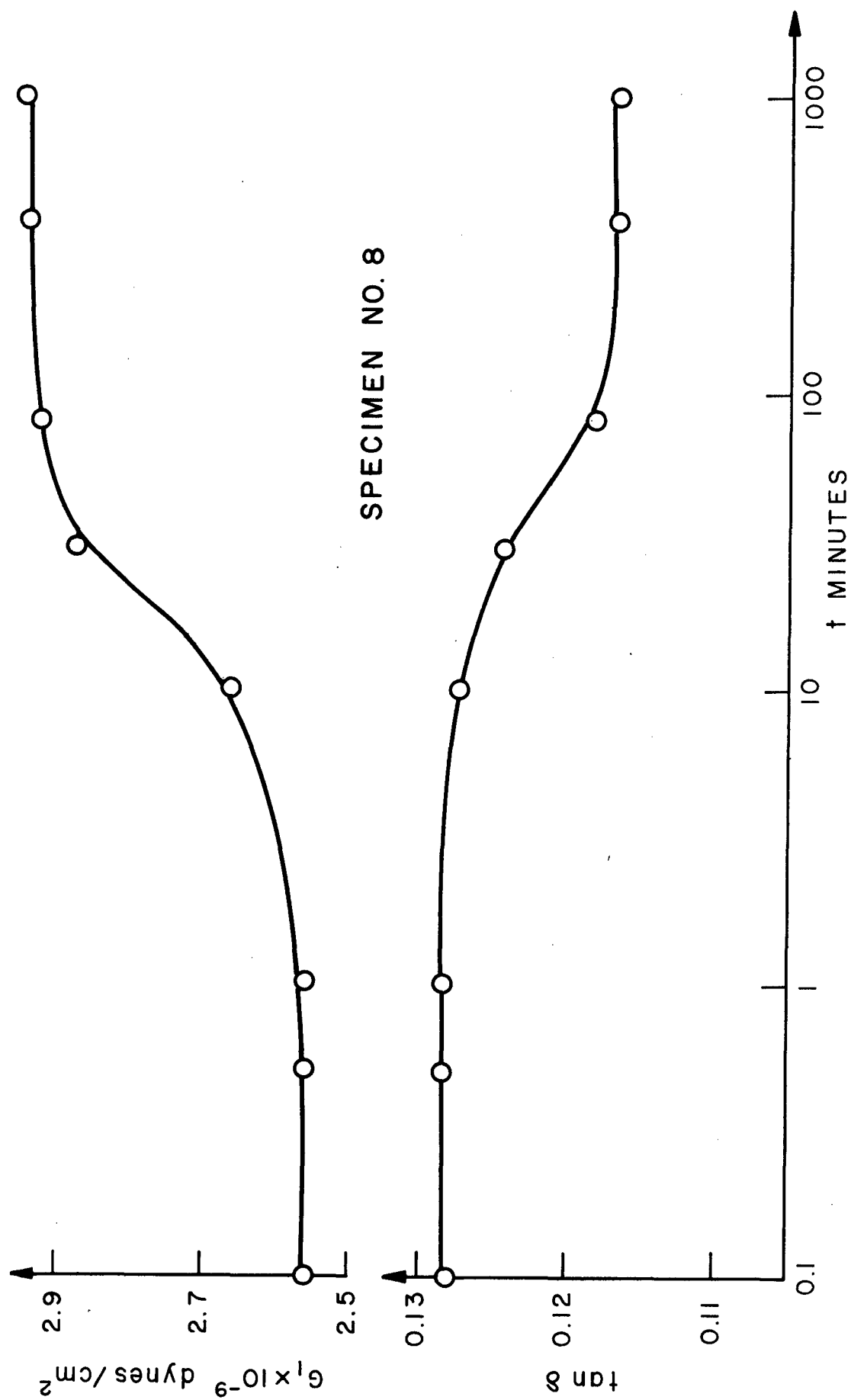


FIG. 16  $G'$  AND  $\tan \delta$  DURING STRESS RELAXATION AT  $\epsilon_x = 115\%$

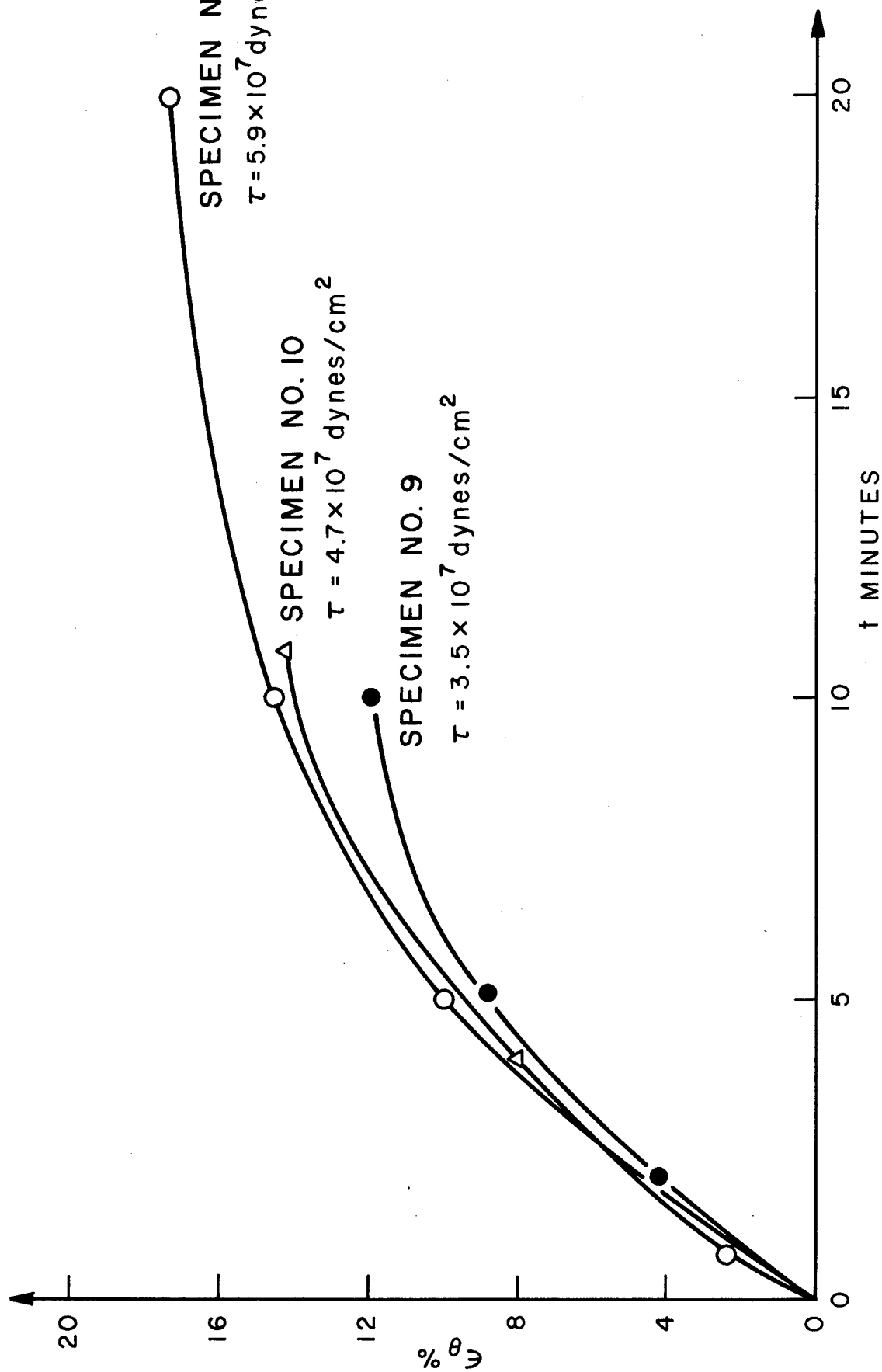


FIG. 17 STRAIN - TIME CURVES DURING TORSIONAL CREEP.



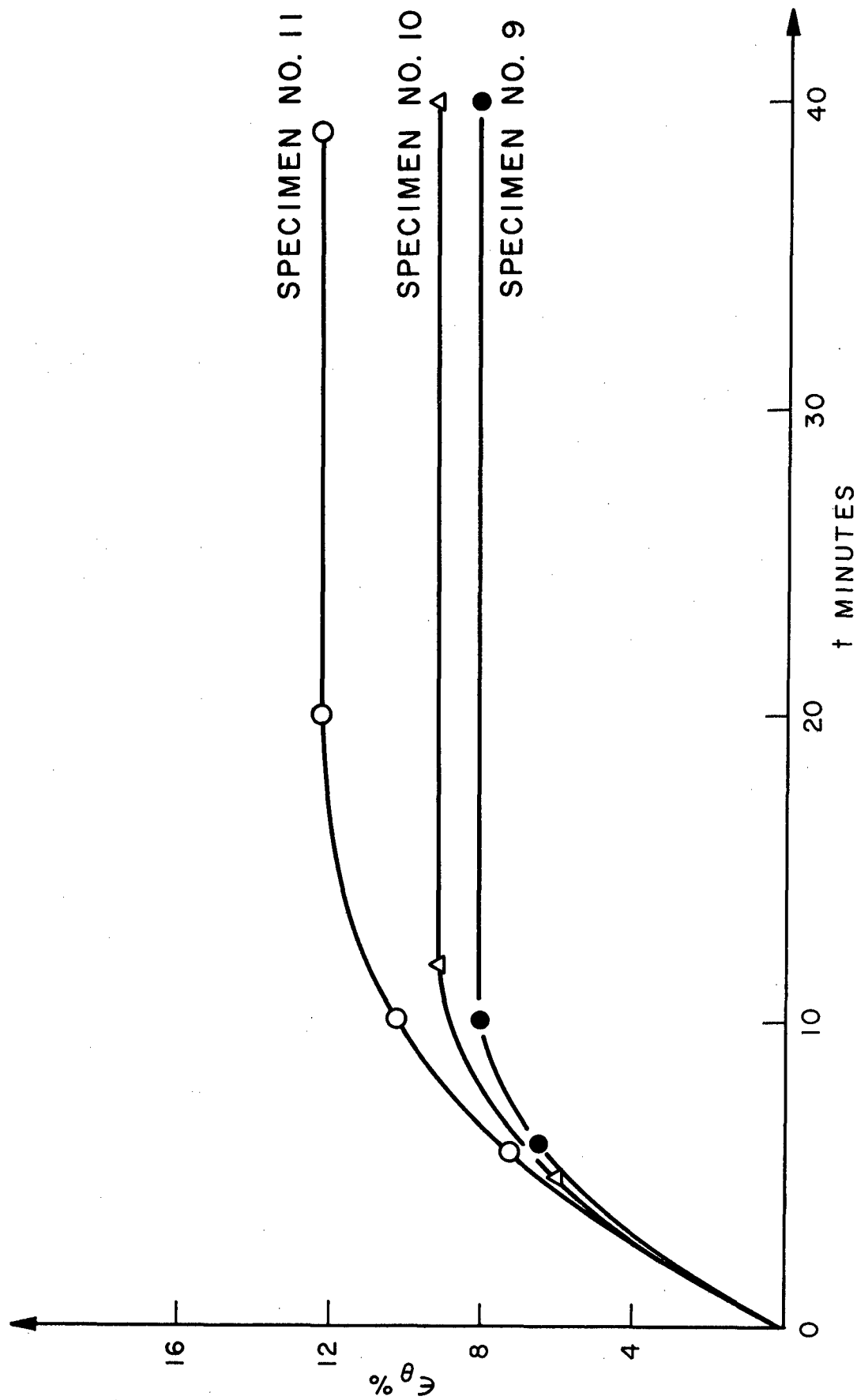


FIG. 18 STRAIN - TIME CURVES DURING TORSIONAL RECOVERY.

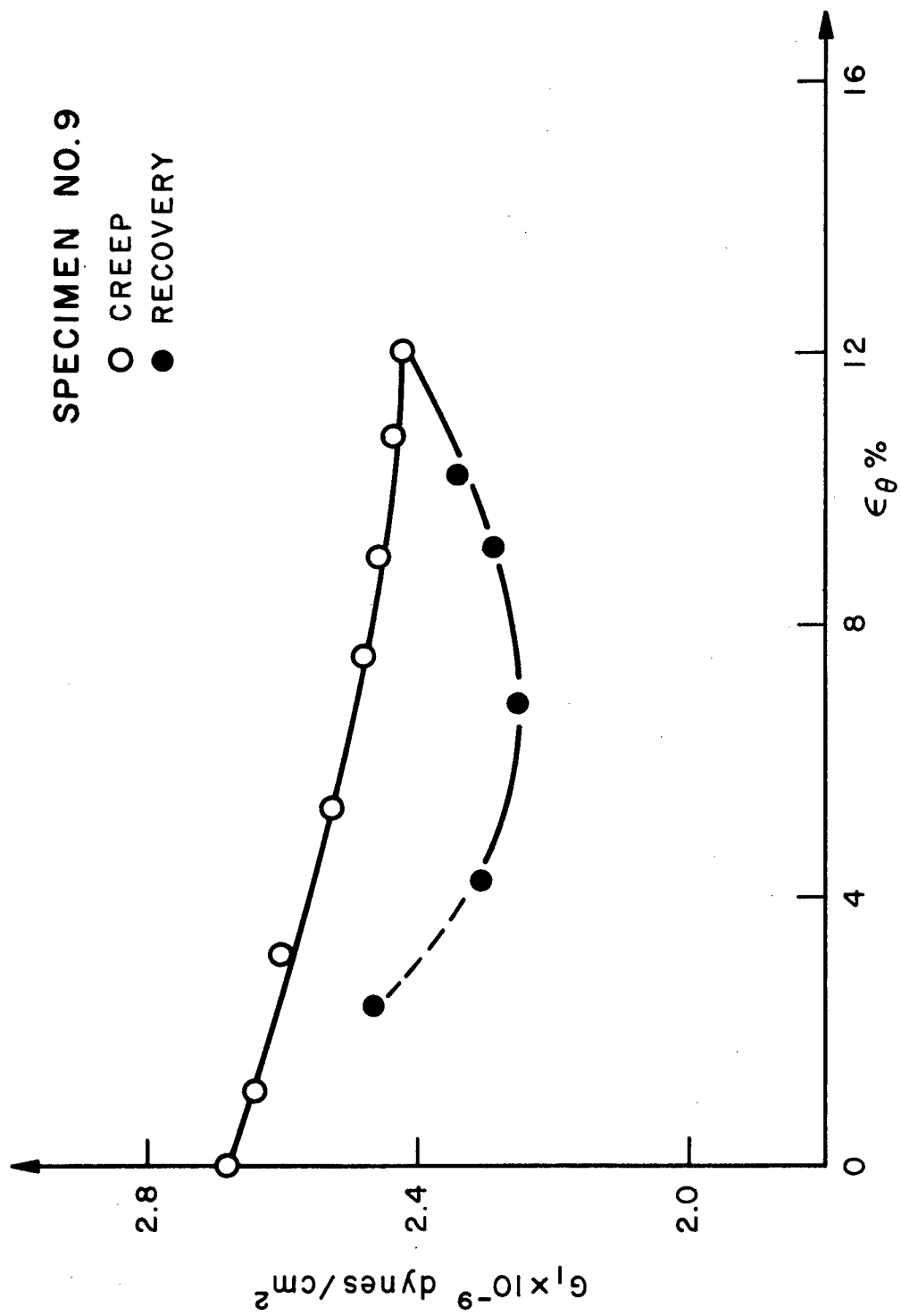


FIG.19  $G_1$  DURING TORSIONAL CREEP AND RECOVERY.

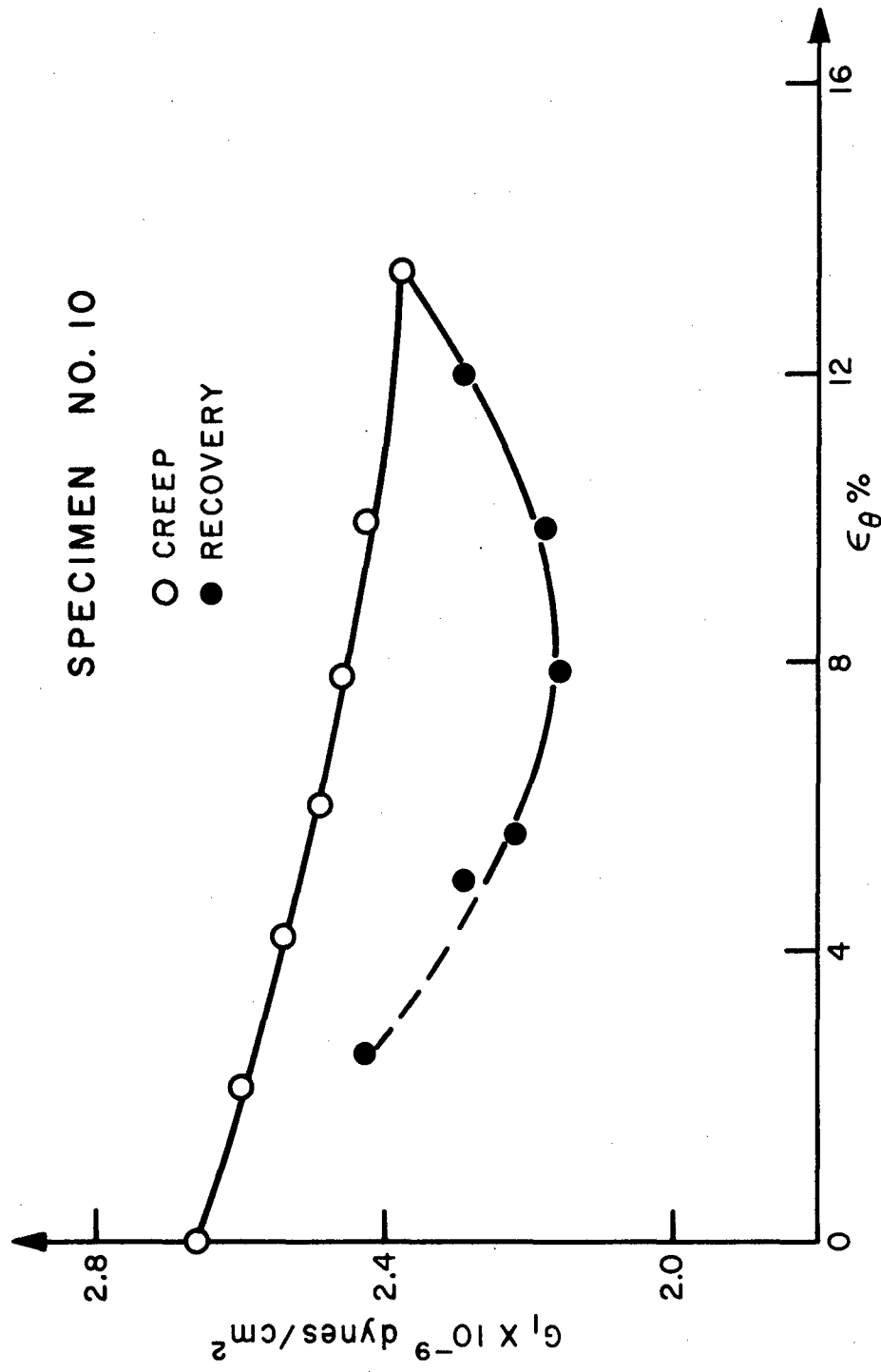


FIG. 20  $G_I$  DURING TORSIONAL CREEP AND RECOVERY

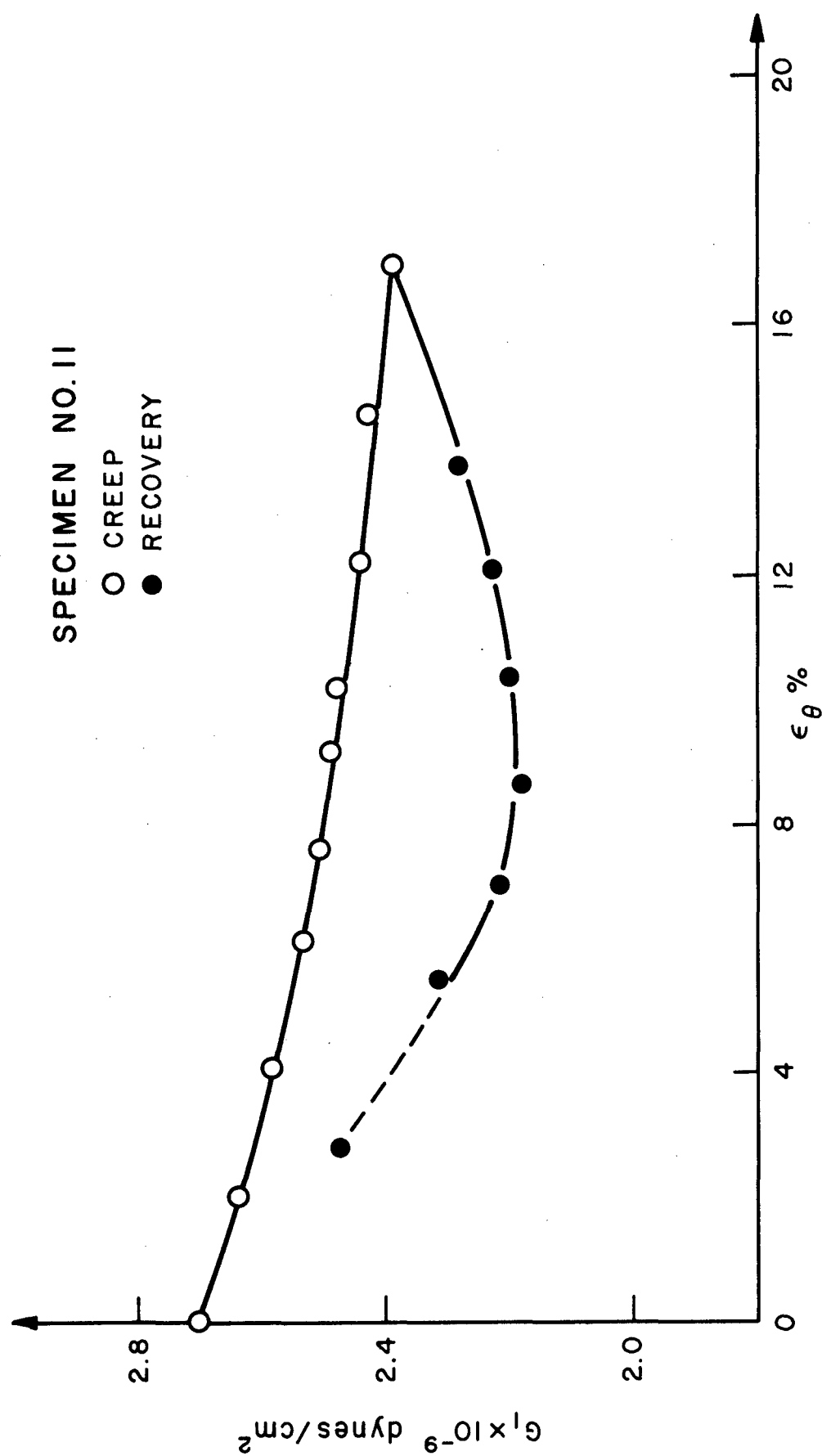


FIG. 21  $G_1$  DURING TORSIONAL CREEP AND RECOVERY.

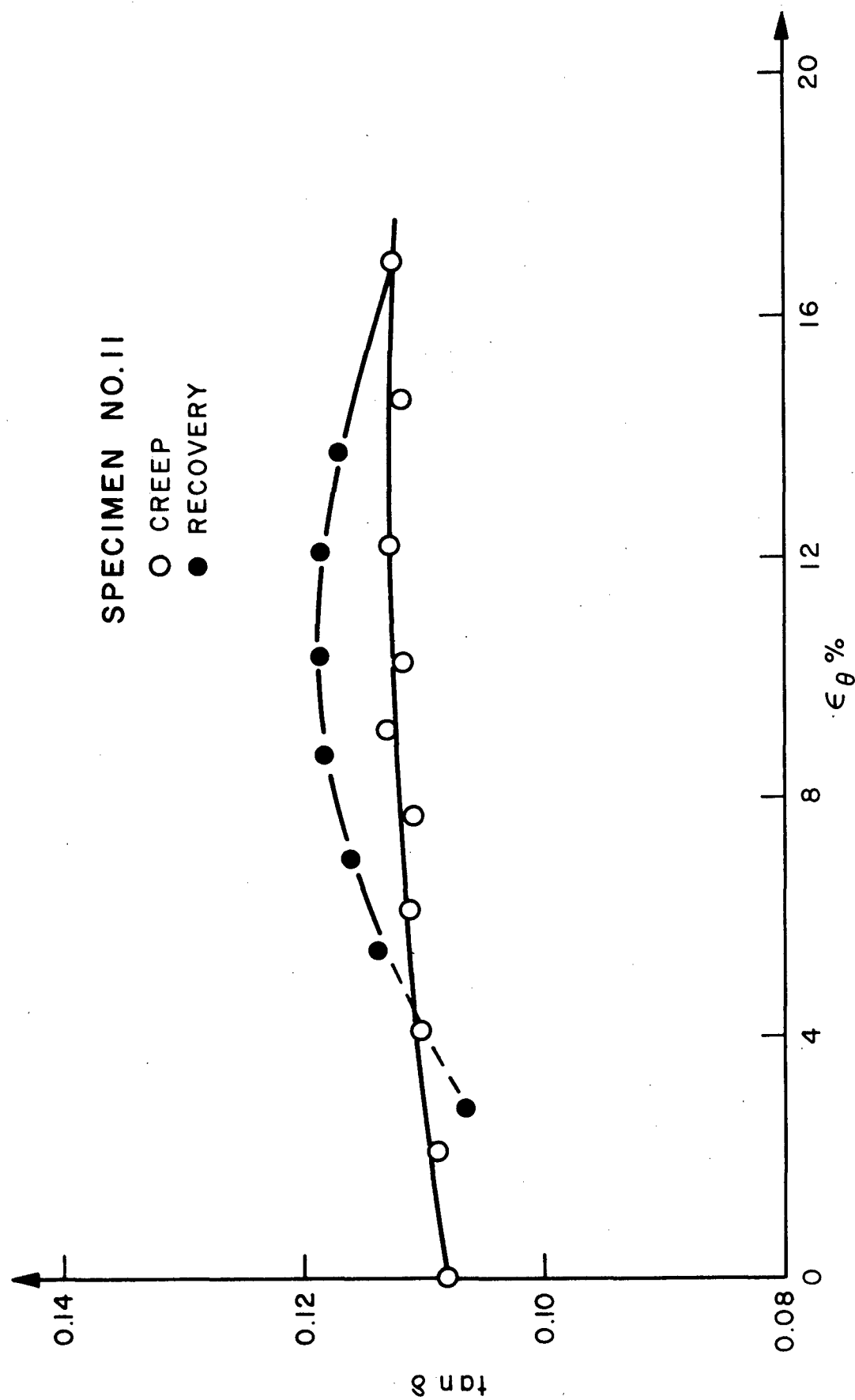


FIG. 22  $\tan \delta = \frac{G_2}{G_1}$  DURING TORSIONAL CREEP AND RECOVERY.

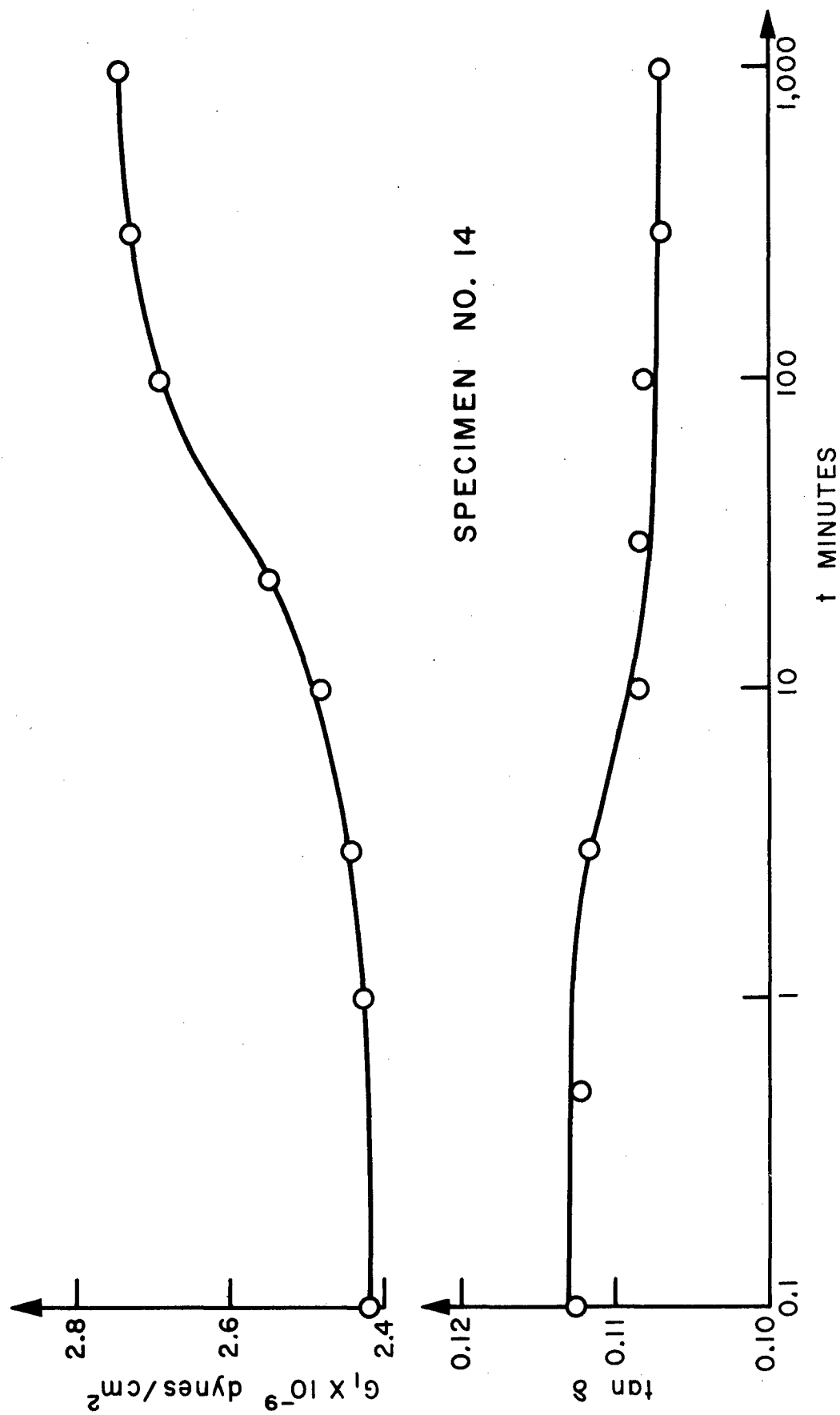


FIG. 23  $G_1$  AND  $\tan \delta$  DURING STRESS RELAXATION AT  $\epsilon_\theta = 16\%$

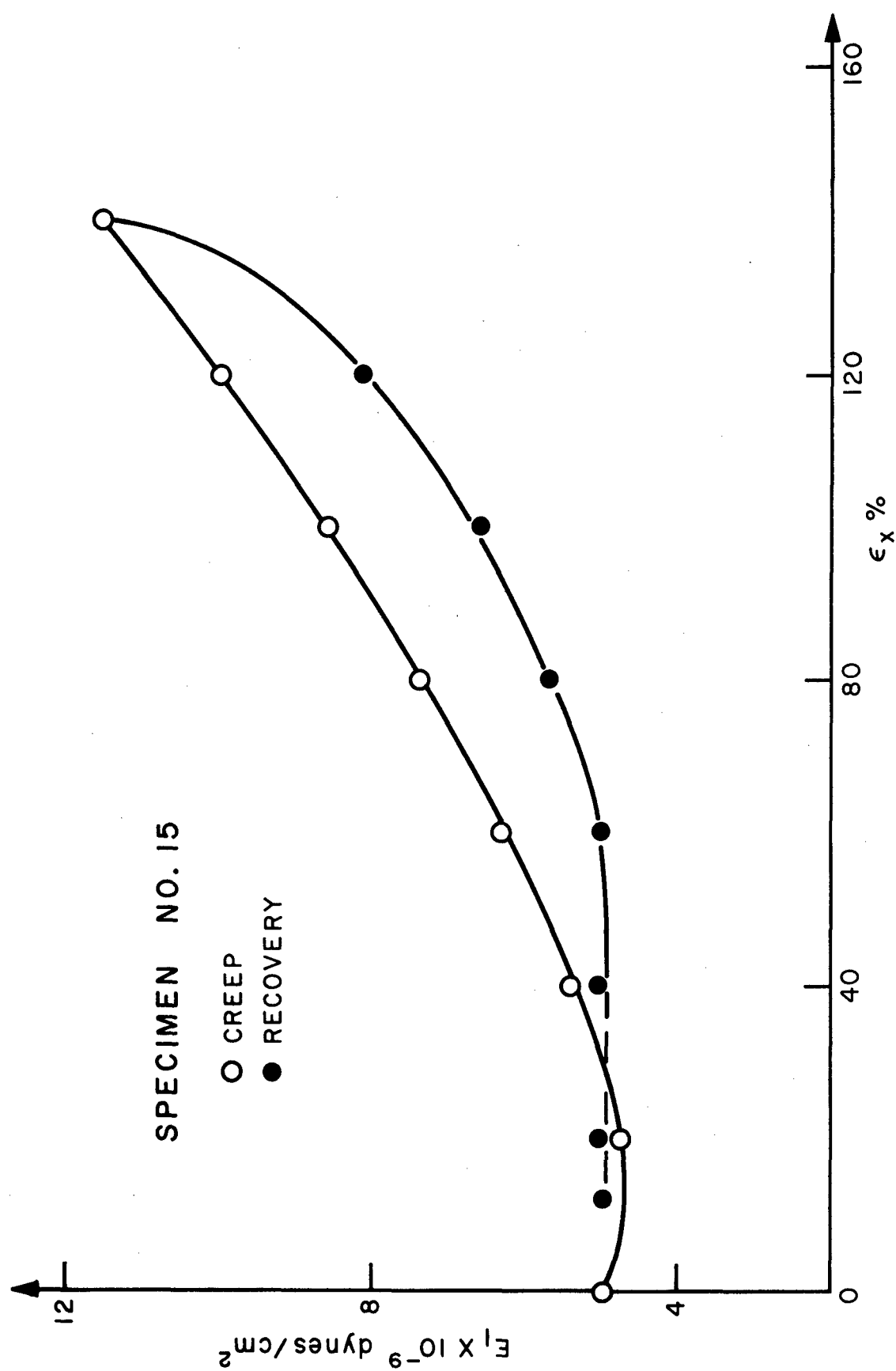


FIG. 24  $E_1$  DURING LONGITUDINAL CREEP AND RECOVERY

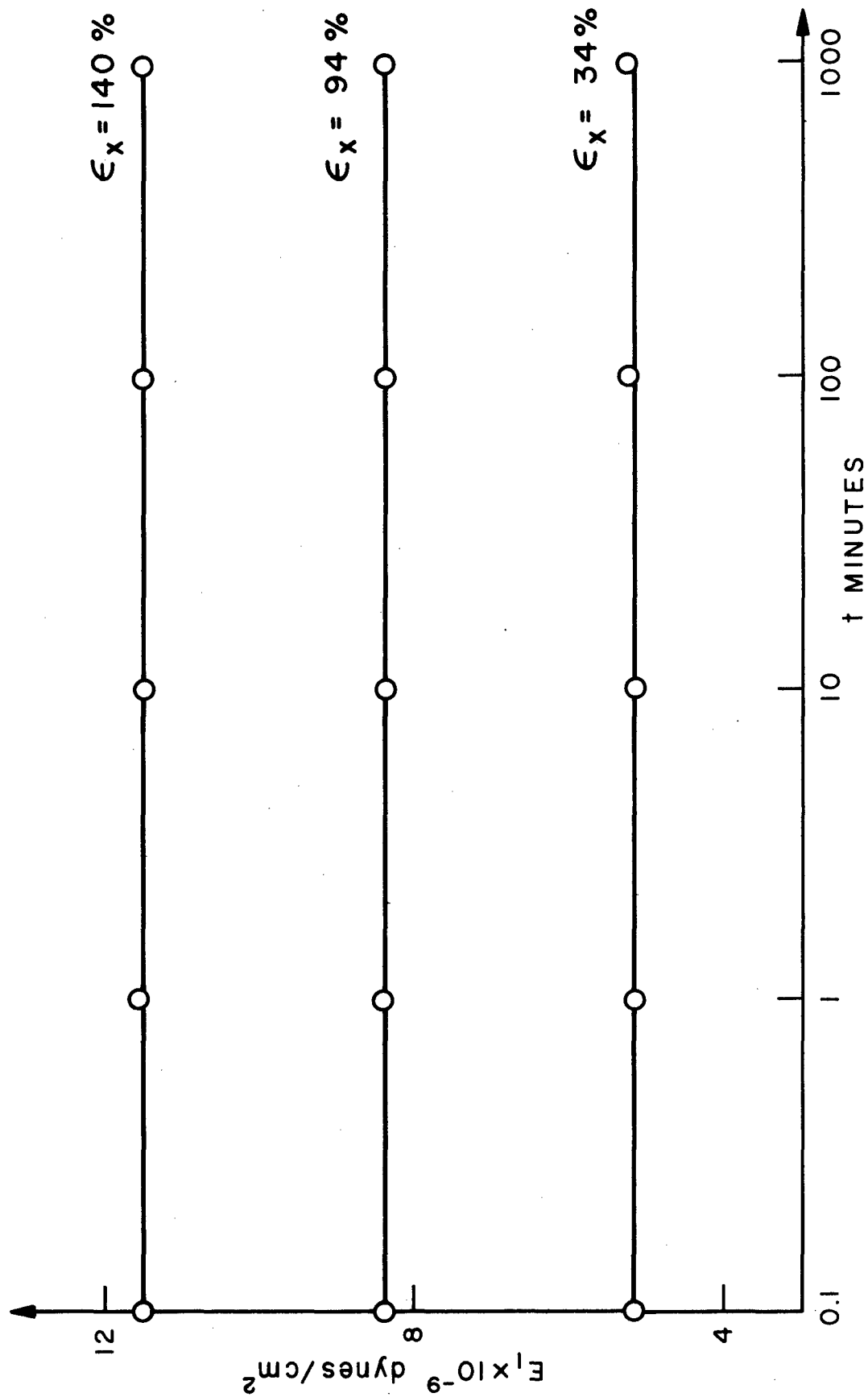


FIG. 25  $E_I$  DURING STRESS RELAXATION AT FIXED LONGITUDINAL STRAINS.



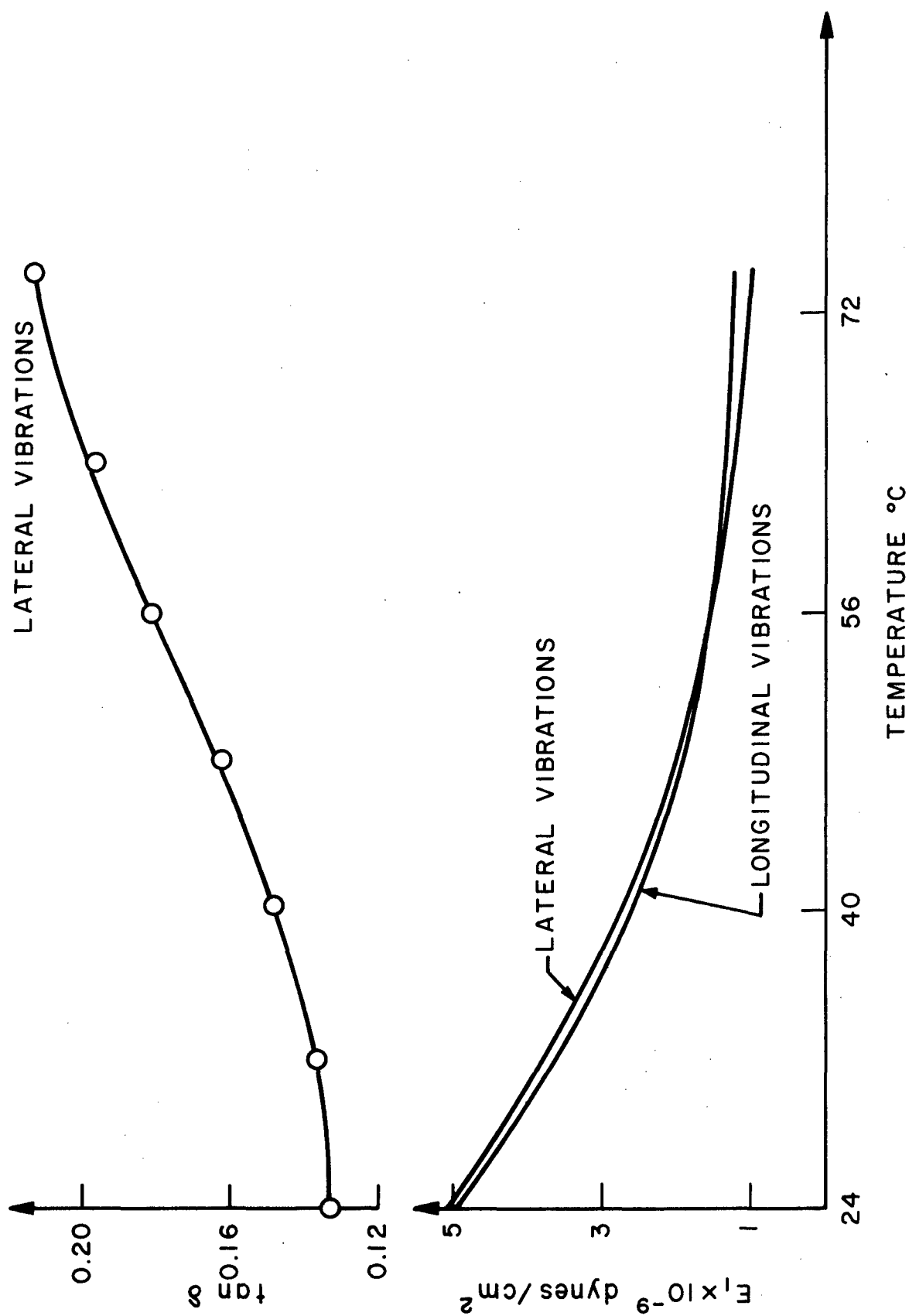


FIG. 26 TEMPERATURE VARIATION OF  $E_1$  AND  $\tan \delta$ .

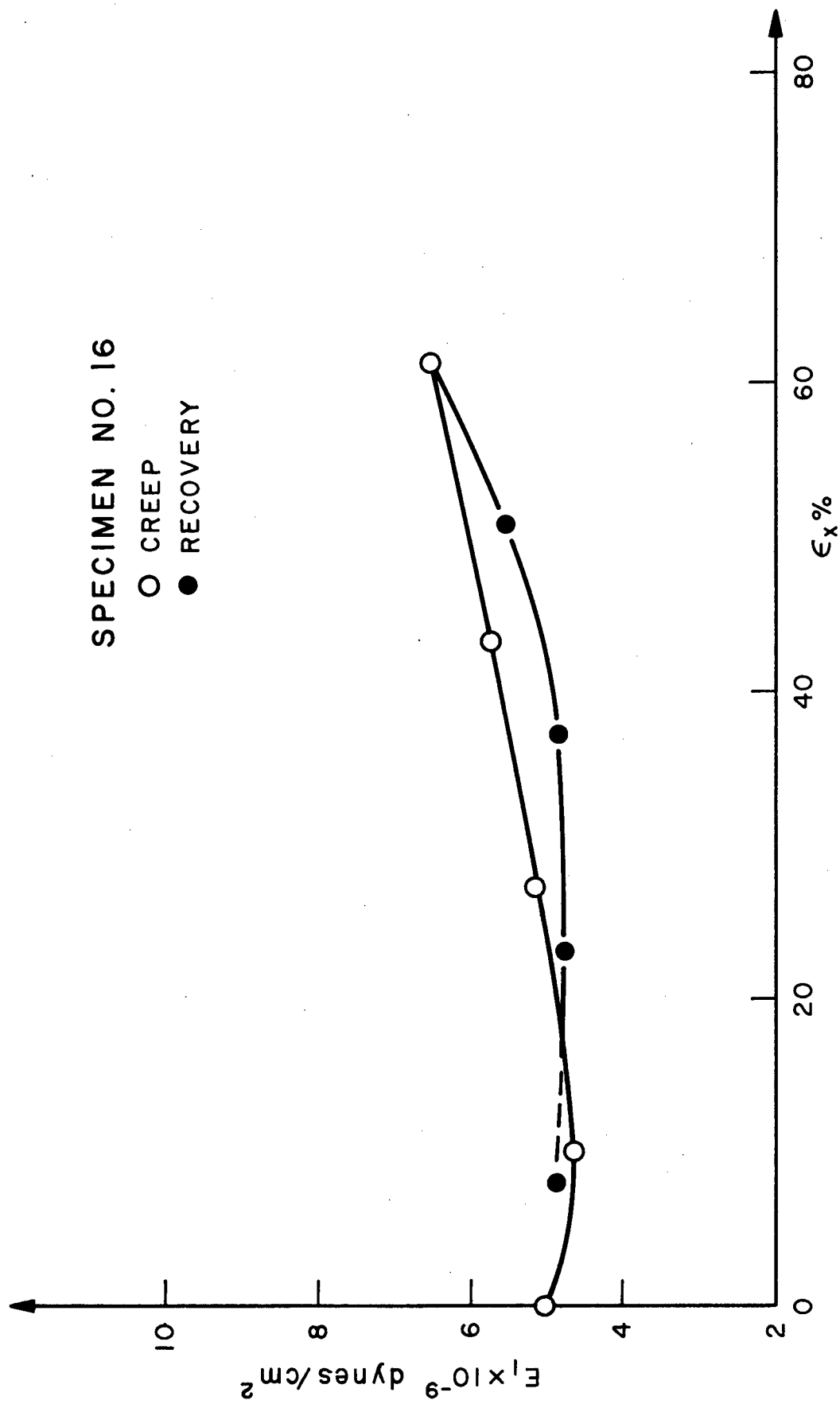


FIG. 27  $E_1$  DURING LONGITUDINAL CREEP AND RECOVERY.

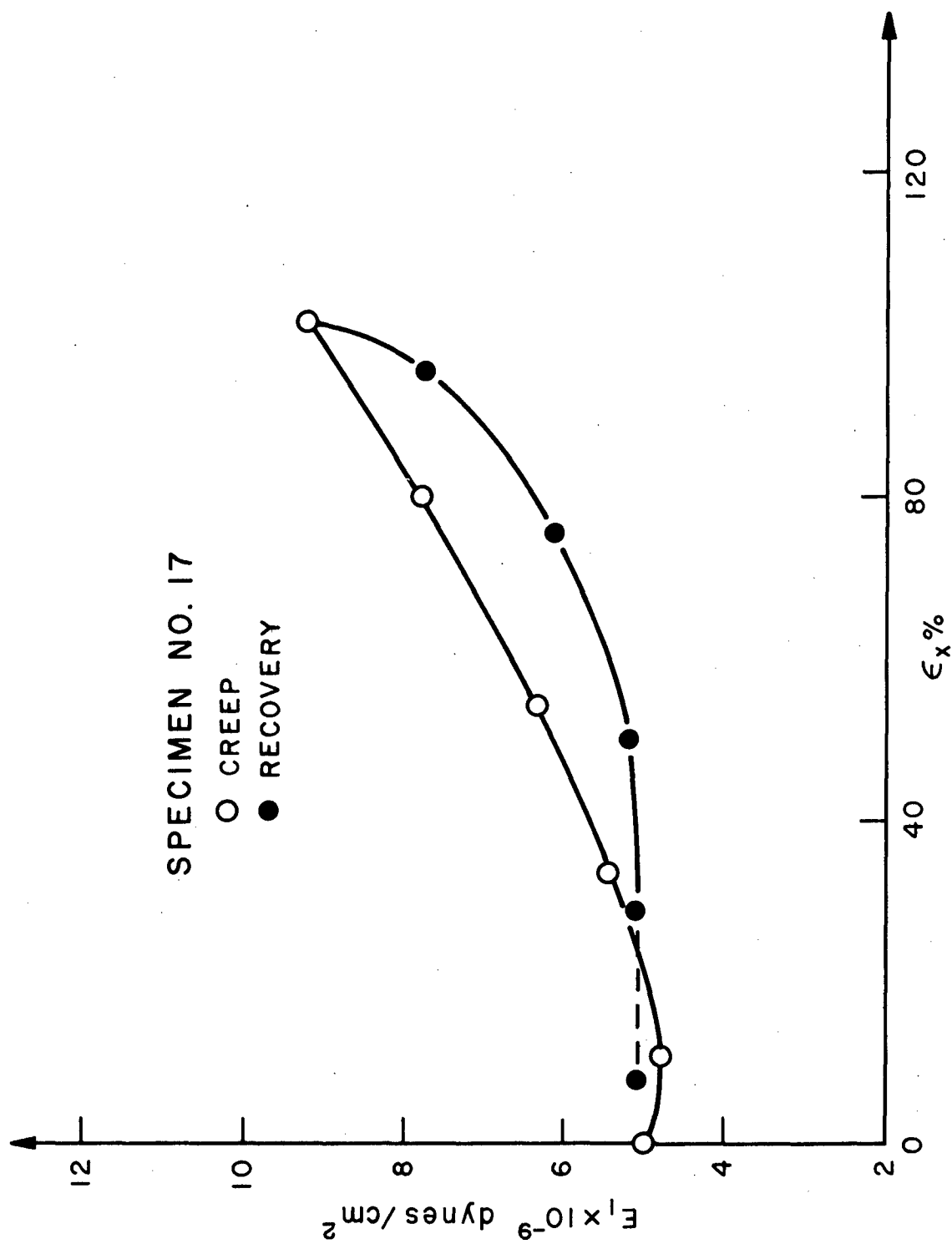


FIG. 28  $E_1$  DURING LONGITUDINAL CREEP AND RECOVERY.

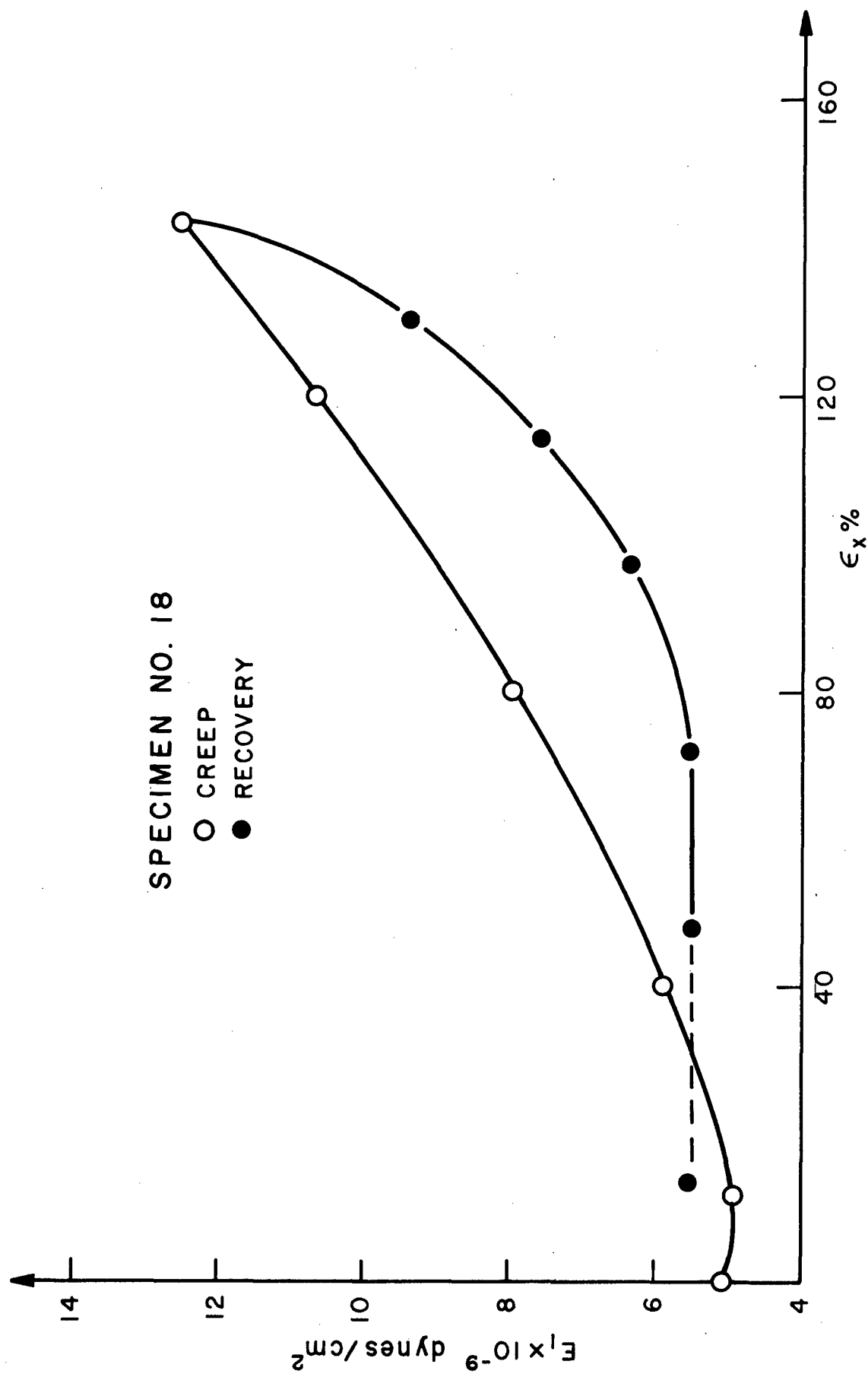


FIG. 29  $E_1$  DURING LONGITUDINAL CREEP AND RECOVERY.

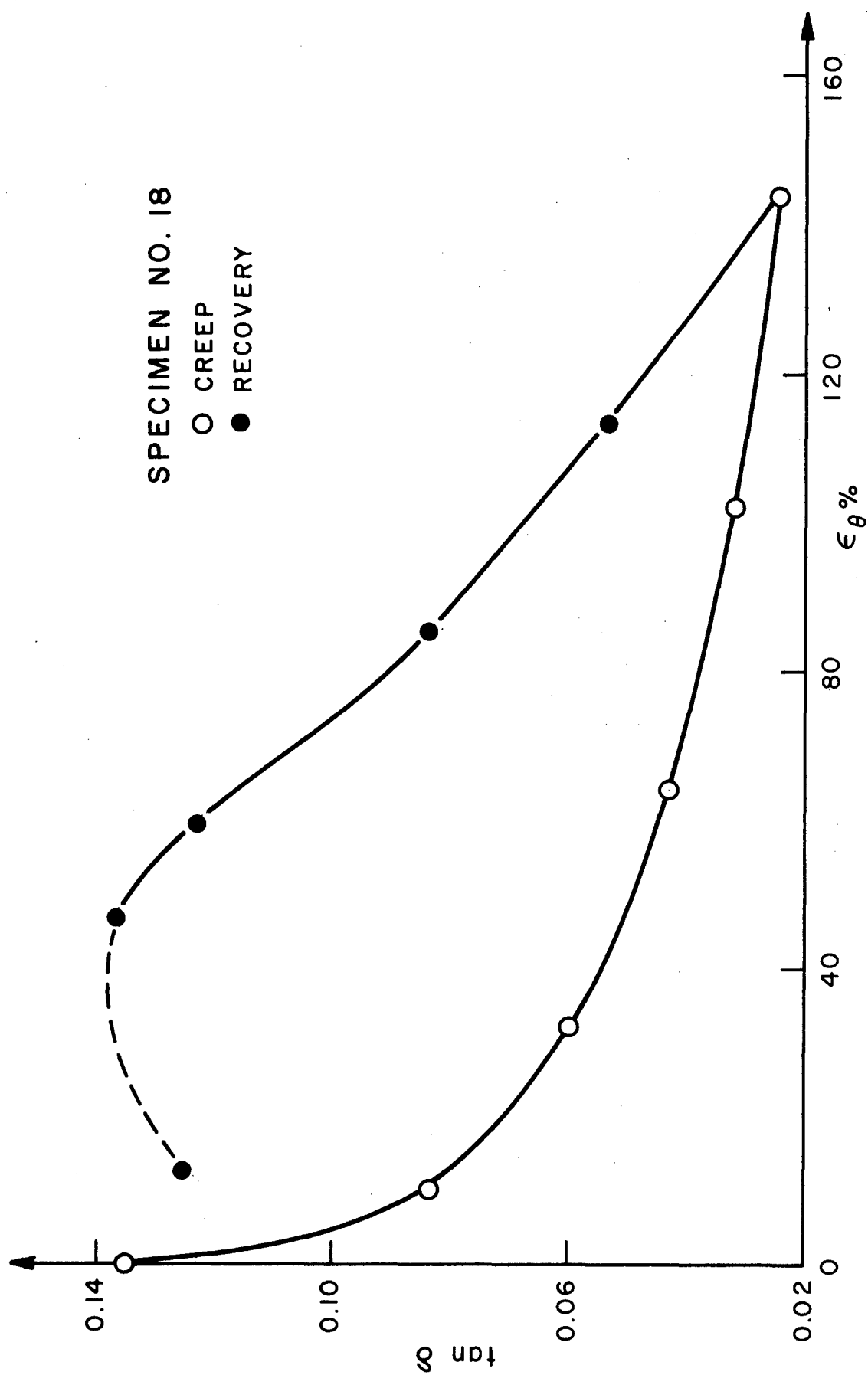


FIG. 30  $\tan \delta = \frac{E_2}{E_1}$  DURING LONGITUDINAL CREEP AND RECOVERY.

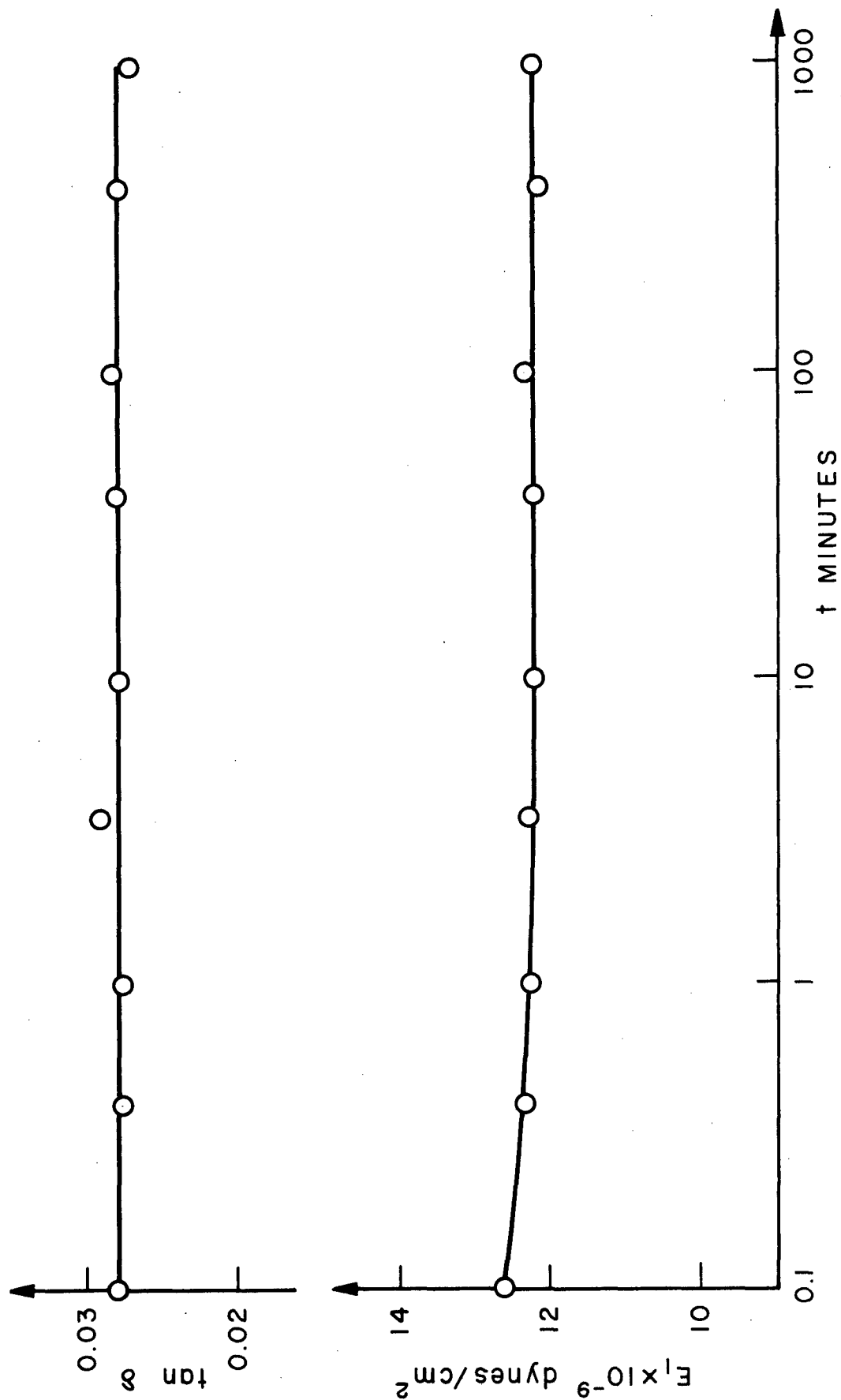


FIG. 31  $E'$ , AND  $\tan \delta$  DURING STRESS RELAXATION AT  $\epsilon_x = 142\%$

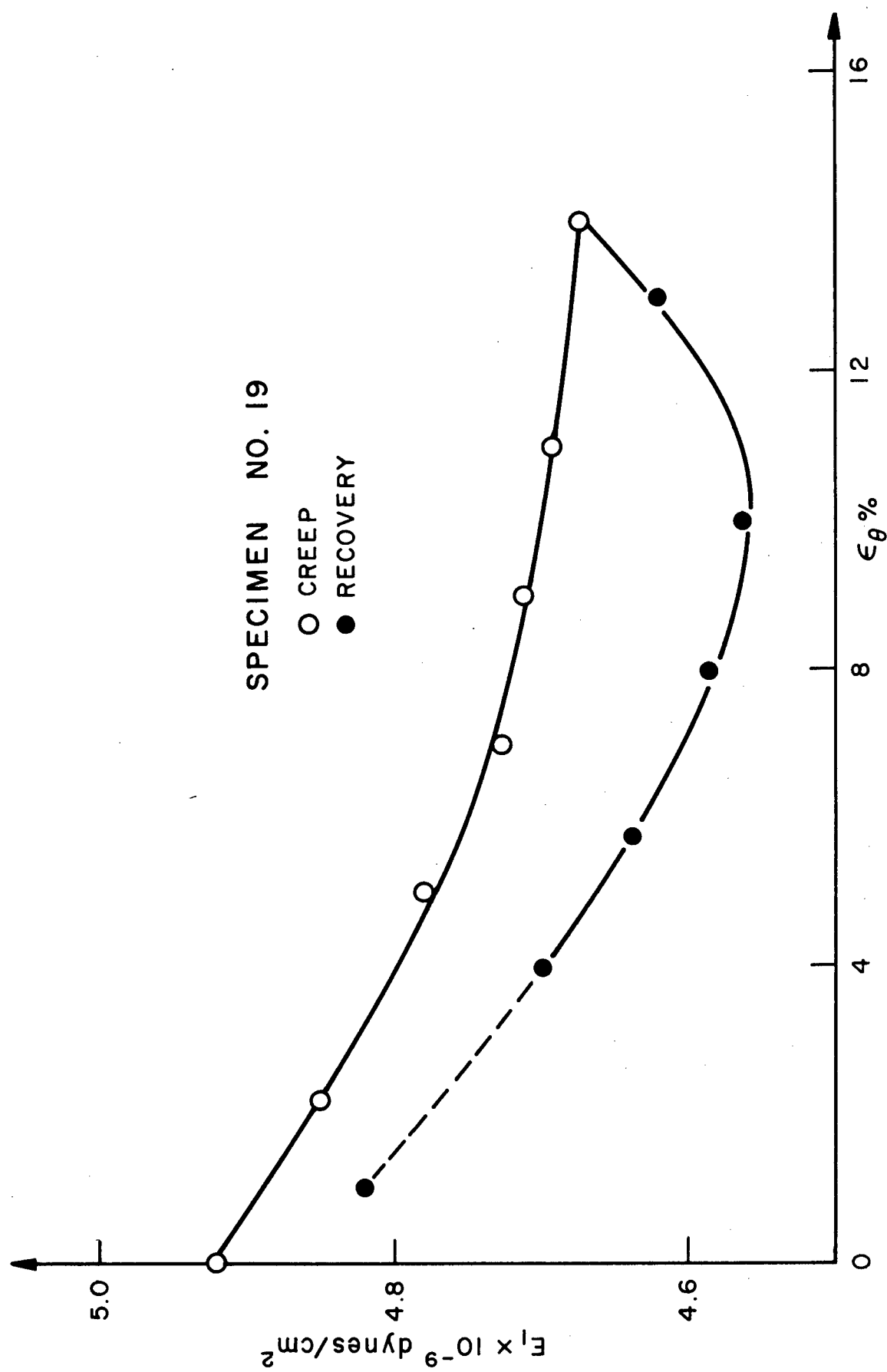


FIG. 32  $E_1$  DURING TORSIONAL CREEP AND RECOVERY.

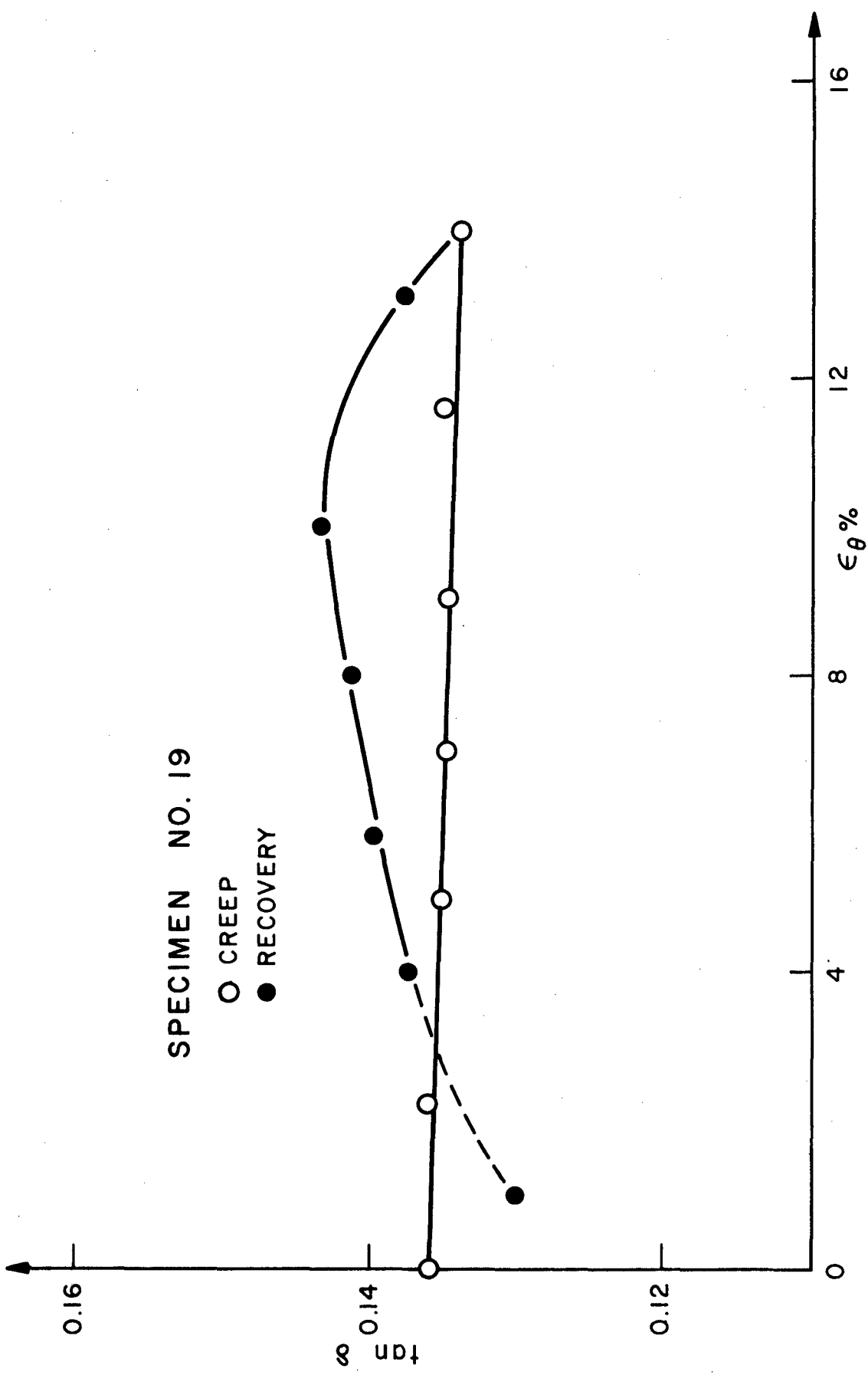


FIG. 33  $\tan \delta = \frac{E_2}{E_1}$  DURING TORSIONAL CREEP AND RECOVERY.



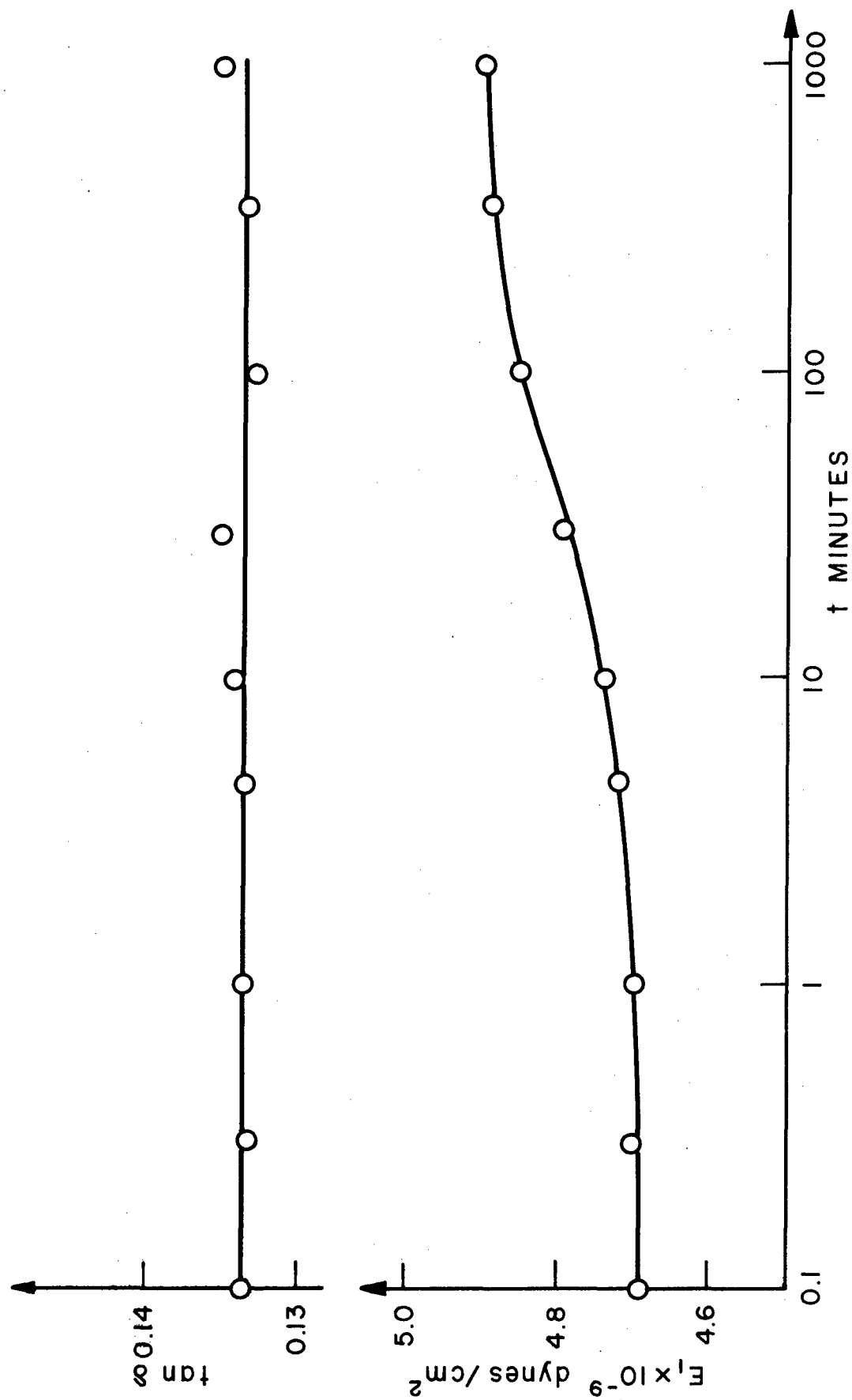


FIG. 34  $E'$  AND  $\tan \delta$  DURING STRESS RELAXATION AT  $\epsilon_{\theta} = 14\%$ .